A Close Look at the Hydrolytic Mechanism of OXA-58, a Class D β-Lactamase from *Acinetobacter baumannii*

KAVEH AMINI

A THESIS SUBMITTED TO THE FACULTY OF GRADUATE STUDIES

IN PARTIAL FULFILLMENT OF THE REQUIREMENTS

FOR THE DEGREE OF MASTER OF SCIENCE

GRADUATE PROGRAM IN CHEMISTRY

YORK UNIVERSITY

TORONTO, ONTARIO

APRIL 2012

Library and Archives Canada

Published Heritage Branch

395 Wellington Street
Ottawa ON K1A 0N4
Canada

Bibliothèque et Archives Canada

Direction du Patrimoine de l'édition

395, rue Wellington
Ottawa ON K1A 0N4
Canada

Your file Votre référence
ISBN: 978-0-494-90084-0

Our file Notre référence
ISBN: 978-0-494-90084-0

ABSTRACT

OXA-58 enzyme from *Acinetobacter baumannii* is a carbepenm-hydrolyzing class-D β-lactamase which uses a carbamylated lysine to activate the nucleophilic serine used for β-lactam hydrolysis. The deacylating water molecule approaches the acylenzyme intermediate formed between the enzyme and the β-lactam from the α-face. According to our findings, OXA-58 uses the same catalytic machinery observed in class D β-lactamases such as OXA-10. Comparison of active site shape in OXA-58, OXA-24 and OXA-48 with the OXA-10 β-lactamase suggests that these carbapenem-hydrolyzing class D β-lactamases have gained the capability of hydrolyzing imipenem, an important carbapenem in clinical use, by slight structural changes in the active site. Also, investigation of the kinetics of β-lactam hydrolysis by Phen113A, Phen114A, Met225A, Phen113Tyr, Phen114Ile and Met225Thr shows that penicillin G is hydrolyzed better than amoxicillin and ampicillin which are hydrolyzed with comparable catalytic efficiencies. Carbenicillin was the poorest substrate.

Contents

Chapter One: β-Lactam resistance in *Acinetobacter baumannii*

1.1 *Acinetobacter baumannii*

1.1.1 Background and history

Being a Gram-negative, coccobacilli aerobic pathogen, *Acinetobacter baumannii* is responsible for many community and hospital-acquired infections worldwide.

Its genetic flexibility and versatility gives *A. baumannii* an exceptional catabolic capability to be highly competent for natural transformation. Also the ability to grow at a wide range of temperature (28-44 °C), humidity and pH range makes the *A. baumannii* capable of adapting to the hospital environment.[1]

During the past decade *A. baumannii* has emerged as an important multidrug-resistant nosocomial pathogen causing pneumonia, septicemia, urinary tract infections and meningitis.[2] Drug families such as β-lactams, aminoglycosides and quinolones are normally used to treat this infections.[1]

β-Lactams are the main antibiotic source and are used in a routine way to treat different bacterial infections. Carbapenems being the last resort of β-lactams are the most efficient antibiotics against a wide variety of Gram-negative bacteria. *Acinetobacter* was initially introduced in 1954 by Brisou and Prévot [3] and in 1968 this genus designation was more widely accepted.[4]

1.2 Antibiotic resistance in *Acinetobacter baumannii*

1.2.1 Mechanisms of antibiotic resistance in *Acinetobacter baumannii*

A wide array of antibacterial resistance mechanisms have been identified for *A. Baumannii*.[5,6] The fast emergence of different strains of *A. Baumannii* resistant to different β-lactams, including carbapenems, indicates the ability of this organism to adapt rapidly to changes in environmental pressure.

1.2.2 Enzymatic mechanisms

Enzymatic degradation of β-lactams by β-lactamases is the most important mechanism of resistance in *A. baumannii*. However, taking the complexity of the nature of this organism into account, in *A. baumannii* multiple mechanisms, often function in a concerted manner.[7,8,9] Out of β-lactamases, carbapenemases are most concerning and include class D OXA type oxacillinases and the metallo- β-lactamases (class B).[10,11,12] So far, the class A carbapenemases have not been described for *A. Baumannii*.[13]

The first OXA-type enzyme with carbapenem-hydrolyzing activity was found in 1985 in a clinical *A. Baumannii* strain isolated in Edinburgh, Scotland.[14] This resistance factor was discovered to be transferable, and the gene was sequenced and named blaOXA-23.[15,16] This type of β-lactamases contributes seriously to carbapenem resistance in *A. Baumannii* all over the world .[7,18,19,20]

1.2.2.1 β-Lactamases

Production of penicillinase by pathogenic *Escherichia coli* was most probably the first antibiotic resistance mechanism reported.[71] Since then, intensive investigations have been performed on β-lactamases, and there are a large number of reviews and

monographs that reveal the details of this broad family of enzymes.[72-76] Here only a brief explanation of the resistance mechanism and structure of β-lactamases will be provided for review purpose.

β-Lactamases hydrolyze β-lactams either by employing an active site Ser nucleophile or through activation of a water molecule via a Zn^{2+} in their structure (Figure 1). These serine active site β-lactamases or metallo-β-lactamases have been categorized according to their three-dimensional structures, amino acid sequences, substrate preferences and inhibition by inhibitors. The β-lactamase family has been categorized in different ways; however, the nomenclature of Bush et al. [78] has been widely accepted. In an investigation on almost 200 β-lactamases, these authors have subdivided these enzymes in four main groups. Groups 1, 2, and 4 are serine β-lactamases, while metallo-β-lactamases fall into group 3. Group 1 consists of cephalosporinases which are poorly inhibited by clavulanic acid; group 2 consists of penicillinases which are sensitive to clavulanic acid and are called extended spectrum β-lactamases (ESBLs) [79]; and group 4 consists of β-lactamases that turn to be poorly inactivated by clavulanic acid and cannot be fit into the other categories. The serine active site β-lactamases act via a covalent catalytic mechanism where an active site serine nucleophile attacks the lactam ring (Figure 1). Then the covalent enzyme intermediate is hydrolytically cleaved. This mechanism is exactly the same as β-lactam inactivation of the extracellular bacterial peptidoglycan transpeptidases (targets for these antibiotics) where an active site serine is modified covalently by the drug. However, in this case, the second step of the lactamase reaction is inhibited by the unavailability of the hydrolyzing water molecule due to the

configuration of the active site of these transpeptidases, and therefore the acyl-enzyme species is a stable complex resulting in enzyme inactivation and consequent breakdown of cell wall biosynthesis.

The high similarity in mechanisms employed by peptidoglycan peptidases and serine β-lactamases is an indicator of the similarities in their three-dimensional structures and also an evolutionary link between them.[80,81]

1.2.2.2 Class D β-lactamases in *Acinetobacter Baumannii*

In general, in serine active-site enzymes including class D β-lactamases, after the formation of a Michaelis complex between the enzyme and substrate, the active site serine is deprotonated by an active site base and activated for a nucleophilic attack on the β-lactam carbonyl.[36] Then a tetrahedral transitional state is formed between the enzyme and the substrate. The collapse of this transition state leads to an acyl-enzyme intermediate between the β-lactam and the attacking serine. Finally activation of a water molecule through general-base mediation results in hydrolysis of the ester bond, releasing the hydrolyzed product.

Two closely related enzymes that form the *bla*OXA-23 gene cluster in *A. Baumannii* are OXA-27 and OXA-49.[21,22] Other OXA-type gene clusters with carbapenemase activity have been discovered to be the blaOXA-24-like (encoding OXA-24, -25, -26, and -40) [21, 23] and the *bla*OXA-58-like [24, 25] carbapenemase genes. The X-ray structure of OXA-24 was recently revealed through which important information for drug development toward this class of carbapenemases was provided.[26] *bla*OXA-58 was described recently and, like *bla*OXA-23, is normally plasmid mediated [27], which may be

the reason for its widespread distribution.[28,29,30] *bla*OXA-58 gene has been also reported in *A. Junii* isolated in Romania and Australia.[31,32] *bla*OXA-51-like genes (encoding OXA-51, -64, -65, -66, -68, -69, -70, -71, -78, -79, -80, and -82) are the final gene cluster, and this cluster is unique in terms of occurring naturally in *A. baumannii* because of its chromosomal location and prevalence.[33,28,34] Like other class D enzymes, its encoded protein has a greater affinity for imipenem than for meropenem.[33, 35]

1.2.2.3 OXA-58, a class D β-lactamase in *A. baumannii*

OXA-58 is the only member of a subgroup of carbepenem hydrolyzing class D β-lactamases and shares less than 50% sequence identity with other carbepenem hydrolyzing class D β-lactamase subgroups.[11,37] OXA-58 was first identified in 2003 in France [27], and since then it has been isolated in different parts of the world.[11,6] It has been proven that OXA-58 employs a carbamylated lysine residue [38] in its active site to activate the serine nucleophile to attack the carbonyl carbon of the β-lactam backbone.

1.2.2.4 Mechanism of action of β-lactams

β-Lactams are the most widely employed antibiotics against bacterial infections due to their high efficiency and specificity.[39-41] The chemical structures of different β-lactam families have been shown in Figure 2. These compounds are small molecules with a four member ring which is known as the β-lactam backbone. The similarity of their chemical structure to that of the terminal D-alanine-D-alanine portion of the pentapeptide moiety of the precursors of the cell wall (peptidoglycan) makes them highly specific.[42,43] Due to this similarity, β-lactams are capable of binding penicillin binding proteins (PBPs) competitively and prevent them from binding to their natural substrate. β-Lactams bind to

the serine active site of PBPs forming an acyl-enzyme species. This acyl-enzyme species is stable in contrast to that formed with the D-alanine-D-alanine peptide of peptidoglycan precursors and irreversibly inhibits the transpeptidation function of PBPs.[43,44] Inhibition of PBPs leads to a failure in cross-linking of the newly synthesized peptidoglycan precursors (The assembly of peptidoglycan and its structure in gram-negative bacteria have been illustrated in Figure 3 and Figure 4). This weakens the cell wall, leaving the cell wall unable to tolerate the osmotic pressure of the growing cell, which eventually leads to the cell breakdown.[45,46]

Scheme 2 illustrates the three step model for inhibition of PBPs by β-lactams.

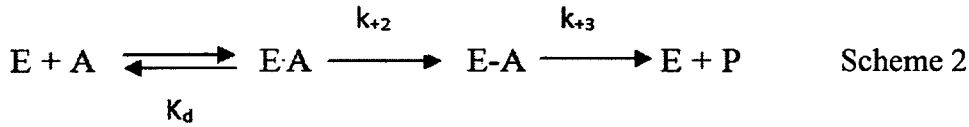

Scheme 2

where E represents the enzyme, A is the β-lactam, E·A is the non-covalent Michaelis complex, E-A represents the covalent acyl-enzyme species and P is the inactive hydrolysis product. K_d is the dissociation constant of the non-covalent complex, k_{+2} and k_{+3} are first order rate constants for the acylation and deacylation reactions, respectively. k_{+2}/K_d is the second order rate constant for the acylation step. In fact the PBPs catalyze the reaction up to the acyl-enzyme formation step therefore; these reactions have large k_{+2}/K_d values but very low k_{+3} values. However in β-lactamases the reaction continues until the inactive hydrolyzed product is produced (Figure 5). The mechanism of β-lactam hydrolysis by OXA-58 has been illustrated in Figure 6.

1.2.2.5 Other enzymatic mechanism of antibiotic resistance

While hydrolysis is considered the most important characterized enzymatic resistance mechanism, there are some other alternative strategies that have been developed by bacteria for detoxification of antibiotics.

1.2.2.5.1 Redox enzymes

Oxidation is a mechanism employed by mammalians for detoxification of xenobiotics. Mainly a group of membrane-bound cytochrome P-450 enzymes with broad substrate specificity use this molecular strategy to hydroxylate xenobiotics to facilitate their elimination.[82] In contrast, pathogenic bacteria have not developed the oxidation or reduction of antibiotics frequently as a mechanism of resistance. Nonetheless, a few examples of this strategy have been introduced in the literature. Oxidation of tetracycline antibiotics by TetX enzyme is the most widely studied of these.[83–86]

TetX monohydroxylates tetracycline antibiotics at their position 11a, which consequently disrupts the Mg^{2+}-binding site of the antibiotic which is essential for antibacterial activity. Following this hydroxylation, the antibiotic is non-enzymatically rearranged into unstable products that polymerize into an inactive product.[86,87]

1.2.2.5.2 Lyase enzymes

Lyases are non-hydrolytic or non-oxidative catalysts of the cleavage of carbon-carbon, carbon-oxygen, carbon-nitrogen, and carbon-sulfur bonds. Double bond formation or ring closure also frequently happens due to these reactions.

There is only one well investigated antibiotic resistance lyase, Vgb, which causes resistance against type B streptogramin antibiotic.[88] Vgb from streptogramin B-resistant *staphylococci* [89,90] was first reported to be a hydrolytic lactonase because of the ring

opening of the antibiotic at the ester bond.[91] Isolation and characterization of the product of *S. aureus* Vgb catalysis, however, showed that water is not required as a co-substrate analogous in the reaction.[88] There was also a double bond in the inactive product at the site of cleavage, which confirmed that the resistance enzyme Vgb is a lyase.

1.2.3 Nonenzymatic mechanism

In addition to the enzymatic mechanism by β-lactamases, nonenzymatic mechanisms have also been described for β-lactam resistance, including carbapenem resistance. These include changes in outer membrane proteins (OMPs) [25,47,48,8], multidrug efflux pumps [49,50,51], and variations in the affinity or expression of penicillin-binding proteins.[8, 52, 53, 54]

1.2.4 Strategies to fight resistance against β-lactams

Development of resistance to β-lactams by bacteria is a complicated phenomenon. Many factors influence the emergence and spread of antibiotic resistance. Knowledge of the mechanism of action and structure of antibiotic hydrolyzing enzymes is critical to develop methods to ultimately fight against resistance. As an example, discovering the 3'-regiospecificity of aminoglycoside resistance by the resistance kinases that appeared in the 1960s lead to the design of aminoglycosides such as tobramycin and gentamicin that did not have the sites of inactivation.[55] This approach has also helped the design and development of many new generations of semi-synthetic β-lactams, by the purpose of keeping one step ahead of evolving β-lactamases.

Among the more recent β-lactam scaffolds are the penems and carbapenems which are developed to overcome resistance. These β-lactams have broad-spectrum activity

against bacterial pathogens and high stability against β-lactamases.[56] Imipenem as the first antibiotic in this class was metabolized by a renal dehydropeptidase and co-administration of cilastatin, an inhibitor of this enzyme, was required although the more novel β-lactams such as ertapenem and faropenem have improved spectrum and stability.[57–59]

Another strategy to fight against antibiotic resistance is development of inhibitors of β-lactamases on the basis of the knowledge of resistance mechanisms. These inhibitors can be administered along with the antibiotics, thereby inhibiting β-lactamases as a main factor of resistance and rescuing the antibacterial activity of the β-lactams. This method has been successfully employed as a strategy to overcome resistance to the penicillinases where the mechanism-based inactivators of β-lactamases clavulanic acid, sulbactam, and tazobactam have been introduced to clinical use.[60] Taking the success of class A β-lactamase inhibitors into account, expanding this strategy to other antibiotics is of great importance.

Mobashery and coworkers [61] showed that 6α-hydroxymethylpenicillanate is an effective inhibitor of TEM-1 β-lactamase, a class A β-lactamase. In the case of OXA-10, a class D non-carbapenemase β-lactamase, it was reported that both α- and β-hydroxyisopropylpenicillanates were inactivators for this class D oxacillinase. [62] Recently, we have shown that 6α-hydroxyoctylpenicillanate rapidly inactivates the OXA-58, a class D carbapenemase β-lactamase ($t_{1/2}$=3 min at 4 °C) forming a very stable acyl-enzyme complex.[38]

Another strategy to fight against antibiotic resistance is to improve the delivery and the accessibility of antibiotics to their sites of action. Liposomal preparations of hydrophobic antibiotics such as ethambutol which have been reported for treatment of mycobacterial infections are an example of this approach.[63,64]

Linking of two different types of antibiotics (for example, β-lactams and quinolones [65], or β-lactams and oxazolidinones [66]) is another method that has been investigated. In this method stable or labile bonds were used to link the antibiotics, although a more clever strategy that employs the enzymatic activity of β-lactamases to release linked antibiotics has been also introduced. For example, the Ala racemase inhibitor β-chloro-Ala was released from cephalosporin–β-chloro-Ala upon β-lactamase action [67], and cephalosporin–triclosan hybrids have been designed so that triclosan is release upon hydrolysis of the β-lactam bond by β-lactamases.[68]

Expanded knowledge of the molecular mechanism of antibiotic resistance is required to develop different strategies to overcome antibiotic resistance. With regards to the ongoing drying of the pipeline of the antibiotic drug discovery [69,70] understanding of the details of enzyme-based resistance plays a crucial role on the treatment of infectious diseases.

1.3 Research objectives

In this project, the hydrolytic mechanism of OXA-58, a class D β-lactamase from *A. Baumannii* in antibiotic resistance has been investigated. Three main goals of this research have been: (I) Study of the inactivation and inhibition kinetics of this enzyme by different β-lactams and novel β-lactam analogues, hydrolytic mechanism and the

conformational changes induced in the presence of different β-lactams. (II) Investigation of the role of the lysine in the active site of this β-lactamase in its catalytic mechanism and (III) the role of Phen 113, Phen 114 and Met 225 residues which lie right above the active site in the activity of this protein.

References

(1) Vallenet, D., Nordmann, P.; Barbe, V., Poirel, L., Mangenot, S., Bataille, E., Dossat, C., Gas, S.; Kreimeyer, A., Lenoble, P., Oztas, S., Poulain, J., Segurens, B., Robert, C., Abergel, C., Claverie, J. M., Raoult, D., Me´digue, C., Weissenbach, J., Cruveiller, S. *PLoS One* **2008**, *19,3* (3), e1805.

(2) Abbo, A., Navon-Venezia, S., Hammer-Muntz, O., Krichali,, T., Siegman-Igra, Y., Carmeli, Y., *Emerg. Infect. Dis.* **2005**, 11:22–29.

(3) Brisou, J., Prevot, A. R.. *Ann. Inst. Pasteur* (Paris) **1954**, 86:722–728.

(4) Baumann, P., M. Doudoroff, and R. Y. Stanier. A. *J. Bacteriol.* **1968**, 95:1520–1541.

(5) Perez, F., Hujer A. M., Hujer K. M., Decker B. K., Rather P. N., Bonomo. R. *Antimicrob. Agents Chemother* **2007**, 51:3471–3484.

(6) Poirel, L., Nordmann P. *Clin. Microbiol. Infect.* **2006**, 12:826–836.

(7) Bou, G., Cervero, G., Dominguez, M. A., Quereda, C., Martinez-Beltran, J. *J. Clin. Microbiol.* **2000**, 38:3299–3305.

(8) Fernandez-Cuenca, F., Martinez-Martinez, L., Conejo, M. C., Ayala, J. A., Perea, E. J., Pascual, A., *J. Antimicrob. Chemother.* **2003**, 51:565–574.

(9) Quale, J., Bratu, S., Landman, D., Heddurshetti, R. *Clin. Infect. Dis.* **2003**, 37:214–220.

(10) Piddock, L. J. *Clin. Microbiol. Rev.* **2006**, 19:382–402.

(11) Queenan, A. M., Bush, K. *Clin. Microbiol. Rev.* **2007**, 20:440–458.

(12) Walsh, T. R., Toleman, M. A., Poirel, L., Nordmann, P. *Clin. Microbiol. Rev.* **2005**, 18:306–325.

(13) Queenan, A. M., Bush, K. *Clin. Microbiol. Rev.* **2007**, 20:440–458.

(14) Paton, R., Miles, R. S., Hood, J., Amyes, S. G. B. *Int. J. Antimicrob. Agents* **1993**, 2:81–88.

(15) Donald, H. M., Scaife, W., Amyes, S. G., Young, H. K. *Antimicrob. Agents Chemother.* **2000**, 44:196–199.

(16) Scaife, W., Young, H. K., Paton, R. H., Amyes, S. G. *J. Antimicrob. Chemother.* **1995**, 36:585–586.

(17) Boo, T. W., Walsh, F., Crowley, B. *J. Antimicrob. Chemother.* **2006**, 58:1101–1102.

(18) Coelho, J. M., Turton, J. F., Kaufmann, M. E., Glover, J., Woodford, N., Warner, M., Palepou, M. F., Pike, R., Pitt, T. L., Patel, B. C., Livermore, D. M. *J. Clin. Microbiol.* **2006**, 44:3623–3627.

(19) Corvec, S., Poirel, L., Naas, T., Drugeon, H., Nordmann, P. *Antimicrob. Agents Chemother.* **2007**, 51: 1530–1533.

(20) Dalla-Costa, L. M., Coelho, J. M., Souza, H. A., Castro, M. E., Stier, C. J., Bragagnolo, K. L., Rea-Neto, A., Penteado-Filho, S. R., Livermore, D. M., Woodford, N. *J. Clin. Microbiol* **2003**, 41:3403–3406.

(21) Afzal-Shah, M., Woodford, N., and Livermore, D. M., *Antimicrob. Agents Chemother.* **2001**, 45:583-588.

(22) Brown, S., Amyes, S. *J. Antimicrob. Chemother.* **2006**, 57:1–3.

(23). Bou, G., Oliver, A., Martinez-Beltran, *J. Antimicrob. Agents Chemother.* **2000**, 44:1556–1561.

(24) Bertini, A., Giordano, A., Varesi, P., Villa, L., Mancini, C., Carattoli, A. *Antimicrob. Agents Chemother.* **2006**, 50:2268–2269.

(25). Bogaerts, P., Naas, T., Wybo, I., Bauraing, C., Soetens, O., Pierard, D., Nordmann, P., Glupczynski, Y. *J. Clin. Microbiol.* **2006**, 44:4189–4192.

(26) Santillana, E., Beceiro, A., Bou, G., Romero, A. *Proc. Natl. Acad. Sci. USA* **2007**, 104:5354–5359.

(27) Poirel, L., Marque, S., Heritier, C., Segonds, C., Chabanon, G., Nordmann, P. *Antimicrob. Agents Chemother.* **2005**, 49:202–208.

(28) Coelho, J., Woodford, N., Afzal-Shah, M., Livermore, D. *Antimicrob. Agents Chemother.* **2006**, 50:756–758.

(29) Marque, S., Poirel, L., Heritier, C., Brisse, S., Blasco, M. D., Filip, R., Coman, G., Naas, T., Nordmann, P. *J. Clin. Microbiol.* **2005**, 43:4885–4888.

(30) Peleg, A. Y., Bell, J. M., Hofmeyr, A., Wiese, P. *J. Antimicrob. Chemother.* **2006**, 57:794–795.

(31) Marque, S., Poirel, L., Heritier, C., Brisse, S., Blasco, M. D., Filip, R., Coman, G., Naas, T., Nordmann, P. *J. Clin. Microbiol.* **2005**, 43:4885–4888.

(32) Peleg, A. Y., Franklin, C., Walters, L. J., Bell, J. M., Spelman, D. W. *Antimicrob. Agents Chemother.* **2006**, 50:399–400.

(33) Brown, S., Young, H. K., Amyes, S. G. *Clin. Microbiol. Infect.* **2005**, 11:15–23

(34) Heritier, C., Poirel, L., Fournier, P. E., Claverie, J. M., Raoult, D., Nordmann, P. *Antimicrob. Agents Chemother.* **2005**, 49:4174–4179.

(35) Heritier, C., Poirel, L., Aubert, D., Nordmann, P. *Antimicrob. Agents Chemother.* **2003**, 47:268–273.

(36) Ledent, P., Raquet, X., Joris, B., Van Beeumen, J., and Frere, J. M. *Biochem. J.* **1993**, 292 (Part 2), 555–562.

(37) Walther-Rasmussen, J., Høiby, N. *J. Antimicrob. Chemother.* **2006**, 57, 373–383.

(38) Verma V., Testero, S. A., Amini, K, Wei, W, Liu J., Balachandran, N., Monoharan, T., Stynes, S., Kotra, L. P., Golemi-Kotra, D., *J. Biol. Chem.* **2011**, 286: 37292–37303.

(39) Dalhoff, A., Thomson, C. J. *Chemotherapy* **2003**, 49, (3), 105-20.

(40) Essack, S. Y. *Pharm. Res.* **2001**, 18, (10), 1391-9.

(41) Siu, L. K., *J. Microbiol. Immunol. Infect.* 2002, 35, (1), 1-11.

(42) Guignard, B., Entenza, J. M., Moreillon, P. *Curr. Opin. Pharmacol.* **2005**, 5, (5), 479-89.

(43) Tipper, D. J., Strominger, J. L. *Proc. Natl. Acad. Sci. USA* **1965**, 54, (4), 1133-41.

(44) Ghuysen, J. M., *Annu. Rev. Microbiol.* **1991**, 45, 37-67.

(45) Giesbrecht, P., Kersten, T., Maidhof, H., Wecke, J. *Microbiol. Mol. Biol. Rev.* **1998**, 62, (4), 1371-414.

(46) Sugai, M., Yamada, S., Nakashima, S., Komatsuzawa, H., Matsumoto, A., Oshida, T., Suginaka, H., *J. Bacteriol.* **1997**, 179, (9), 2958-62.

(47) Costa, S. F., Woodcock, J., Gill, M., Wise, R., Barone, A. A., Caiaffa, H., Levin, A. S. *J. Antimicrob. Agents* **2000**, 13:175-182.

(48) del Mar Tomas, M., Beceiro, A., Perez, A., Velasco, D., Moure, R., Villanueva, R., Martinez-Beltran, J., Bou, G. *Antimicrob. Agents Chemother.* **2005**, 49:5172–5175.

(49) Heritier, C., Poirel, L., Lambert, T., Nordmann, P. *Antimicrob. Agents Chemother.* **2005**, 49:3198–3202.

(50) Higgins, P. G., Wisplinghoff, H., Stefanik, D., Seifert, H. *J. Antimicrob. Chemother.* **2004**, 54:821–823.

(51) Magnet, S., Courvalin, P., Lambert, T. *Antimicrob. Agents Chemother.* **2001**, 45:3375– 3380.

(52) Gehrlein, M., Leying, H., Cullmann, W., Wendt, S., Opferkuch, W. *Chemotherapy* **1991**, 37:405–412.

(53) Obara, M., Nakae, T. *J. Antimicrob. Chemother.* **1991**, 28:791–800.

(54) Siroy, A., Cosette, P., Seyer, D., Lemaitre-Guillier, C., Vallenet, D., Van Dorsselaer, A., Boyer-Mariotte, S., Jouenne, T., De, E. *J. Proteome Res.* **2006**, 5:3385–3398.

(55) Wright G.D., Berghuis A.M., Mobashery S. *Adv. Exp. Med. Biol.* **1998**, 456:27–69.

(56) Edwards J.R., Betts M.J. *J. Antimicrob. Chemother.* **2000**, 45:1–4.

(57) Dalhoff, A., Nasu, T., Okamoto, K. *Chemotherapy* **2003**, 49:229– 236.

(58) Jones, M.E., Blosser-Middleton, R.S., Critchley, I.A., Karlowsky J.A., Thornsberry, C., Sahm, D.F. *J. Antimicrob. Chemother.* **2003**, 51:196–199.

(59) Hammond, M.L. J. *Antimicrob. Chemother.* **2004**, 53:7– 9.

(60) Lee, N., Yuen, K.Y., Kumana, C.R. *Drugs* **2003**, 63:1511– 1524.

(61) Golemi, D., Maveyraud, L., Ishiwata, A., Tranier, S., Miyashita, K., Nagase, T., Massova, I., Mourey, L., Samama, J. P., and Mobashery, S. *J. Antibiot.* **2000**, 53, 1022–1027.

(62) Maveyraud, L., Golemi-Kotra, D., Ishiwata, A., Meroueh, O., Mobashery, S., Samama, J. P. *J. Am. Chem. Soc.* **2002**, 124: 2461–2465

(63) Wiens, T. Redelmeier, T., Av-Gay, Y. *Agents Chemother.* **2004**, 48:1887–1888.

(64) Khuller, G.K., Kapur, M., Sharma, S. *Curr. Pharm. Des.* **2004**, 10:3263– 3274.

(65) Albrecht, H.A., Beskid, G., Christenson, J.G., Deitcher, K.H., Georgopapadakou, N.H., Keith, D.D., Konzelmann, F.M., Pruess, D.L., Wei, C.C., *J. Med. Chem.* **1994**, 37:400– 407.

(66) Gordeev, M.F., Hackbarth, C., Barbachyn, M.R., Banitt, L.S., Gage, J.R., Luehr, G.W., Gomez, M., Trias, J., Morin, S.E., Zurenko, G.E., Parker, C.N., Evans, J.M., White, R.J., Patel, D.V. *Bioorg. Med. Chem. Lett.* **2003**, 13:4213–4216.

(67) Mobashery, S., Johnston, M. *Biochemistry* **1987**, 26:5878– 5884.

(68) Stone, G.W., Zhang, Q., Castillo, R., Doppalapudi, V.R., Bueno, A.R., Lee, J.Y., Li, Q., Sergeeva, M., Khambatta, G., Georgopapadakou, N.H., *Antimicrob. Agents Chemother.* **2004**, 48:477– 483.

(69) Projan, S.J. *Curr. Opin. Microbiol.* **2003**, 6:427– 430.

(70) Wenzel, R.P. *N. Engl. J. Med.* **2004**, 351:523–526.

(71) Abraham, E.P., Chain, E., *Nature* **1940**, 146:837.

(72) Bush, K. *Curr. Opin. Investig. Drugs* **2002**, 3:1284-1290.

(73) Bush, K. *Clin. Infect. Dis.* 1998, 27:S48–S53.

(74) Bush, K., Mobashery, S. *Adv. Exp. Med. Biol.* **1998**, 456:71-98.

(75) Kotra, L.P., Mobashery, S. *Arch. Immunol. Ther. Exp. (Warsz)* **1999**, 47:211-216.

(76) Poole, K. *Cell. Mol. Life Sci.* **2004**, 61:2200-2223.

(77) Wright, G. D. *Adv. Drug. Del. Rev.* **2005**, 57:1451- 1470

(78) Bush, K., Jacoby, G.A., Medeiros, A.A. *Antimicrob. Agents Chemother.* **1995**, 39:1211 –1233.

(79) Shah, A.A., Hasan, F., Ahmed, S., Hameed, A. *Crit. Rev. Microbiol.* **2004**, 30:25–32.

(80) Massova, I., Mobashery, S. *Antimicrob. Agents Chemother.* **1998**, 42:1-17.

(81) Knox, J.R., Moews, P.C., Fre`re, J.M. *Chem. Biol.* **1996**, 3:937–947.

(82) Guengerich, F.P. *Chem. Res. Toxicol.* **2001**, 14:611 – 650.

(83) Park, B.H., Levy, S.B., *Antimicrob. Agents Chemother.* **1988**, 32:1797-1800.

(84) Speer, B.S., Salyers, A.A. *J. Bacteriol.* **1988**, 170:1423–1429.

(85) Whittle, G., Hund, B.D., Shoemaker, N.B., Salyers, A.A. *Appl. Environ. Microbiol.* **2001**, 67:3488-3495.

(86) Yang, W., Moore, I.F., Koteva, K.P., Bareich, D.C., Hughes, D.W., Wright, G.D. *J. Biol. Chem.* **2004**, 279:52346–52352.

(87) Speer, B.S., Bedzyk, L., Salyers, A.A. *J. Bacteriol.* **1991**, 173:176-183.

(88) Mukhtar, T.A., Koteva, K.P., Hughes, D.W., Wright G.D. *Biochemistry* **2001**, 40:8877– 8886.

(89) Allignet, J., Liassine, N., el Solh, N. *Antimicrob. Agents Chemother.* 1998, 42:1794–1798.

(90) Allignet, J., Loncle, V., Mazodier, P., el Solh, N. *Plasmid* **1988**, 20:271– 275.

(91) Le Goffic, F., Capmau, M.L., Abbe, J., Cerceau, C., Dublanchet, A., Duval, J. *Ann. Microbiol.* (Paris) **1977**, 128B:471–474.

(92) T. G. Kenneth, Todar's Online Textbook of Bacteriology, www.textbookofbacteriology.net

(93) Green, D. W. *Expert Opin. Ther. Targets* **2002**, 1:1-19.

(94) http://www.chem.ox.ac.uk/oc/cjschofield/biosynthesis.htm

Figures

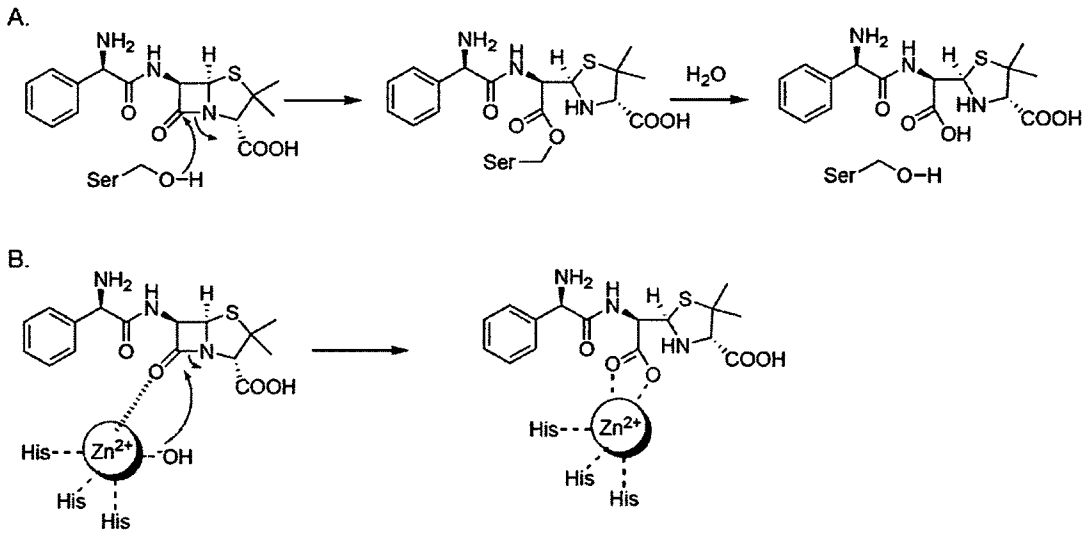

Figure 1. General mechanism of Ser-β-lactamases and metallo-β-lactamases. The hydrolysis of the penicillin amoxicillin is shown catalyzed by a Ser-β-lactamase (A) and a metallo-β -lactamase (B). (Taken from Wright et al[77])

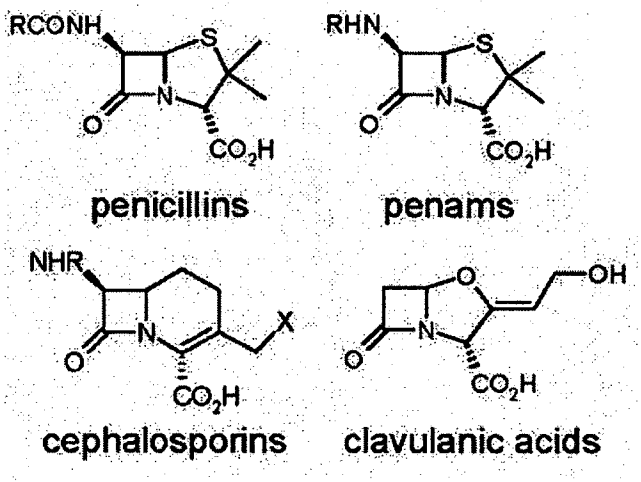

Figure 2. Structure of different β-lactam families

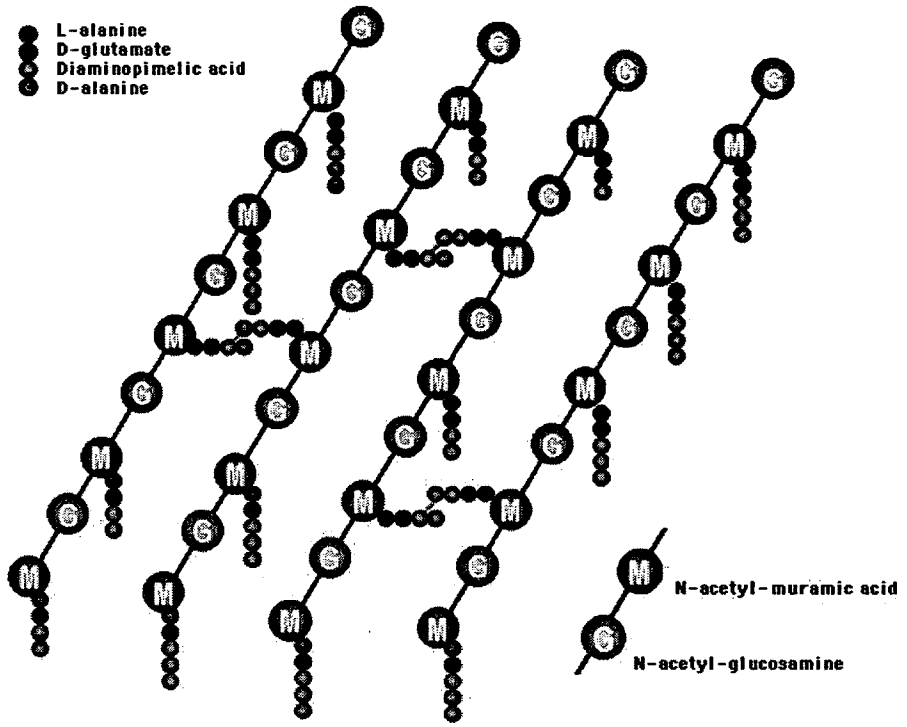

Figure 3. The assembly of gram-negative peptidoglycan (Taken from Todar et al [92])

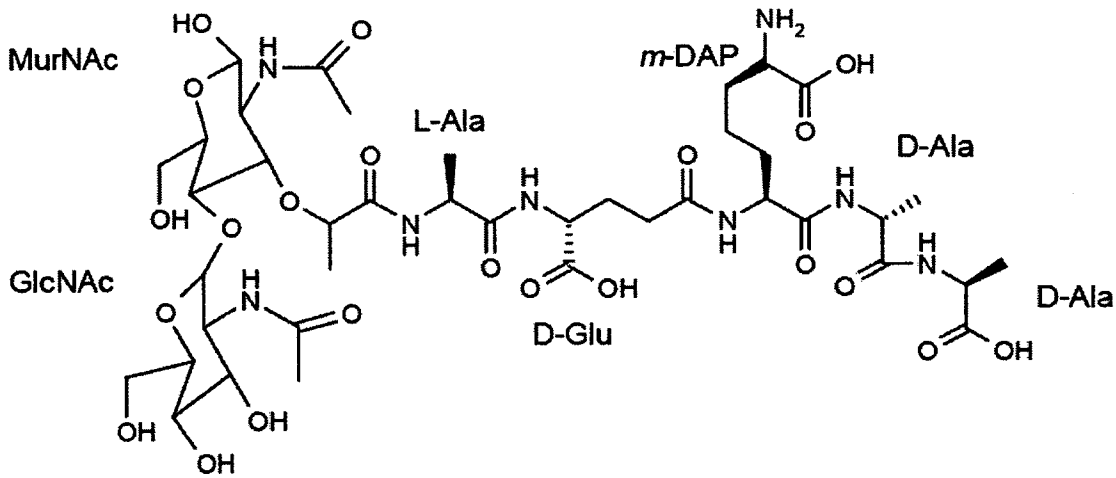

Figure 4. Structure of peptidoglycan precursors found in gram-negative bacteria which is L-Ala, D-Glu, m-DAP, D-Ala, D-Ala. (GlcNAc: N-acetyl glucosamine, MurNAc: N-acetyl-muramic acid) (Taken from Green et al [93])

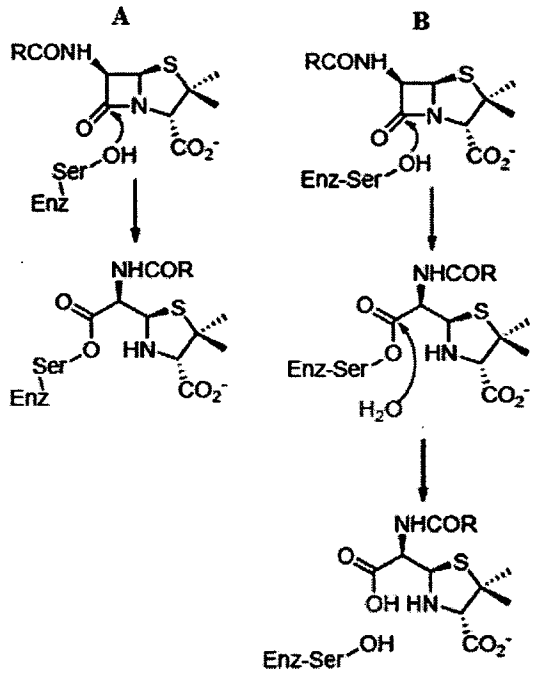

Figure 5. The metabolic pathway of (A) penicillin-Binding proteins and (B) β-lactamases. (Taken from Schofield et al[94])

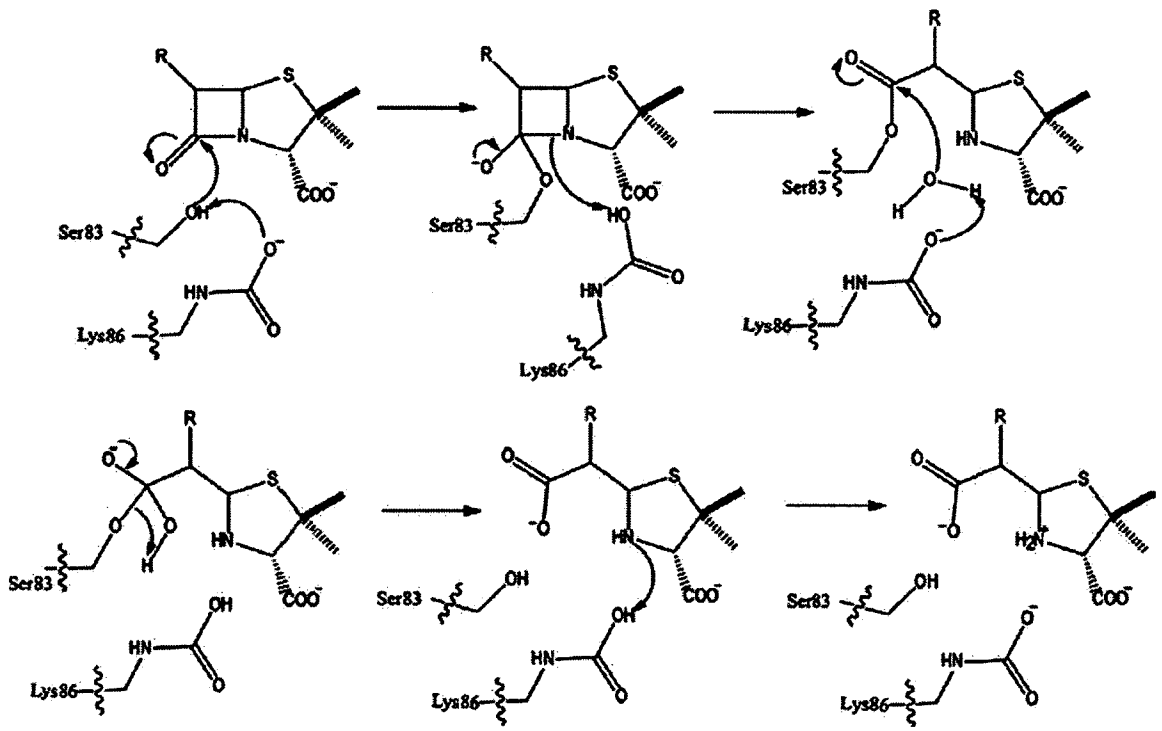

Figure 6. General catalytic mechanism of OXA-58 (Prepared by Dr. Golemi-Kotra[38]

Chapter Two: Hydrolytic mechanism of OXA-58, a carbepenem hydrolyzing class D β-lactamase

2.1 Introduction

2.1.1 OXA-58 an OXA-type carbapenem-hydrolyzing β-lactamase

Normally, severe *Acinetobacter* infections are treated with carbapenems.[1,2] Carbapenems are a family of β-lactams which are the most efficient antibiotics against bacteria and had initially been designed and developed to fight β-lactam resistance because of their stability toward hydrolysis by most β-lactamases[1,2], however, resistant *Acinetobacter baumannii* isolates are increasingly reported [3,4] and due to selective pressure, carbapenems have become inactive against β-lactamases. β-Lactamases are subdivided into four general classes. Classes A, C, and D are serine active site β-lactamases where Class B consists of metalloenzymes.[5, 6]

After the introduction of carbepenems to clinical use ~30 years ago, emergence of members of all four classes of β-lactamases capable of hydrolyzing carbapenems has been reported.[7-9] Outburst of carbapenem-resistant *A. baumannii* around the world is closely related to the new carbapenem-hydrolyzing class D β-lactamases.[10-13] Carbapenemase activity have been reported in Around 45 variants of class D β-lactamases.[14] Due to their ability to hydrolyze oxacillin, a penicillin β-lactam, class D β-lactamases are sometimes called as oxacillinases or OXA β-lactamases. It was in late 1980s that OXA β-lactamases were recognized as a resistance mechanism against imipenem, the first carbapenem which was used clinically.[15] Class D β-lactamases and

oxacillinases have 18% sequence identity, however they share 40-90% sequence identity with each other.[9,14]

Carbapenem-hydrolyzing class D β-lactamases have been categorized in nine groups.[9,14] OXA-23, OXA-24, and OXA-58, which represent three different Carbapenem-hydrolyzing class D β-lactamase groups, are the most prevalent carbapenemases in *A. baumannii*.[10,16] Out of these, only the structure of OXA-24 has been revealed.[17-19] Investigations on the structure and the role of different residues in OXA-24 uncovered that the extended substrate specificity of these enzymes is due to a hydrophobic cleft over their active sites.[17]

Solution of the crystal structure of OXA-48, a Carbapenem-hydrolyzing class D β-lactamases from *Klebsiella pneumoniae* showed that unlike OXA-24 this enzyme lacks the hydrophobic cleft over the active site and also the shape of the active site in this enzyme is different from that of OXA-24.[20] It was concluded that a different catalytic mechanism may be used by OXA-48.[20]

Details of the structural investigations performed on these different carbapenem-hydrolyzing class D β-lactamase subgroups reveals that they have gone through different evolutionary pathways. The diversity of carbapenem-hydrolyzing class D β-lactamases and their direct association with bacterial antibiotic resistance makes mechanistic studies on hydrolytic activity more important than ever.

2.2 Sequence analysis of OXA-58

All serine active site β-lactamases possess three conserved catalytic motifs which are also found in OXA-58 (Figure 1). The Arg residue which interacts with the carboxylic group of β-lactams in OXA-10 (Arg-244) is also present in OXA-58 (Arg-263). All the residues that form the hydrophobic cleft, in which the carbamylated lysine lies, as in OXA-10, OXA-24, and OXA-48, are present also in OXA-58 (Phe-85, Val-132, Phe-135, Trp-169, and Leu-170). Alignment of the sequence of OXA-58 with those of OXA-24 and OXA-48 and its comparison with the sequence of OXA-10 (Prepared by Dr. Golemi-Kotra) indicates that these carbapenem-hydrolyzing class D β-lactamases share the same catalytically important residues with OXA-10 (Figure 1).

2.3 Mechanism of β-lactam turnover by OXA-58

Penicillinate derivatives (Figure 2) were used to probe the mechanism of β-lactam hydrolysis in OXA-58. These derivatives have already been used to elucidate the mechanism of β-lactam turnover in different β-lactamases.[22] These compounds have a hydroxyalkyl side chain at C6 position of the β-lactam ring which is either at α or β face of the plane of the molecule. After acylation of the β-lactamase by these penicillinates and formation of the acyl-enzyme intermediate, hydrolysis or stabilization of this intermediate will depend on the face from which the hydrolyzing water molecule approaches the ester bond and the orientation of the side chain in C6 position of the β-lactam (Figure 3).

2.4 Experimental section

Materials and chemical reagents

All chemicals and antibiotics were purchased from Sigma or Fisher unless otherwise stated. Growth media were purchased from EMD Biosciences (Mississauga, Ontario, Canada). Chromatography media and columns were purchased from GE Healthcare.

2.4.1 Purification of OXA-58 and K86A Mutant

OXA-58 was cloned by Jerome Liu and OXA-58 K86A mutant was constructed (pET24d (+) vector was used) by Dr. Vidhu Verma (Dr. Golemi-Kotra's laboratory). The purification protocol was also developed by Dr. Vidhu Verma. A seed culture of E. coli BL21 (DE3) containing the appropriate expression vector was grown overnight at 37 °C in Luria Bertani medium containing 50 μg/ml kanamycin. A 2.5 ml aliquot of the seed culture was used to inoculate 800 ml of Terrific Broth medium containing 50 μg/ml kanamycin. The cell culture was grown at 37 °C until an absorbance at 600 nm (A600 nm) of 0.6 was reached, at which point overexpression was induced by the addition of isopropyl β-D-thiogalactopyranoside to a final concentration of 0.1 mM. The cells were allowed to overexpress the requisite protein for 16 h at 25 °C with shaking. The cells were then harvested by centrifugation at 7,000 × g for 10 min at 4 °C. The cell pellet (3 g) was resuspended in 90 ml of 10 mM sodium phosphate buffer, pH 6.4. The cytoplasmic contents were liberated by sonication, and the resulting cell extract was spun down at 18,000 × g to remove insoluble cell debris. The supernatant was then loaded onto an SP-Sepharose cation exchange column equilibrated with 10 mM sodium phosphate

buffer, pH 6.4. The protein was eluted with a linear gradient of 10-200 mM sodium phosphate buffer, pH6.4. Fractions containing the protein were concentrated and loaded onto a desalting column to exchange the buffer to 50 mM sodium phosphate buffer, pH 7.0. All purification steps were carried out at 4 °C. To confirm the purity the purified protein was loaded on a 12.5% SDS-PAGE (Figure 4).

2.4.2 Determination of the catalytic parameters by UV-visible spectrophotometry

The catalytic parameters (K_m and k_{cat}) of OXA-58 with nitrocefin (studies by monitoring the production of the hydrolyzed product at 486 nm according to the instruction provided by the company, Calbiochem) and cephapirin (studied by monitoring the consumption of the substrate at 259 nm, figure 5(A)) were determined under steady state conditions at room temperature using a Cary 100 Bio UV-visible spectrophotometer (Varian Inc., Palo Alto, CA). Briefly, each β-lactam (20-100 μM) was mixed with enzyme (5 nM in the case of nitrocefin, $\Delta_{\varepsilon 486}$ = 20,500 M^{-1} cm^{-1}; 120 nM in the case of cephapirin, $\Delta_{\varepsilon 259}$ = 7000 $M^{-1}cm^{-1}$). The initial rates were measured at 5% substrate turnover. All the kinetic reactions were carried out at room temperature in 50 mM sodium phosphate buffer, pH 7.0. The reaction volume was 250 μl. Linewever-Burk plots for these experiments have been presented in Figure 5 (B and C).

2.4.3 Inactivation kinetics

A Cary 100 Bio UV-visible spectrophotometer was used to perform kinetic measurements. Inactivation experiments were carried out with compounds 1–6 (Scheme 1). In a typical inactivation experiment, the β-lactam compound at different

concentrations (100, 200, 300, 500, or 700 μM) was incubated on ice with the enzyme (1.25 μM) in 50 mM sodium phosphate buffer, pH 7.0. To monitor the residual activity of enzyme by time, at different time intervals, a 20-μl aliquot of the incubation mixture was diluted 12.5-fold (to a final assay volume of 250 μl), and the remaining enzyme activity was monitored immediately at 240 nm using penicillin G (1 mM) as the reporter substrate ($\Delta_{\varepsilon 240}$ = 570 M^{-1} cm^{-1}). Data were analyzed using the Kitz-Wilson method.[23] The rate of recovery of enzyme activity was determined by monitoring the enzyme activity of the above mixtures over 24 h at 4 °C.

The β-lactam compounds 1–6 were also assessed as competitive inhibitors using nitrocefin as a reporter substrate (Figure 6-2). The steady state parameters for nitrocefin are k_{cat} = 99 ± 8 s^{-1} and K_m = 21 ± 2 μM. In a typical competitive inhibition experiment, the enzyme was added to the reaction mixture containing nitrocefin and inhibitor. The final concentration of the enzyme was maintained at 5 nM. Two concentrations of nitrocefin, 30 and 100 μM were used. The reaction volume was 250 μl. Enzyme activity was monitored at 486 nm ($\Delta_{\varepsilon 486}$ = 20,500 M^{-1} cm^{-1}). The concentrations of the inhibitors in these assays were selected such that they would flank 50% inhibition of enzyme activity. The experiments were repeated at least three times. The dissociation constants (K_i) were determined by the Dixon plot (Figures 6).[21]

2.4.4 Circular dichroism spectroscopy

The far-UV CD spectra of OXA-58 (10 μM) in the absence and presence of a β-lactam (100 μM) were recorded using a Jasco J-810 instrument. In experiments with the β-lactam substrates, CD spectra were recorded immediately after substrate and enzyme

were mixed together. All measurements were carried in 50 mM sodium phosphate buffer, pH 7.0, in a rectangular cuvette with a path length of 0.1 cm. Spectra were recorded from 260 to 200 nm at a scan rate of 10 nm/min and a 1.0-nm bandwidth, at 20 °C. All spectra were corrected for buffer and inhibitor as appropriate.

2.4.5 Electrospray Ionization Mass Spectrometry

OXA-58 at a concentration of 110 μM in 50 mM sodium phosphate, pH 7.0, was incubated individually with 5mM of each of the compounds 1–6 for 1 h at room temperature. The mixture was then desalted using Zeba mini centrifugal columns (Pierce) equilibrated with water, concentrated using a SpeedVac, and frozen at -20 °C. The samples were sent to the Advanced Protein Technology Centre, The Hospital for Sick Children (Toronto, Ontario, Canada) to be analyzd using an Applied Biosystems/MDS Sciex API QSTAR XL Pulsar mass spectrometer.

2.5 Results

2.5.1 Purification of OXA-58 and K86A Mutant

High level expression of the protein in the cytoplasm (20 mg/liter) enabled isolation of > 95% homogeneous protein (Figure 4).

The K86A mutant was purified using the same protocol. Expression levels and purity were the same as for the wild-type protein.

2.5.2 Study of the enzyme kinetics of OXA-58

Table 1 shows the kinetic constants (K_m and k_{cat} values) for the hydrolysis of nitrocefin and cephapirin by OXA-58 β-lactamase obtained by Lineweaver-Burk method.[21]

Isothermal titration calorimetry investigations, performed by Dr. Vidhu Verma (Dr. Golemi-Kotra's laboratory) in our research group showed that OXA-58 readily hydrolyzed ampicillin, oxacillin, benzylpenicillin, amoxicillin, and cephalothin. Biphasic kinetics had been observed for the hydrolytic activity of OXA-58 on ampicillin, amoxicillin, and cephalothin in the absence of carbon dioxide. Penicillins were hydrolyzed better than cephalosporins. Imipenem had a slow turnover rate, but according to its low K_m, it was a moderate substrate. Carbenicillin was reported not to be turned over by OXA-58.[21]

2.5.3 Mode of interaction of OXA-58 with the 6-hydroxyalkylpenicillinate derivatives

The structures of the 6-hydroxyalkylpenicillinate derivatives used have been illustrated in Figure 2. Out of six penicillinates examined only 6-α-hydroxyoctylpenicillinate (compound 5) inactivated OXA-58 at 4 °C (Table 2). The inactivation persisted even after 24 hrs incubation of OXA-58 with concentrations as low as 100 μM of compound 5 at 4 °C. However, the 6β-hydroxyoctylpenicillanate derivative (compound 6) did not undergo hydrolysis as investigated by UV spectrophotometry, but this compound inhibited OXA-58 competitively (Table 3). By contrast, the 6-β-hydroxymethylpenicillinate derivative (compound 2, ε_{203} = 200 $s^{-1}M^{-1}$) behaved as a moderate substrate with $k_{cat}/K_m = 79 \times 10^4$ $M^{-1}s^{-1}$ ($k_{cat} = 32.2 \pm 0.5$ s^{-1}; $K_m = 41 \pm 1$ μM). Incidentally, the Michaelis-Menten constant for 6β-hydroxyoctylpenicillanate (compound 6) is the same as the dissociation constant which indicates that the rate-limiting step is

likely to be acylation. On the other hand, all the penicillanate derivatives (compounds 1-6) inhibited OXA-58 competitively (Table 3).

2.5.4 Mass spectrometry analysis of the interaction between penicillinate derivatives and OXA-58

The interaction modes of compounds 1–6 were also investigated by ESI-MS. These experiments showed that compound 5 resulted in the formation of quantitative and stable acyl-enzyme species, whereas compound 6 resulted in the formation of a smaller amount of acyl-enzyme species (Fig. 7). The lack of measurable time-dependent inactivation of the enzyme by compound 6, as investigated by UV-visible spectrophotometry, suggests that the observed acyl-enzyme species could result from the formation of a short lived covalent complex. However, at the level of the detection limit of the UV-visible spectrophotometer, we were not able to measure any hydrolysis. Other inhibitors do not show any acylation with the enzyme. The mass spectra for OXA-58 incubated with compound 1-3 have been illustrated in figure 8.

2.5.5 Structural investigation of the interactions between β-lactams and OXA-58 β-lactamase

Far UV CD was used to investigate the effect that β-lactam binding has on the secondary structures of OXA-58. These studies showed that the protein undergoes a conformational change in the presence of different β-lactams, albeit at different levels (Figure 9).

2.6 Discussion

2.6.1 Mechanism of β-lactam hydrolysis by OXA-58

Serine active site β-lactamases hydrolyze β-lactams in two steps as shown in scheme 2.

$$E + A \underset{k_{-1}}{\overset{k_1}{\rightleftharpoons}} E.A \xrightarrow{k_2} E\text{-}A \xrightarrow{k_3} E + P$$

In the first step, the enzyme (E) employs a serine active site residue to form a transient acyl-enzyme intermediate (E-A). This is a ring opening reaction. In the second step, hydrolysis of the acyl-enzyme intermediate happens by a water molecule. A general base within hydrogen-bonding proximity to the serine residue transforms the weakly nucleophilic alcohol of the serine into a strong nucleophile, by deprotonating it and makes the formation of the acyl-enzyme species in the first step possible. In class A β-lactamases, this role is played by Lys-73 and Glu-166.[24-28] In class C, either Lys-67 or Tyr-105 may act as the general base to activate the serine.[29-31] In class D β-lactamases, a carbamylated lysine acts as the general base in both steps.[31-33]

The role of the carbamylated lysine in the hydrolysis is shown schematically in Figure 10. After activation of Ser-83, the carbamate species might be deprotonated by the N-4 of the penam.[18] At the end of hydrolysis, the carbamylated lysine is protonated and returns to its basic form, probably by receiving the proton from the protonated species of carbamylated lysine by the N-4 amine group of the penam.[18]

The possibility of rendering the β-lactamase deacylation-deficient by stabilizing the acyl-enzyme species by disturbing of the hydrogen bonding network of the hydrolyzing water molecule or the physical displacements of this water molecule

sterically by bulky C6 side chains of β-lactams has been already shown.[22,39-41] This is an important aim in designing new β-lactams that are stable toward the hydrolytic activity of β-lactamases.[22]

In this project a set of 6α- and 6β-hydroxyalkylpenicillanate derivatives (compounds 1–6) have been used to probe the face from which the deacylating water molecule approaches the ester carbonyl of the acyl-enzyme species.[22, 42] Mobashery and coworkers [22] reported that compound 1 is an inactivator of TEM-1 β-lactamase, a class A β-lactamase. According to their study, the deacylating water molecule comes from the α-face in TEM-1. In OXA-10, it was shown that 6β-hydroxymethylpenicillanate (compound 2) behaved as a substrate for this class D oxacillinase, and hence it was concluded that the water molecule approaches from the α-face.[34] The α- and β-face refer to the stereochemistry of the hydroxyalkyl side chain at the C6 position of the β-lactam molecule.

In our study of the interactions of these penicillanate derivatives with OXA-58, compound 2 was shown to be a substrate for this enzyme, and compound 5 was proven to be an inactivator (Figure 6-1). Compound 6 was not hydrolyzed by OXA-58 which indicates that the increase in the bulkiness of the side chain at the C6 position could interfere with the catalytic machinery of OXA-58, for example by decarbamylating the enzyme.[35]

Results from ESI-MS and competitive experiments also reinforce this; by revealing that compound 6 is capable of binding to OXA-58, but only a small percentage of the noncovalent Michaelis complex built between compound 6 and the enzyme form an acyl-

enzyme species. Time-dependent inactivation experiments show that compound 6 is not capable of inactivating the enzyme even after 24 h. In contrast, the 6β-hydroxyoctylpenicillanate derivative (compound 5) inactivates the enzyme building a very stable acyl-enzyme complex (Figures 6-1 and 7). This shows that the water molecule approaches the ester bond of the acyl-enzyme species from the α-face (that of the side chain of compound 5). The knowledge obtained from the investigations on the binding interaction of compound 5 with OXA-58 provides insights which can help to design potential inactivators of these class D enzymes. For instance, a bulky side chain at the C6 position may increase the binding affinity of β-lactams, and the presence of a 6β-hydroxylalkyl substituent as displayed by compound 5 may provide an obstacle on the way of the hydrolyzing water molecule. A recent study by Bou et al. [18] also has shown that OXA-24 is rapidly inactivated in the presence of β-lactams with a bulky side chain at their C6 position.

2.6.2 Insights into the Mechanism of Imipenem Hydrolysis

Although high resolution structures for OXA-24 and OXA-48 have been obtained[17,20], the fundamentals of gaining carbapenemase activity by oxacillinases to a large extend is still unknown.

Investigations on the structure of OXA-24 showed a hydrophobic cleft right above the active site that might be responsible for the preference of this enzyme for imipenem over oxacillin.[17] However, this hydrophobic cleft is not observed in OXA-48.[20]

Alignment of the Sequence of OXA-58 with those of OXA-24 and OXA-48 and its comparison with the sequence of OXA-10[21] indicates that the residues that are involved

with catalysis in OXA-10 are conserved in these carbapenem-hydrolyzing class D β-lactamases (Figure 1). According to the study that we have performed these carbapenem-hydrolyzing class D β-lactamases employ the same catalytic mechanism as OXA-10 and even in contrast to OXA-10 they are capable of hydrolyzing imipenem.

References

(1) Bonfiglio, G., Russo, G., and Nicoletti, G. Expert Opin. Investig. Drugs **2002**, 11:529–544.

(2) Testero, A., Fisher, J. F., and Mobashery, S. in Burger Medicinal Chemistry, Drug Discovery and Development (Abraham, D. J., and Rotella, D. P., eds) **2010,** 7th Ed., pp. 259–404, John Wiley & Sons, Inc., New York

(3) Ayan, M., R. Durmaz, E. Aktas, and B. Durmaz. *J. Hosp. Infect.* **2003**, 54:39-45.

(4) Landman, D., Quale, J. M., Mayorga, D., Adedeji, A., Vangala, K., Ravishankar, J., Flores, C., Brooks, S. *Arch. Intern. Med.* **2002**, 162:1515–1520.

(5) Livermore, D. M. *J. Antimicrob. Chemother.* **1998**, 41:25–41.

(6) Bush, K., and Jacoby, G. A. *Antimicrob. Agents Chemother.* **2010**, 54:969–976.

(7) Walsh, T. R. *Curr. Opin. Infect. Dis.* **2008**, 21:367–371.

(8) Poirel, L., Pitout, J. D., Nordmann, P. *Future Microbiol.* **2007**, 2, 501–512.

(9) Queenan, A. M., and Bush, K. *Clin. Microbiol. Rev.* **2007**, 20:440–458.

(10) Poirel, L., and Nordmann, P. *Clin. Microbiol. Infect.* **2006**, 12, 826–836.

(11) Marqué, S., Poirel, L., Héritier, C., Brisse, S., Blasco, M. D., Filip, R., Coman, G., Naas, T., and Nordmann, P. *J. Clin. Microbiol.* **2005**, 43, 4885–4888.

(12) Héritier, C., Dubouix, A., Poirel, L., Marty, N., Nordmann, P. *J. Antimicrob. Chemother.* **2005**, 55, 115–118.

(13) Zarrilli, R., Giannouli, M., Tomasone, F., Triassi, M., Tsakris, A. *J. Infect. Dev. Ctries.* **2009**, 3, 335–341.

(14) Walther-Rasmussen, J., and Høiby, N. *J. Antimicrob. Chemother.* **2006**, 57:373–383.

(15) Paton, R., Miles, R. S., Hood, J., Amyes, S. G., Miles, R. S., Amyes, S. G. *Int. J. Antimicrob. Agents* **1993**, 2:81–87.

(16) Higgins, P. G., Dammhayn, C., Hackel, M., and Seifert, H. *J. Antimicrob. Chemother.* **2010**, 65:233–238.

(17) Santillana, E., Beceiro, A., Bou, G., and Romero, A. *Proc. Natl. Acad. Sci. U.S.A.* **2007**, 104, 5354–5359.

(18) Bou, G., Santillana, E., Sheri, A., Beceiro, A., Sampson, J. M., Kalp, M., Bethel, C. R., Distler, A. M., Drawz, S. M., Pagadala, S. R., van den Akker, F., Bonomo, R. A., Romero, A., and Buynak, J. D. *J. Am. Chem. Soc.* **2010**, 132:13320–13331.

(19) Schneider, K. D., Ortega, C. J., Renck, N. A., Bonomo, R. A., Powers, R. A., Leonard, D. A. *J. Mol. Biol.* **2011**, 406:583–594.

(20) Docquier, J. D., Calderone, V., De Luca, F., Benvenuti, M., Giuliani, F., Bellucci, L., Tafi, A., Nordmann, P., Botta, M., Rossolini, G. M., Mangani, S. *Chem. Biol.* **2009**, 16, 540–547.

(21) Verma V., Testero, S. A., Amini, K, Wei, W, Liu J., Balachandran, N., Monoharan, T., Stynes, S., Kotra, L. P., Golemi-Kotra, D. *J. Biol. Chem.* **2011**, 286: 37292–37303.

(22) Golemi, D., Maveyraud, L., Ishiwata, A., Tranier, S., Miyashita, K., Nagase, T., Massova, I., Mourey, L., Samama, J. P., and Mobashery, S. *J. Antibiot.* **2000**, 53:1022–1027.

(23) Kitz, R. J., Ginsburg, S., and Wilson, I. B. *Biochem. Pharmacol.* **1967**, 16:2201–2209.

(24) Golemi-Kotra, D., Meroueh, S. O., Kim, C., Vakulenko, S. B., Bulychev, A., Stemmler, A. J., Stemmler, T. L., and Mobashery, S. *J. Biol. Chem.* 2004, 279:34665–34673.

(25) Herzberg, O., and Moult, *J. Science* **1987**, 236:694–701.

(26) Strynadka, N. C., Adachi, H., Jensen, S. E., Johns, K., Sielecki, A., Betzel, C., Sutoh, K., and James, M. N. *Nature* **1992**, 359:700–705.

(27) Lamotte-Brasseur, J., Dive, G., Dideberg, O., Charlier, P., Frére, J. M., Ghuysen, J. M. *Biochem. J.* **1991**, 279:213–221.

(28) Nukaga, M., Mayama, K., Hujer, A. M., Bonomo, R. A., and Knox, J. R. *J. Mol. Biol.* **2003**, 328:289–301

(29) Oefner, C., D'Arcy, A., Daly, J. J., Gubernator, K., Charnas, R. L., Heinze, I., Hubschwerlen, C., and Winkler, F. K. *Nature* **1990**, 343:284–288

(30) Dubus, A., Ledent, P., Lamotte-Brasseur, J., and Fre`re, J. M. *Proteins* **1996**, 25:473–485.

(31) Sun, T., Nukaga, M., Mayama, K., Braswell, E. H., and Knox, J. R. *Protein Sci.* **2003**, 12:82–91.

(32) Vercheval, L., Bauvois, C., di Paolo, A., Borel, F., Ferrer, J. L., Sauvage, E., Matagne, A., Fre`re, J. M., Charlier, P., Galleni, M., and Kerff, F. *Biochem. J.* **2010**, 432:495–504.

(33) Golemi, D., Maveyraud, L., Vakulenko, S., Samama, J. P., Mobashery, S. *Proc. Natl. Acad. Sci. U.S.A.* **2001**, 98:14280–14285.

(34) Golemi, D., Maveyraud, L., Vakulenko, S., Tranier, S., Ishiwata, A., Kotra, L. P., Samama, J. P., and Mobashery, S. *J. Am. Chem. Soc.* **2000**, 122:6132–6133.

(35) Maveyraud, L., Golemi-Kotra, D., Ishiwata, A., Meroueh, O., Mobashery, S., and Samama, J. P. *J. Am. Chem. Soc.* **2002**, 124, 2461–2465.

(36) Maveyraud, L., Golemi, D., Kotra, L. P., Tranier, S., Vakulenko, S., Mobashery, S., and Samama, J. P. *Structure* **2000**, 8:1289–1298.

(37) Chen, Y., McReynolds, A., and Shoichet, B. K. *Protein Sci.* **2009**, 18:662–669.

(38) Swarén, P., Golemi, D., Cabantous, S., Bulychev, A., Maveyraud, L., Mobashery, S., and Samama, J. P. *Biochemistry* **1999**, 38, 9570–9576.

(39) Miyashita, K., Massova, I., Taibi, P., and Mobashery, S. *J. Am. Chem. Soc.* **1995**, 117:11055–11059.

(40) Maveyraud, L., Massova, I., Birck, C., Miyashita, K., Samama, J. P., and Mobashery, S. *J. Am. Chem. Soc.* **1996**, 118, 7435–7440.

(41) Mourey, L., Miyashita, K., Swaren, P., Bulychev, A., Samama, J. P., and Mobashery, S. *J. Am. Chem. Soc.* **1998**, 120:9382–9383.

(42) Nagase, T., Golemi, D., Ishiwata, A., and Mobashery, S. *Bioorg. Chem.* **2001**, 29:140–145.

(43) Yang , J., Jamei, M., Rowland Yeo, K., Tucker, G.T., Rostami-Hodjegan, A., *Eur. J. Pharm. Sci.* **2005**, 26:334–340.

Figures

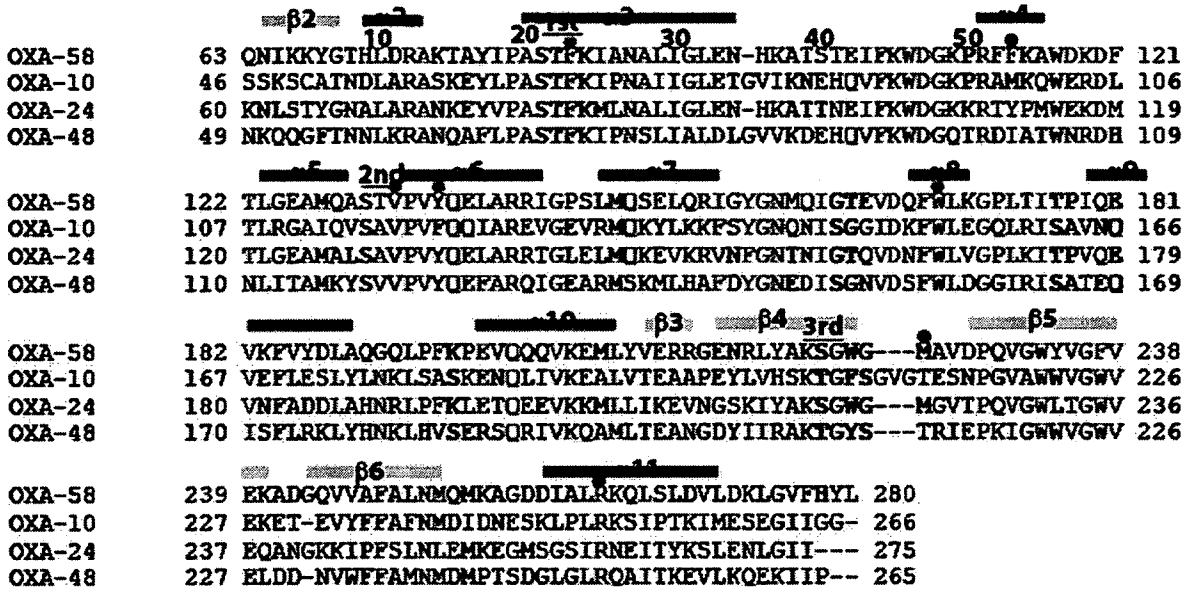

Figure 1. Sequence alignment of OXA-58 with OXA-10, OXA-24, and OXA-48. Highlighted in *red* are the three conserved motifs in serine β-lactamases. The *green dots* indicate the residues that form the hydrophobic cleft around the conserved lysine residue. The *blue dots* indicate the residues that form the hydrophobic cleft in OXA-24. The secondary structures correspond to those predicted by the OXA-58 homology model. (Prepared by Dr. Golemi-Kotra)

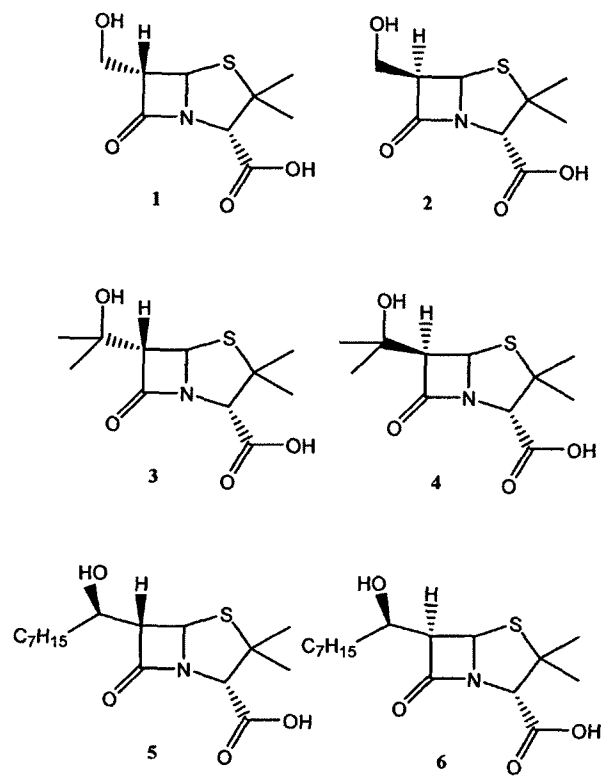

Figure 2 The structure of penicillinate derivatives

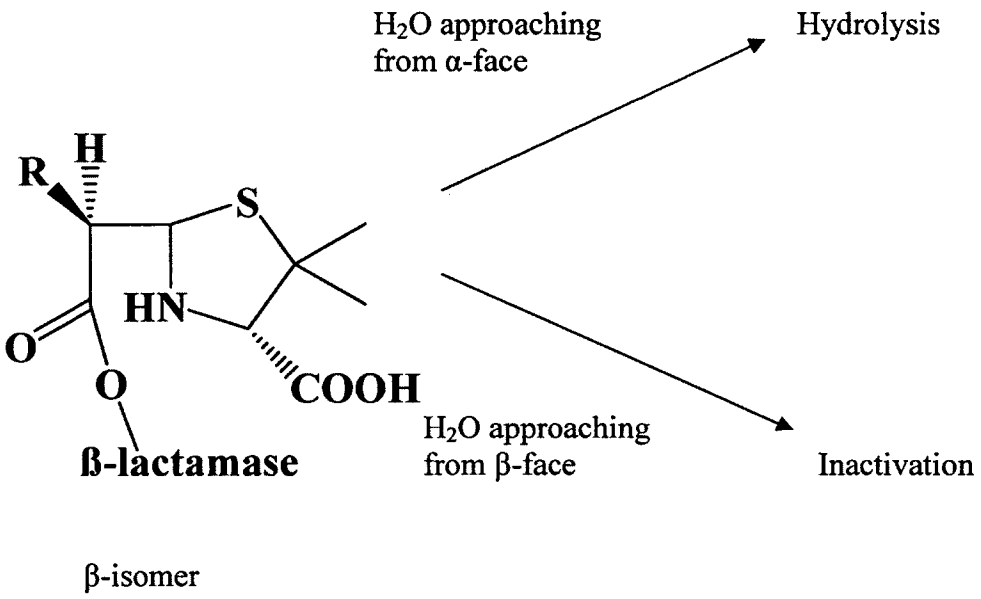

Figure 3. Schematic presentation of the process of studying the mechanism of hydrolysis of β-lactamases by penicillinates.

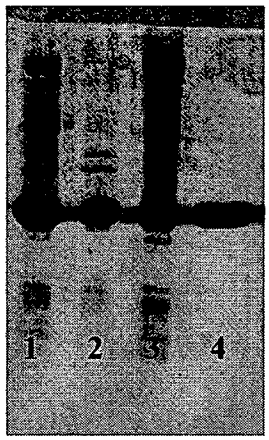

Figure 4. Isolation and purification of OXA-58 to homogeneity. 12.5% SDS-polyacrylamide gel stained with Coomassie Blue. Lane 1, cell extract after sonication. Lane 2, pellet collected after centrifugation. Lane 3, supernatant obtained after centrifugation, Lane 4, OXA-58 after purification with a SP-Sepharose column.

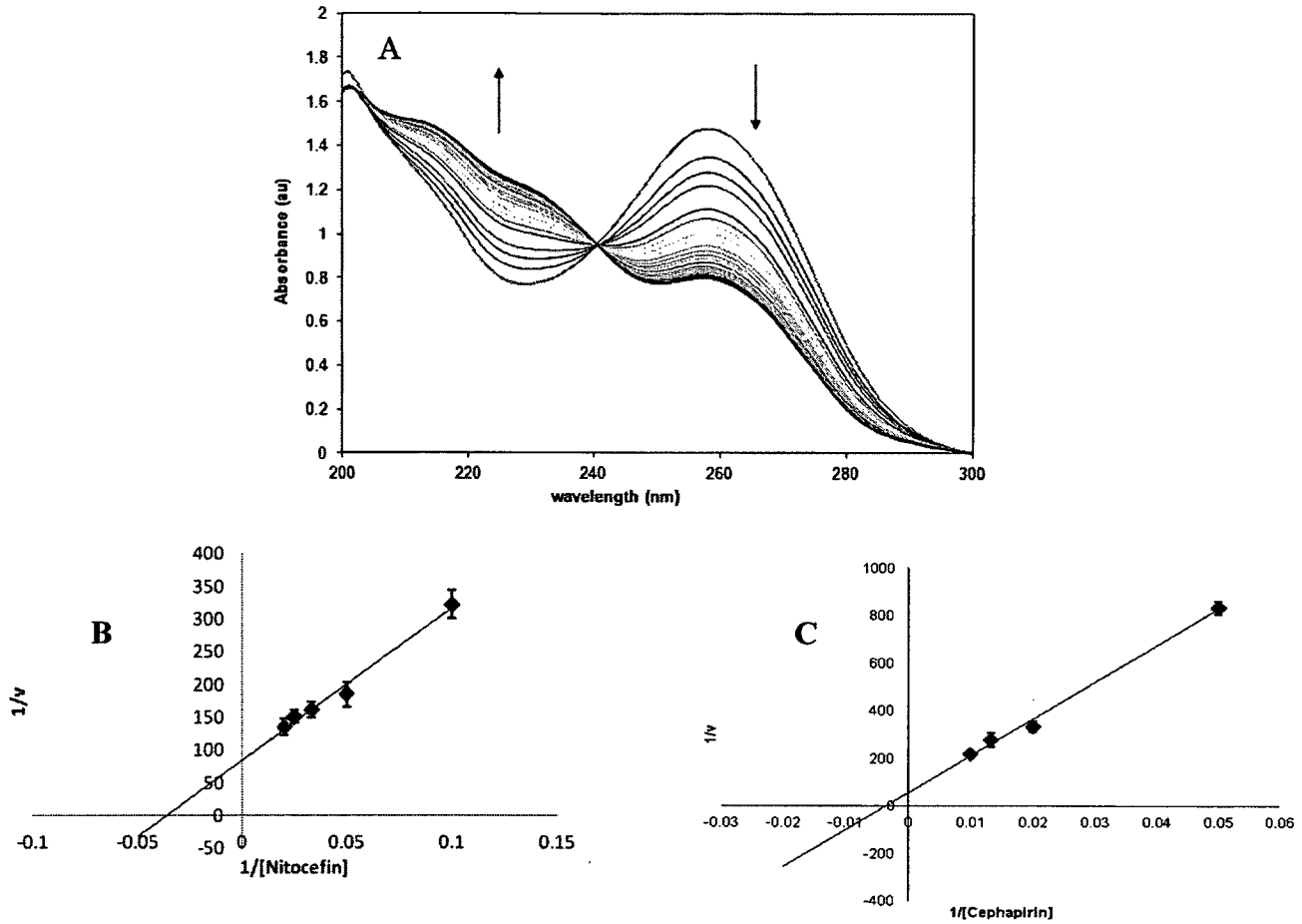

Figure 5. (A) UV-Vis spectral profile for the hydrolysis of cephapirin at 100 μM by 100 nM OXA-58. The hydrolysis progress curves were obtained by monitoring at 260 nm. Lineweaver-Burk plots for the extraction of kinetic parameters for the hydrolysis of (B) nitrocefin and (C) cephapirin by OXA-58.

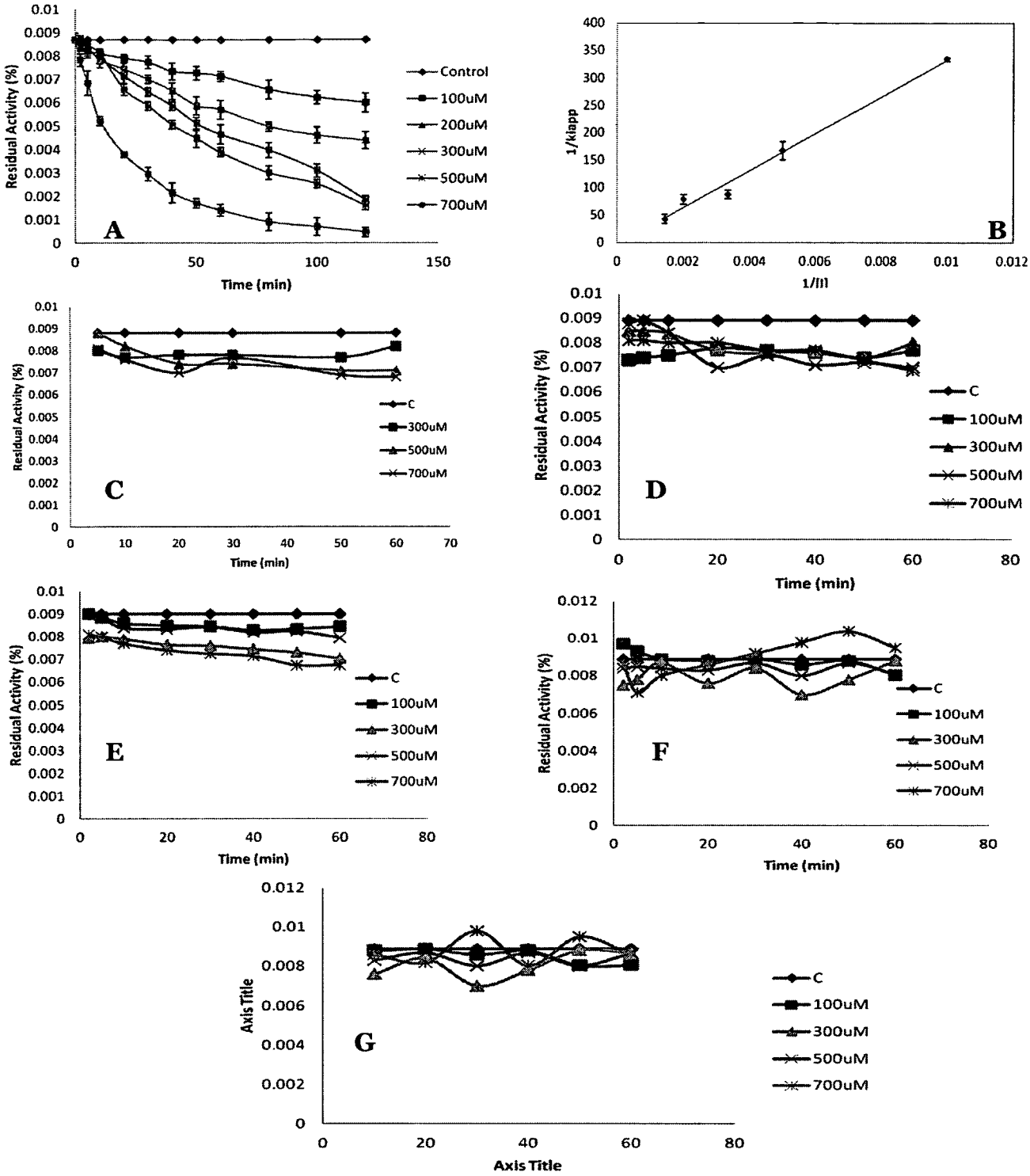

Figure 6-1. Graphical representations of the experimental procedure for inactivation studies. (A) Time- and concentration-dependent inactivation of enzyme by compound 5. (B) The Kitz–Wilson plot, of the observed inactivation rate constant (k_{obs}) as a function of compound 5 concentration ([I]). Graphs for monitoring residual activity (%) of OXA-58 versus time (min) in the presence of different concentrations of (C) compound 6, (D) compound 3, (E) compound 4, (F) compound 1 and (G) compound 2.

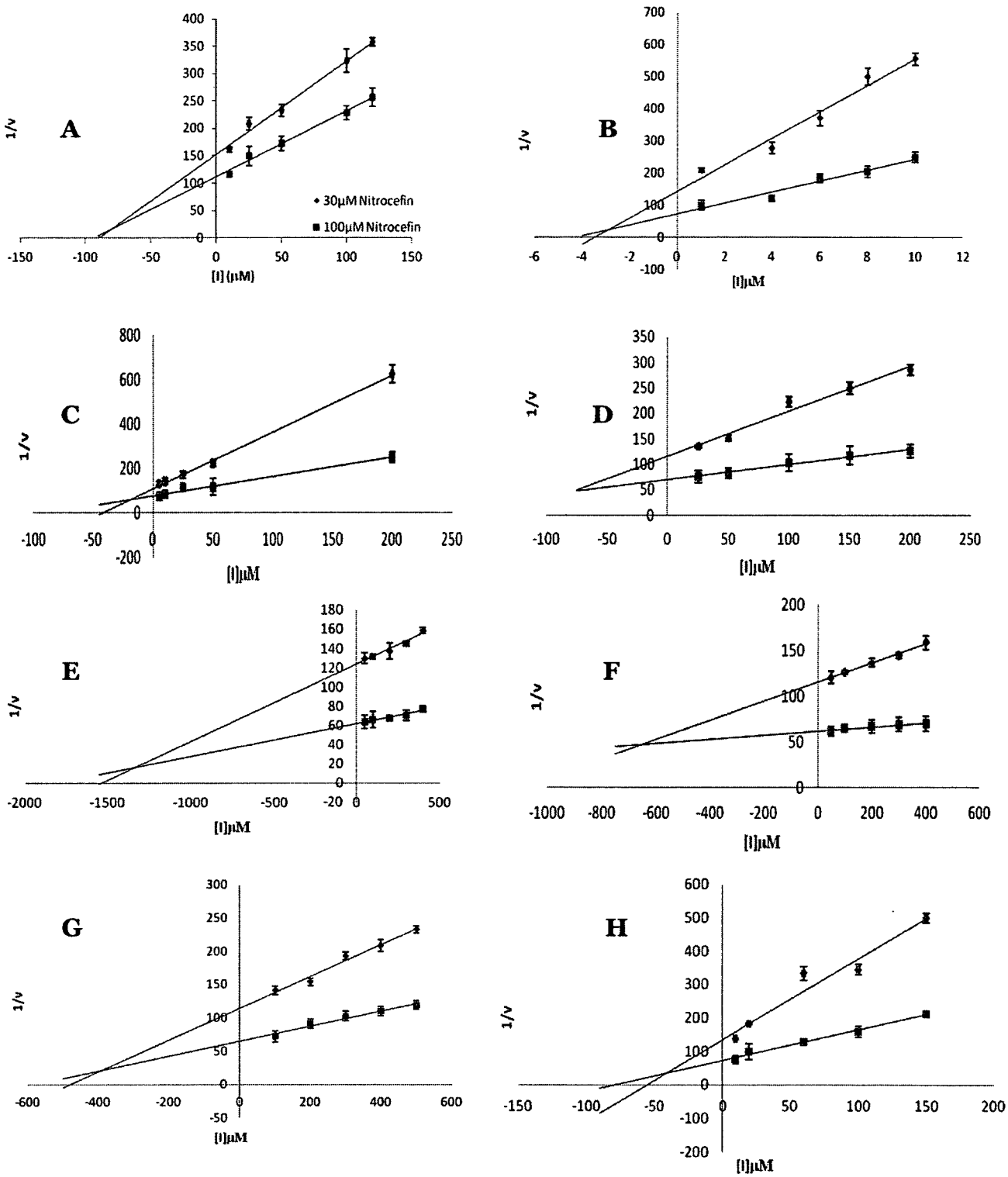

Figure 6-2. Dixon plot obtained for the competitive inhibition of (A) carbenicillin, (B) Imipenem, compounds (C) 1, (D) 2, (E) 3. (F) 4, (G) 5 and (H) 6 on the activity of OXA-58 using nitrocefin as a reporter substrate at 30 and 100 µM.

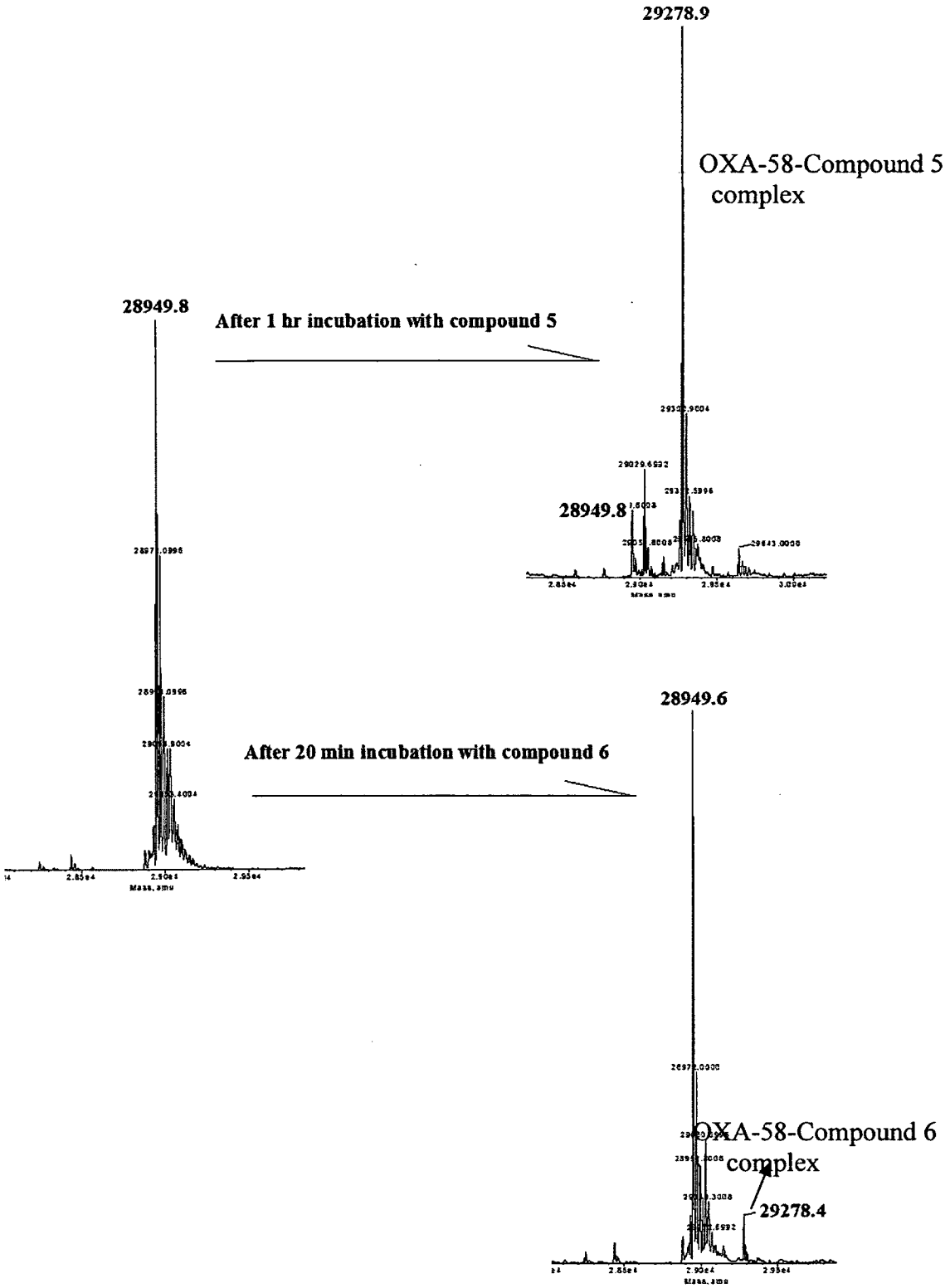

Figure 7. Examination of OXA-58 inactivation by compounds 5 and 6 with ESI-MS. In these experiments OXA- 58 at 110 μM was incubated with compounds 5 or 6 at 5 mM for 1 h or 20 min, respectively, in 50mM sodium phosphate, pH 7.0, at room temperature. The mixtures were desalted and subjected to ESI-MS for analysis.

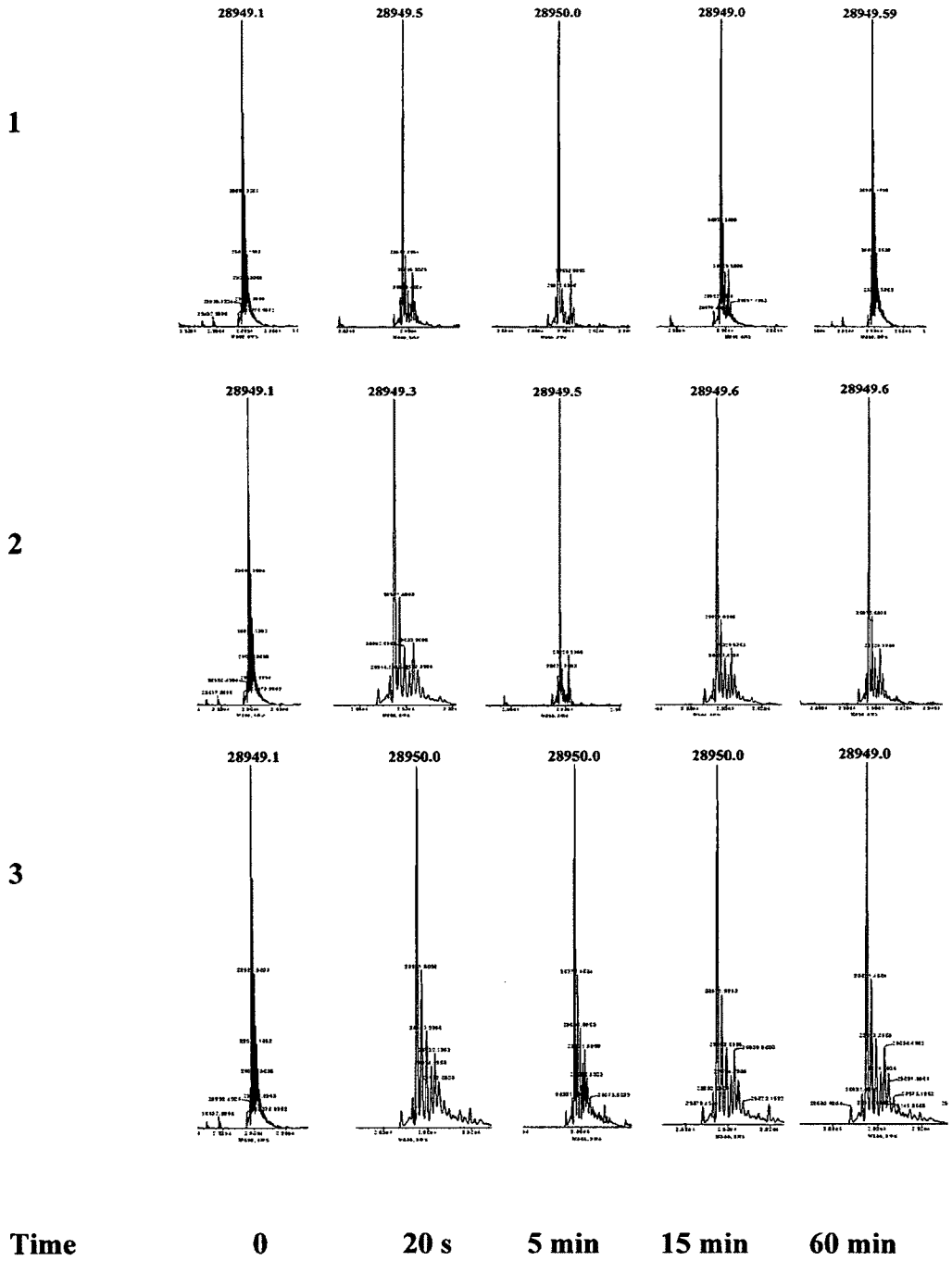

Figure 8. Examination of the interaction of OXA-58 and compounds 1, 2 and 3 with ESI-MS. In this experiment OXA- 58 at 110 μM was incubated individually with compounds 1, 2 and 3 at 5 mM for 1 h, in 50mM sodium phosphate, pH 7.0, at room temperature. At different time intervals samples were taken, the mixture was desalted and subjected to ESI-MS for analysis.

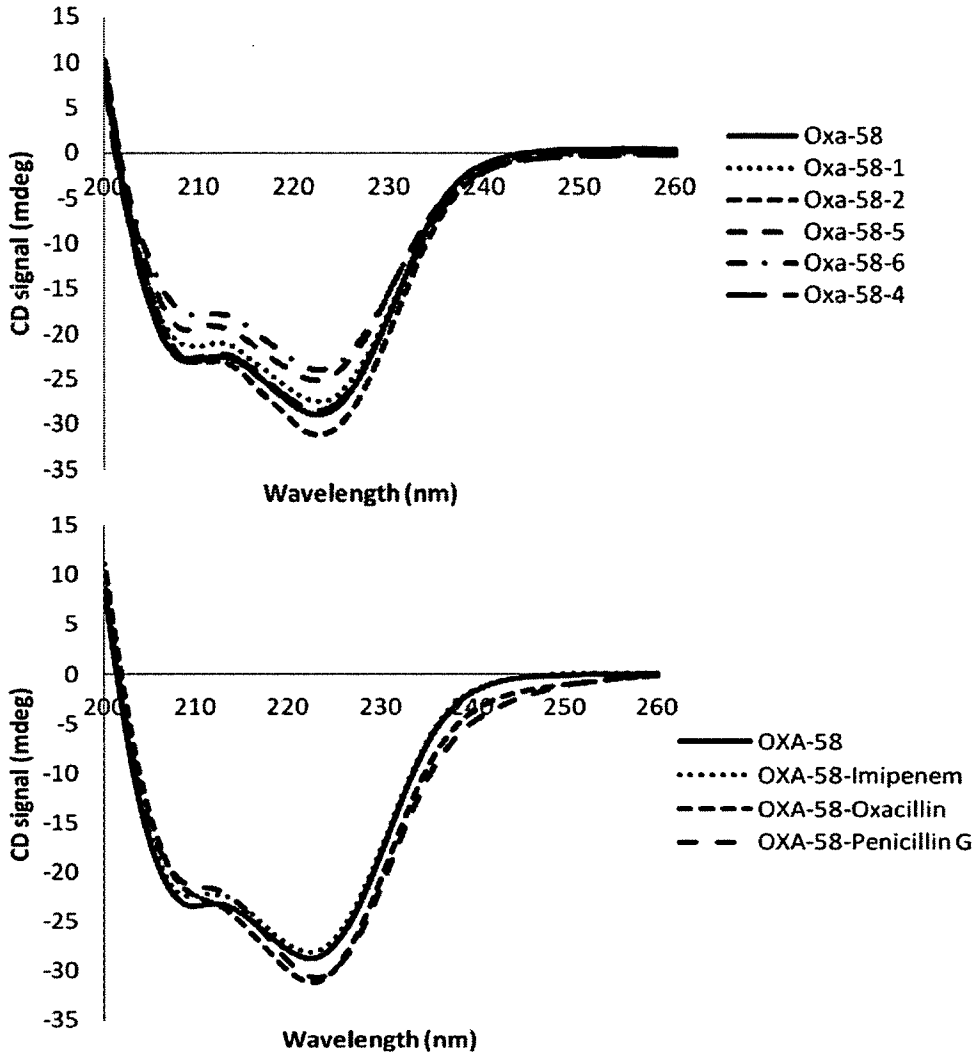

Figure 9. Effect of different β-lactams on the structure of OXA-58 investigated by CD. In these experiments OXA-58 at 10 μM was incubated with 100 μM of each β-lactam individually and the CD spectrum was acquired immediately.

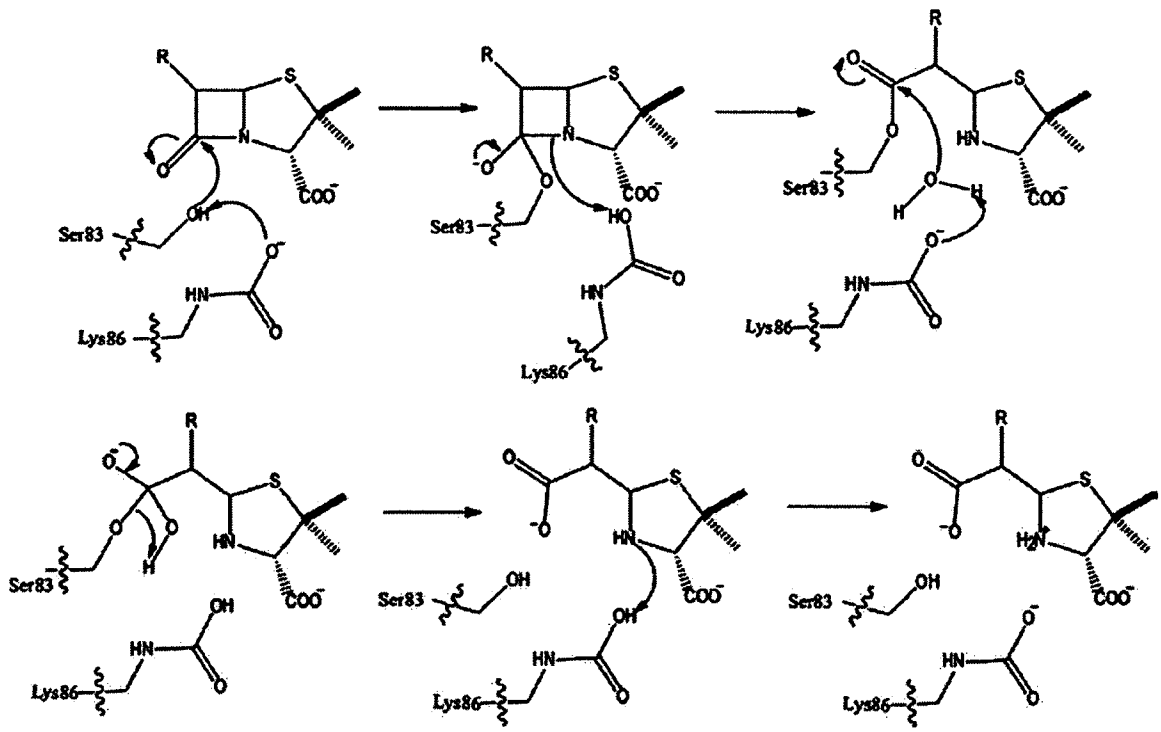

Figure 10. General catalytic mechanism of OXA-58 (Prepared by Dr. Golemi-Kotra)

Tables

Table 1 Kinetic parameters for the hydrolysis of nitrocefin and cephapirin by OXA-58

Substrate	K_m (μM)±*SD*	K_{cat} (s^{-1})±*SD*	K_{cat}/K_m ($\mu M^{-1} s^{-1}$)
Nitrocefin	21±2	99±8	4.7
Cephapirin	262±18	22±1	0.08

Table 2 Kinetic parameters of inactivation

Inhibitor	k_{inact}***±SD*** (min^{-1})	K_I***±SD***(μM)
1	N/A	N/A
2	N/A	N/A
3	N/A	N/A
4	N/A	N/A
5	0.22±0.01	7804±366
6	N/A	N/A

Table 3 Competitive inhibition of OXA-58 by different inhibitors at 25°C and pH 7

Inhibitor	***K_I±SD (μM)***
1	29 ± 4
2	82 ± 3
3	644 ±8
4	1276 ± 58
5	404 ± 10
6	42 ± 1
Imipenem	3.1 ± 0.2
Carbenicillin	78 ± 2

Chapter Three: Elucidation of the role of active site lysine residue (Lys86) in catalytic activity of OXA-58

3.1 Introduction

3.1.1 The involvement of a crucial carbamylated lysine residue in the catalytic mechanism of OXA-58

One of the characteristics of the catalytic mechanism of class D β-lactamases is employment of the same residues for both acylation and deacylation steps of hydrolysis.[1] In addition, all these enzymes use a carbamylated lysine residue which is of central significance for catalysis (Figure 1). Studies on different β-lactamases suggest that this carbamylated lysine residue is responsible for activation of both the active site serine for acylation by the substrate and the hydrolyzing water molecule in the deacylation step of the hydrolysis mechanism.[2]

Carbamylated lysine has also been reported in some other proteins such as rubisco[3], urease [4] and phosphotriesterase.[5] In most of these proteins the carbamylated lysine plays the role of a ligand for a metal ion.

In class D β-lactamases carbamylated lysine is the general base that activates the hydroxyl group of the active site serine residue to get acylated by the substrate. According to a study performed previously in our lab by UV-visible spectrophotometry, replacement of this residue with an alanine leads to practical inactivation of the enzyme.[6] However, here we have shown that OXA-58 still is capable of hydrolyzing β-lactams

without the critical carbamylated lysine residue and also investigated the effect of absence of the carbamylated lysine on the catalytic activity of OXA-58.

3.2 Experimental section

Materials and methods

All chemicals and antibiotics were purchased from Sigma-Aldrich (St. Louis, MO, USA) or Fisher (Fairlawn, NJ, USA) unless otherwise stated. Growth media were purchased from EMD Biosciences (Mississauga, Ontario, Canada). Chromatography media and columns were purchased from GE Healthcare (Chalfont St. Giles, Buckinghamshire, UK). *Escherichia coli Nova Blue* and BL21 (DE3) strains and cloning and expression plasmids were purchased from Novagen (Mississauga, Ontario, Canada).

3.2.1 Circular dichroism spectroscopy

The far-UV CD spectra of OXA-58 and OXA-58 K86A (10 μM) were recorded using a Jasco J-810 instrument. All measurements were carried in 50 mM sodium phosphate buffer, pH 7.0, in a rectangular cuvette with a path length of 0.1 cm. The volume of the cell was 200 μL. Spectra were recorded from 260 to 200 nm at a scan rate of 10 nm/min and a 1.0-nm bandwidth, at 20 °C. All spectra were corrected for buffer as appropriate.

3.2.2 Cibacron blue 3GA titrations

Tryptophan fluorescence quench of OXA-58 and OXA-58 K86A by Cibacron Blue 3GA was conducted in a Cary Eclipse fluorescence spectrophotometer (Varian Inc., Palo Alto, CA, USA). The fluorescence spectra of OXA-58 and OXA-58 K86A (1 μM) were acquired in the presence of increasing concentrations of Cibacron Blue from 0.5 to 6 μM

in 50 mM sodium phosphate buffer pH 7.0. The fluorescence (F_I) was fit to the equation below:

$$F_I = F_{max} - F_{change}\{[\text{Cibacron Blue}] / (K_d + [\text{Cibacron Blue}])\}$$

where F_{max} is the initial fluorescence intensity, F_{change} is the total fluorescence quench, and K_d is the dissociation constant.[7] The excitation wavelength was 295 nm and the emission was recorded at 345 nm.

3.2.3 Tryptophan fluorescence quenching experiments

All the experiments were performed at room temperature. Quenching experiments with different β-lactams were performed by addition of aliquots of β-lactam solutions (25 or 10 mM) into the wild type OXA-58 and OXA-58 K86A solutions. These experiments were performed to probe the interaction of the enzyme with the β-lactams. The final concentration of the enzyme was 1 μM and that of β-lactams were, 0.5 to 27 mM for penicillin G, carbenicillin, ampicillin and oxacillin, 0.5 to 6 mM for amoxicillin and 25 to 100 μM for imipenem. The assay volume was 150 μL. The experiments were performed in 50 mM sodium phosphate buffer (pH 7.0). The excitation wavelength was set at 295 nm, and the fluorescence emission spectra were scanned from 300 to 400 nm. A cuvette with a path length of 1 cm was used. The effect of presence of different β-lactams on the variation of the fluorescence intensity of the proteins (1 μM for carbenicillin and 0.5 to 3 μM for penicillin G, ampicillin, oxacillin and amoxicillin) as a function of time time was investigated by monitoring the intensity at 345 nm in the presence of different β-lactams (0.5 to 27 mM carbenicillin (For 0 and 0.5 mM at 345 nm, for 1 mM at 350 nm, for 3 at

355 nm, for 6 and 8 mM at 360 nm and for 12,18 and 27 mM at 365 nm), 2 to 10 mM penicillin G (at 345 nm) and ampicillin (at 345 nm), 0.5 to 8 mM for oxacillin (at 345 nm) and 2 to 6 mM for amoxicillin (at 345 nm)) for up to 5 min in 50 mM sodium phosphate buffer.

Quenching titrations with acrylamide were performed by addition of aliquots of concentrated acrylamide solution (100 mM) into the enzyme solution in the absence and presence of one or two different concentrations of each β-lactam. The final concentration of the proteins was 1 μM and that of the β-lactams was 1 and 6 mM for carbenicillin, 1 and 12 mM for penicillin G, 50 μM for imipenem and 1 or 2 mM for the rest of the β-lactams. The experiments were performed in 50 mM sodium phosphate buffer. The fluorescence quenching data in the presence of acrylamide were first analyzed by the Stern-Volmer equation which has been presented below:[8]

$$F/F_0 = 1 + K_{sv}[Q]$$

where F_o and F are the fluorescence intensities (at 345 nm) in the absence and presence of the quencher (β-lactam), respectively. K_{sv} is the Stern-Volmer constant, and [Q] is the concentration of the quencher. Also, the fluorescence intensity of OXA-58 and OXA-58 K86A was monitored by time in the presence of different β-lactams. These experiments were performed at different concentrations of β-lactams and each protein.

3.2.4 Investigation of the binding affinity of Bocillin for OXA-58 K86A

Acyl-enzyme species formed between OXA-58 K86A and different β-lactams were detected using the fluorescent substrate BOCILLIN FL (Invitrogen, Carlsbad, CA). For K_d with BOCILLIN FL, OXA-58 K86A was incubated at 1 μM with different

concentrations (0 to 20 μM) BOCILLIN FL in 50 mM sodium phosphate buffer pH 7.0, for 30 s. The reaction volume was 25 μL. Following the incubation the reaction was stopped by addition of 10 μl SDS loading dye and the 20 μL of samples were loaded on a 12.5 % SDS-PAGE. The gel was scanned using a Typhoon Trio+ Variable Mode Imager (GE Healthcare) at 488 nm excitation and 520 nm emission. The gel images were analyzed using ImageJ software (NIH, USA). The Fluorescence (F_{obs}) was fitted using the hyperbolic equation below as the K_d for OXA-58 K86A and Bocillin was close to the concentration of protein:

$$F_{obs}=F_0+(F_{max}-F_0)(1/2P_t)[(K_d+P_t+L_t)-(((K_d+P_t+L_t)^2-4K_dL_t)^{1/2}]$$

where F_{obs} is the intensity observed, P_t is the concentration of receptor, L_t is the concentration of the ligand, F_{max} is the maximum fluorescence intensity, F_0 is the background fluorescence and K_d is the dissociation constant.[9,10]

3.2.5 Determination of the acylation (k_2) and deacylation (k_3) rate constants

For the acylation rate constant of the acyl-enzyme species formed between carbenicillin and OXA-58 K86A, cabenicillin at 64 μM was incubated with 1 μM of OXA-58 K86A and at different time intervals (0 to 60 min) a 25 μL aliquot was taken and BOCILLIN FL at final concentration of 10 μM was added to it and the solution was further incubated for 30 s and then the reaction was stopped by addition of SDS sample buffer (composed of 50 mM Tris-HCl pH 6.8,. 2% SDS, 10% glycerol, 1% β-mercaptoethanol, 12.5 mM EDTA, 0.02 % bromophenol blue). All samples were loaded on a 12.5% SDS-PAGE. The gel was imaged using a Typhoon Trio$^+$ Variable Mode Imager (GE Healthcare) at 488 nm excitation and 520 nm emission. The gel images were

analyzed using ImageJ software (NIH, USA). The fluorescence (F_I) was fitted using the equation below:

$$F_I = F_{base} + F_{max}e^{kt}$$

where k is the acylation rate constant (k_2), F_{max} is fluorescence intensity at time zero, and F_{base} is the background fluorescence.

For the deacylation rate constant of the acyl-enzyme species formed between OXA-58 K86A and BOCILLIN FL, the protein (3 μM) was incubated with 50 μM BOCILLIN FL for 30 s and was desalted using Zeba mini centrifugal columns (Pierce, Rockford, IL, USA) equilibrated with 50 mM sodium phosphate buffer pH 7.0, to remove the excess of BOCILLIN FL. At different time intervals (30 s to 20 min) 25 μL aliquots were taken and the reaction was quenched by addition of 10 μL SDS sample buffer. All samples were loaded on a 12.5% SDS-PAGE. The gel was imaged using a Typhoon Trio$^+$ Variable Mode Imager (GE Healthcare) at 488 nm excitation and 520 nm emission. The gel images were analyzed using ImageJ software (NIH, USA). The fluorescence (F_I) was fitted using the equation below:

$$F_I = F_{base} + F_{max}e^{-kt}$$

where k is the deacylation rate constant (k_3), F_{max} is fluorescence intensity at time zero, and F_{base} is the background fluorescence.

3.2.6 Determination of half maximal inhibitory concentrations (IC_{50}) of different β-lactams with OXA-58 K86A

OXA-58 K86A at 1 μM was individually incubated with 5 to 400 μM penicillin G, ampicillin, amoxicillin or carbenicillin or with 1 to 8 mM oxacillin, cephalothin and imipenem for 2 min and then BOCILLIN FL at final concentration of 10 μM was added to the incubation solution and the samples were further incubated for 30 s. The volume of all reaction mixtures was 25 μL. Following the incubations SDS sample buffer was added to each sample to stop the reaction. The samples were loaded on a 12.5 % SDS-PAGE and the gel was illuminated using a Typhoon Trio+ Variable Mode Imager (GE Healthcare) at 488 nm excitation and 520 nm emission. The gel images were analyzed using ImageJ software (NIH, USA). The data obtained were fitted using the GraFit software to the equation below:

$$\text{Bound} = ([L].\text{Capacity}) / (IC_{50} + [L])$$

where Bound is the amount bound which is directly proportional with the fluorescence intensity, L is the concentration of the β-lactam and capacity is the binding capacity.

3.2.7 Study of the turnover of different β-lactams by OXA-58 K86A

The hydrolytic catalytic activity of OXA-58 K86A on different β-lactams was studied by detection of the BOCILLIN FL bound to the mutant enzyme. OXA-58 K86A at 1 μM was incubated individually with 64 μM of penicillin G, amoxicillin, carbenicillin or imipenem and 1 mM of cephalothin and at different time intervals (1 to 120 min) BOCILLIN FL at a final concentration of 10 μM was added to the samples and further incubated for 30 s and then the reaction was quenched by addition of SDS loading dye. The samples were loaded on a 12.5 % SDS-PAGE and the gel was scanned at 488 nm

excitation and 520 nm emission. The gel images were analyzed using imageJ software (NIH, USA).

3.2.8 Electrospray ionization mass spectrometry

OXA-58 K86A at a concentration of 10 μM in 50 mM sodium phosphate, pH 7.0, was incubated individually with 200 μM BOCILLIN FL for 1 min and 800 μM carbenicillin for 1 hour at room temperature. The volume of the reaction mixtures in both cases was 100 μL. The mixture was then desalted using Zeba mini centrifugal columns (Pierce, Rockford, IL, USA) equilibrated with 50 mM sodium phosphate buffer pH 7.0. Then the reaction was stopped immediately by addition of 10 % final concentration of trichloroacetic acid and the protein precipitate was separated by centrifugation at 18000 × g for 5 min and dissolved in 10 μL water and frozen at -20 °C. The samples were sent for analysis in the Advanced Protein Technology Centre, The Hospital for Sick Children (Toronto, Ontario, Canada) on an Applied Biosystems/MDS Sciex API QSTAR XL Pulsar mass spectrometer.

3.4 Results and discussion

3.4.1 Kinetics of OXA-58 K86A

Half maximal inhibitory concentrations (IC_{50}) for different β-lactams were extracted using BOCILLIN FL as a reporter substrate for OXA-58 K86A (Table 1, Figures 2 and 3). BOCILLIN FL is a fluorescent penicillin β-lactam which acylates OXA-58 K86A. Formation of the acyl-enzyme species between OXA-58 K86A and BOCILLIN FL was also confirmed using ESI-MS (Figure 4). IC50 values for penicillin G, ampicillin, amoxicillin and carbenicillin were in μM range (Figure 2) however,

oxacillin, cephalothin and imipenem interacted with OXA-58 K86A with mM range IC50s (Figure 3 and Table 1). The dissociation constant (K_d) for BOCILLIN FL with OXA-58 K86A was determined to be 1.05 ± 0.03 μM.

Investigation of the hydrolysis of penicillin G and amoxicillin by OXA-58 K86A using BOCILLIN FL as the reporter substrate (Figure 5) showed a dramatic decrease in the reaction rate in comparison to the wild-type OXA-58. Although these penicillins undergo fast acylation by mutant enzyme, deacylation of the acyl-enzyme species happens very slowly. This is observed in the case of the hydrolysis of BOCILLIN FL. The deacylation rate constant (k_3) of OXA-58 K86A-BOCILLIN FL was determined to be 0.0056 ± 0.001 s^{-1} (Figure 6). However, penicillins are still hydrolyzed better than the member of carbapenem group, imipenem. Only ~ 20 % recovery in the activity of enzyme was observed after 24 hrs of elimination of the extra imipenem from the acyl-enzyme solution by desalting using Zeba minicentrifugal columns (Pierce, Rockford, IL, USA). For cephalothin, as a member of the cephalosporin group no significant hydrolysis was observed (Figure 5). The ~ 20 % decrease in the intensity which was not recovered for up to 3 hrs is probably due to the competitive inhibition of cephalothin on the activity of OXA-58 K86A. In spite of the fact that carbenicillin acylated OXA-58 K86A rapidly (Figure 7), the deacylation of the acyl-enzyme species happened very slowly and full recovery of enzyme activity (n the case of incubation of 64 μM carbenicillin with 1 μM OXA-58 K86A) was observed after 24 hrs. The ability of carbenicillin to acylate OXA-58 K86A was also assessed by ESI-mass spectrometry (Figure 8).

3.4.2 Evaluation of the effect of mutation on the active site shape

To ensure that the significant decrease in hydrolytic activity was not caused by the misfolding of the mutant (OXA-58 K86A) or a change in the active site shape, fluorescence spectroscopy was used to observe the binding of the known class D active site probe, Cibacron Blue 3GA to the wild type and mutant protein. This anthraquinone dye has already been proven to be a strong ligand to probe the proper active site formation in class D β-lactamase mutants.[7] The quenching effect of this dye on wild type OXA-58 and OXA-58 K86A fluorescence was observed. This hydrophobic dye was previously shown to bind specifically to the active site of other class D β-lactamases (OXA-1 and OXA-2) with low micromolar affinities and also quench the wild-type OXA-1 tryptophan emission.[7] We found that Cibacron Blue 3GA also quenched wild-type OXA-58 and OXA-58 K86A fluorescent emissions with a large magnitude. No significant shift in the wavelength of maximal emission was seen. The K_d values were calculated to be 3.4 ± 0.2 μM and 4.0 ± 0.4 μM for the wild type OXA-58 and OXA-58 K86A mutant respectively by fitting the fluorescence intensity as a function of the concentration of cibacron blue to an inverted hyperbola single-site model (Figure 9). This indicates that the affinity of Cibacron Blue with OXA-58 K86A is similar to OXA-58. These results show that the mutant (K86A) forms an active site structurally similar to that of the wild-type enzyme.

3.4.3 Tryptophan fluorescence quenching studies

Under the conditions described in the experimental section, good fluorescence spectra for both OXA-58 and OXA-58 K86A were obtained. A regular decrease in the fluorescence intensity of both wild type and mutant enzyme was observed by increasing

concentrations of different β-lactams. Among the β-lactams studied, carbenicillin and penicillin G caused a red shift in the emissions of OXA-58 and OXA-58 K86A which indicates that the side chain of the tryptophan residue(s) responsible for fluorescence intensity is located in a polar microenvironment in the presence of this β-lactam (Figure 10). In the case of the wild type enzyme carbenicillin caused the red shift at concentrations as low as 0.5 mM, however only at 3mM and above it could cause a red shift in the fluorescence spectrum of the K86A mutant of OXA-58. The red shift caused by penicillin G was only observed at 8 mM and above for both wild type and K86A mutant. Other β-lactams quenched the fluorescence emission of these proteins without any shift (Figure 11). Figure 12 illustrates a comparison of the effect of carbenicillin, penicillin G and imipenem on the fluorescence emissions of wild type OXA-58 and OXA-58 K86A mutant. Although the fluorescence emission of the OXA-58 K86A mutant was quenched slightly more than that of the wild type protein by carbenicillin, in general, carbenicillin and penicillin G had similar quenching effects on both the wild type OXA-58 and OXA-58 K86A mutant. However, imipenem quenched the fluorescence of wild type enzyme more efficiently that the K86A mutant. Another technique, tryptophan emission quenching by acrylamide[11], was used to further analyze the events that occurred upon binding of β-lactams to the wild type OXA-58 and the OXA-58 K86A mutant. The Stern-Volmer plots were obtained to determine the solvent accessibility of Trp residue responsible for the fluorescence intensity (Figure 13). These plots displayed linear trends in the absence and presence of penicillin G, indicating that acrylamide molecules directly contact the indole group of Trp-158.[11] The calculated Stern-Volmer constants (K_{SV}) value

decreased in the presence of all β-lactams except imipenem (Table 2), indicating a decrease in solvent accessibility of the Trp residue responsible for fluorescence intensity in the presence of these β-lactams. However, in the presence of imipenem an increase in solvent accessibility is observed. Acrylamide quenched the fluorescence intensity of wild type and K86A mutant of OXA-58 with comparable efficiencies. The results obtained can be taken as evidence that β-lactam binding to both wild type OXA-58 and OXA-58 K86A mutant affects the tertiary structure of these proteins (and also in a similar way) as well.

When monitoring the fluorescence intensity of the wild type OXA-58 as a function of time time in the presence of different β-lactams, we surprisingly observed a sudden increase in the fluorescence intensity at a certain point in time which seemed to be the inactivator of a certain step of hydrolysis (Figure 14, 15, 16 and 17). The time at which this sudden increase in fluorescence intensity happened was found to be dependent upon the concentrations of the substrate (β-lactam) and the protein. Increasing concentrations of the substrate caused a delay in the sudden fluorescence intensity increase. In contrast, when higher concentrations of protein were employed the sudden increase in fluorescence intensity happened earlier. Also fluorescence intensity of wild type OXA-58 did not show any increase with time during its interaction with carbenicillin (The previous studies by Dr. Verma of Golemi-Kotra lab showed no hydrolysis of carbenicillin by OXA-58 [6] however, here in this studies carbenicillin was hydrolyzed). No sudden increase was observed as well for the florescence intensity of the mutant enzyme OXA-58 K86A in 5 min, when interacting with penicillin G; the hydrolysis of 64 μM penicillin

G takes place in 1 hour by 1 μM OXA58K86A. In these experiments a higher concentration of penicillin G (2 mM) has been used which will increase the hydrolysis time. All these reinforced the hypothesis that this phenomenon may pertain to a conformational change in the protein which happens at a certain stage of hydrolysis. Investigation of the hydrolysis of penicillin G at different concentrations of substrate and protein shows that the sudden increase in the fluorescence intensity happens when the hydrolysis is completed. A possible theory could be that, the fluorescence emission of the protein is quenched due to the conformational changes caused by the binding and interaction of β-lactam and when the substrate is hydrolyzed, the protein returns to its previous conformation and the fluorescence intensity is recovered (Figures. 14,15,16, 17 and 18). To investigate whether the sudden increase happens due to the β-lactam hydrolysis, wild type OXA-58 at 20 nM was added to the incubation solution of OXA-58 K86A and penicillin G to remove the unreacted penicillin G. Under these conditions, sudden increase in the fluorescence intensity of K86A mutant was observed which reinforces the idea that this phenomenon happens at the end of hydrolysis (Figure 19). The fluorescence intensity is not fully recovered which might be due to a non-covalent interaction between the hydrolyzed product of the β-lactam with the protein. In the presence of carbenicillin and imipenem, no recovery of the fluorescence of either OXA-58 or K86A mutant was observed during 5 min observation (Figure 18).

3.4.4 Circular dichroism spectroscopy

Comparison of the CD spectra of OXA-58 and OXA-58 K86A shows that no significant change is introduced to the structure of the protein due to the mutation. Also, the thermal melting of the wild type OXA-58 and K86A mutant did not show a significant change in the melting point (i.e. the stability) of the protein because of mutation (melting point for the wild type and K86A mutant were 57 and 59 respectively) (Figure 20).

Using the Lys86Ala mutant we were also able to study the interactions of OXA-58 K86A and different β-lactams by following the acyl-enzyme species formed between the enzyme and the β-lactam.

Both acylation and deacylation rates can be influenced by elimination of the general base of a β-lactamase.[12] Acyl-enzyme intermediate accumulation in Lys86Ala mutant evidently shows that in this mutant the deacylation rate is less than the acylation rate. Enzyme active sites are normally plastic, and the residual catalytic activity after removal of an important functional residue may simply indicate adaptations within the active site that compensates the missing functionality.[13] The fact that acylation activity is not removed in the Lys86Ala mutant does not preclude a general base role for carbamylated Lys86 during the activation of active site Ser83. We should note that the action of a general base is only one part of the complicated series of strategies used by an enzyme to trigger catalysis. As suggested before positive charge of Lys212 can enhance the deprotonation of Ser67 in OXA-1.[7] It could be suggested that the in OXA-58 the role of the eliminated Lys86 is played by Lys220. This Lys residue is located in the close proximity to the Lys 86 in the structure of OXA-58 (Figure 21). The spatial arrangement

of the active site in OXA-1 shows that The Lys 212 residue is closer to the Ser67 than it is to the expected position of a deacylating water molecule which explain the reason for the preferential enhancement of acylation over deacylation in the absence of K70.[7] In the case of OXA-58 also this can be the reason for the fast acylation step in comparison to deacylation step in OXA-58.

Because there is no other residue close enough to act as a general base, it is possible that the elimination of Lys86 side chain or the binding of substrate, or both in a concerted manner introduce a new active site architecture that allows such a residue to fill in for the Lys86.

References

(1) Golemi, D., Maveyraud, L., Vakulenko, S., Tranier, S., Ishiwata, A., Kotra, L. P., Samama, J. P., and Mobashery, S. *J. Am. Chem. Soc.* **2000**, 122:6132–6133.

(2) Maveyraud, L., Golemi, D., Kotra, L. P., Tranier, S., Vakulenko, S., Mobashery, S., and Samama, J. P. *Structure* **2000**, 8:1289–1298.

(3) Lorimer, G. H., Badger, M. R., Andrews, T. J. *Biochemistry* **1976**, 15:529.

(4) Jabri, E., Carr, M. B. Hausinger, R. P., Karplus, P. A. *Science,* **1995**, 268:998-1004.

(5) Shim, H., Raushel, F. M., *Biochemistry* **2000**, 39:7357.

(6) Verma V., Testero, S. A., Amini, K, Wei, W, Liu J., Balachandran, N., Monoharan, T., Stynes, S., Kotra, L. P., Golemi-Kotra, D., *J. Biol. Chem.* **2011**, 286:37292–37303

(7) Schneider K. D., Bethel C. R., Distler A. M., Hujer A. M., Bonomo R. A, and Leonard D. A. *Biochemistry* **2009**, 48:6136–6145.

(8) Eftink, M. R., and Ghiron, C. A. *Anal. Biochem.* **1981**, 114:199-227.

(9) Olson, S. T., Shore, J. D., *J. Biol. Chem.* **1981**, 256:1165.

(10) Bernat, B. A., Armstrong, R. N. *Biochemistry* **2001**, 12712.

(11) Eftink, M. R., and Ghiron, C. A. *Biochemistry* **1976**, 15:672–680.

(12) Guillaume, G., Vanhove, M., Lamotte-Brasseur, J., Ledent, P., Jamin, M., Joris, B., and Frere, J. M. *J. Biol. Chem.* **1997**, 272, 5438–5444.

(13) Peracchi, A. Enzyme catalysis: Removing chemically 'essential' residues by site-directed mutagenesis. Trends Biochem. Sci. **2001**, 26:497–503.

(14) Steyaert, J., Hallenga, K., Wyns, L., and Stanssens, P. *Biochemistry* **1990**, 29:9064–9072.

Figures

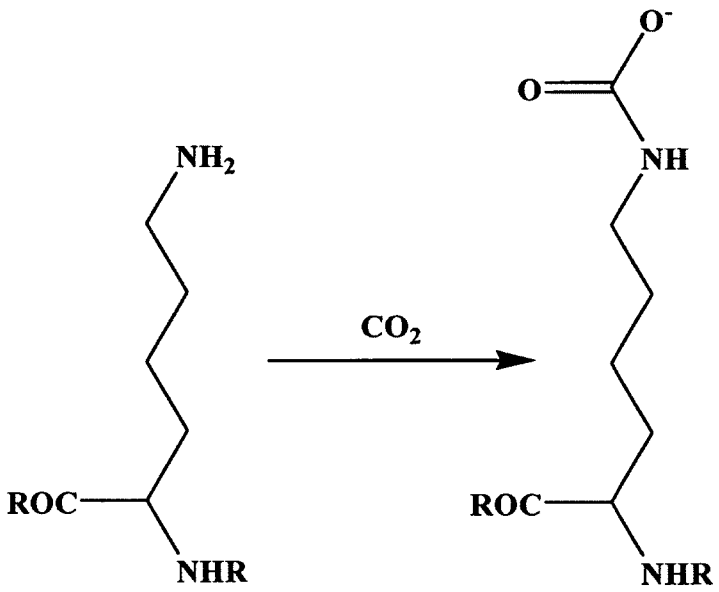

Figure 1. Carbamylation of lysine residue

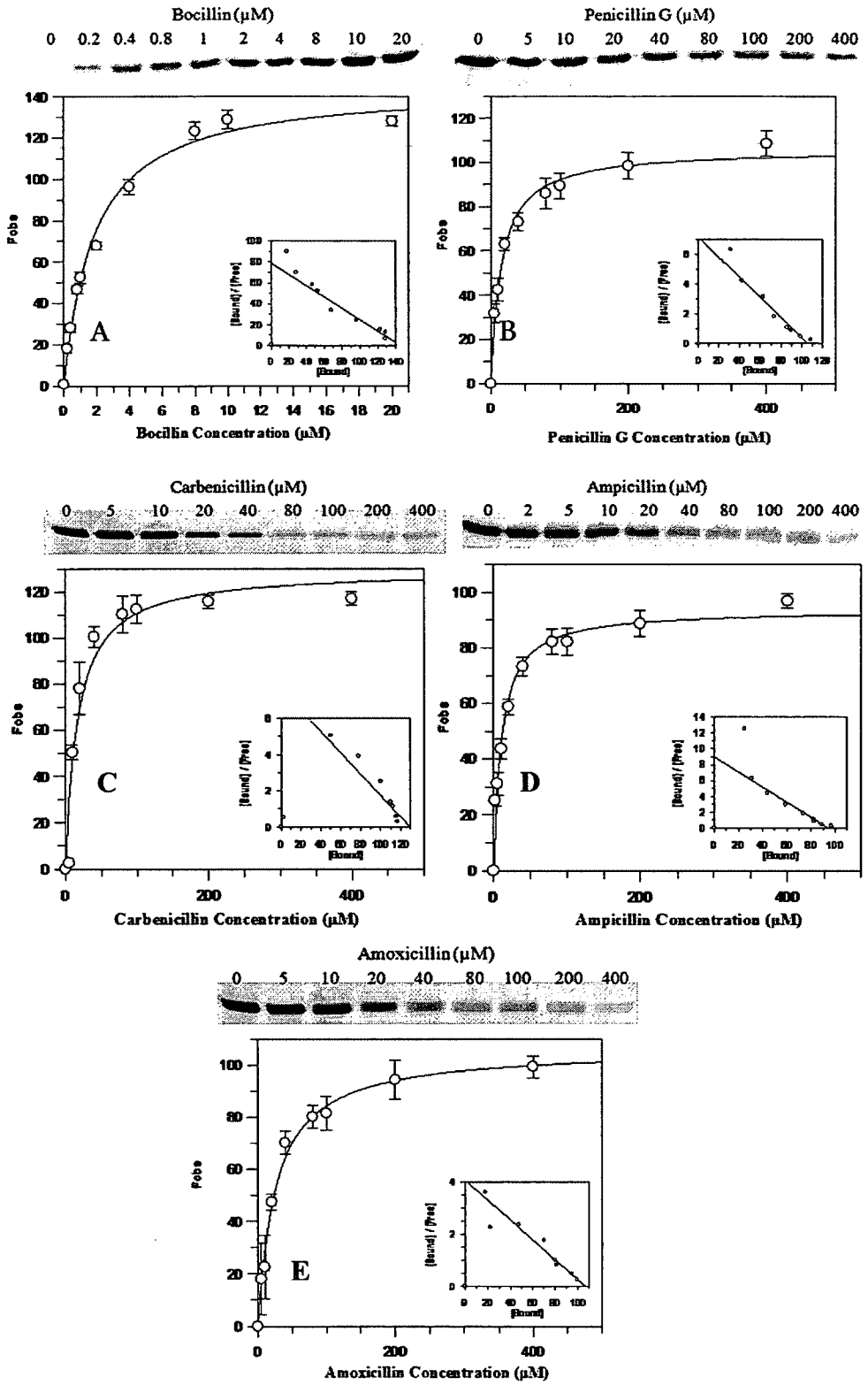

Figure 2. Extraction of K_d for (A) Bocillin and IC50 values for (B) penicillin G, (C) carbenicillin, (D) Ampicillin and (E) Amoxicillin and OXA-58 K86A using BOCILLIN FL as a reporter substrate.

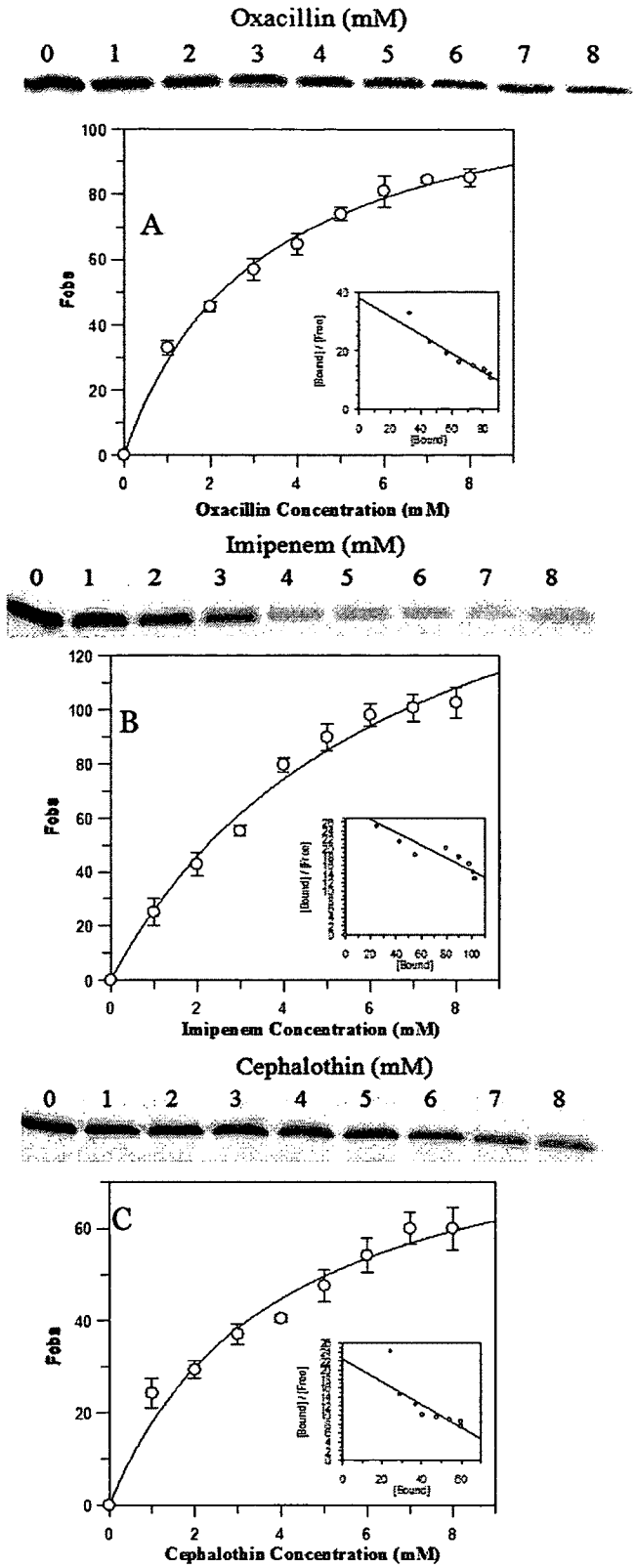

Figure 3. Extraction of IC_{50} values for (A) oxacillin, (B) imipenem and (C) cephalothin and OXA-58 K86A using BOCILLIN FL as a reporter substrate.

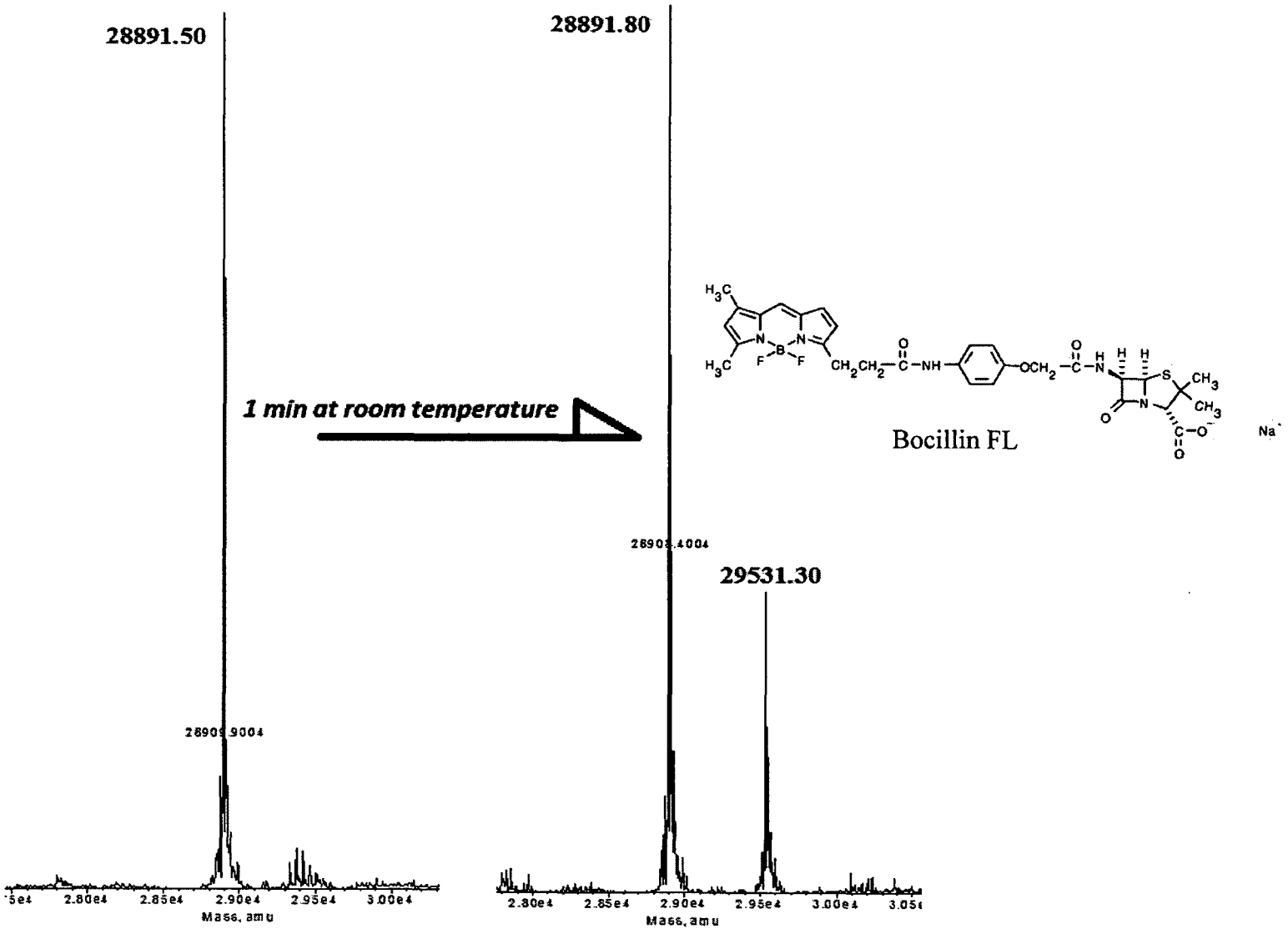

Figure 4. Examination of the formation of an acyl-enzyme species between OXA-58 K86A and BOCILLIN FL with ESI-MS (deconvoluted ESI-MS spectra). In these experiments OXA-58 K86A at 10 μM was incubated with BOCILLIN FL at 200 μM for 1 min, in 50mM sodium phosphate, pH 7.0, at room temperature (total volume = 100 μL). Then the solution was desalted and the reaction was immediately stopped by addition of trichloroacetic acid (10 % final concentration). The protein precipitate was separated by centrifuge at 13'000 rpm for 5 min and resuspended in 10 μL water (final concentration of the protein = 100 μM). The mixture was subjected to ESI-MS for analysis.

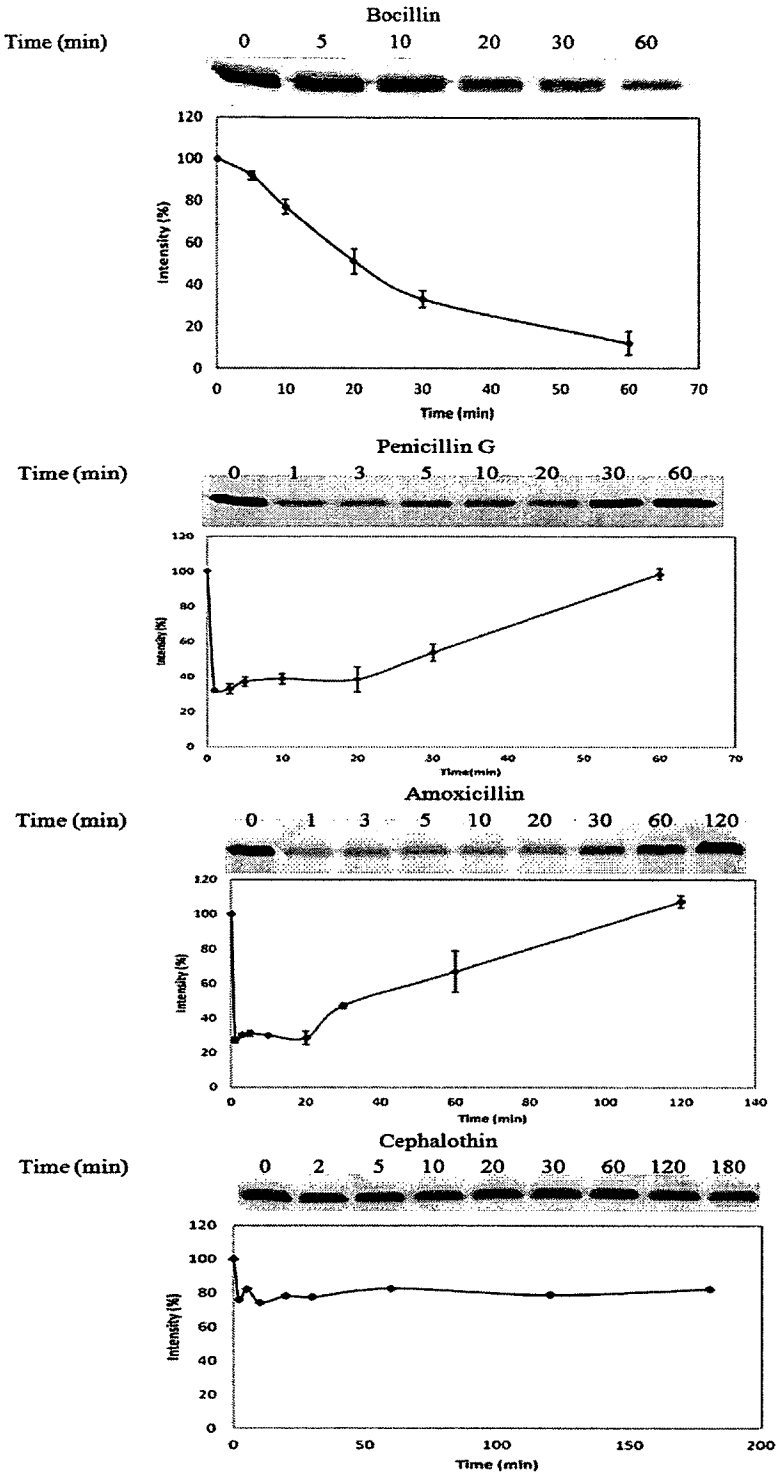

Figure 5. Examination of the hydrolysis of Bocillin, penicillin G and amoxicillin by OXA-58 K86A using BOCILLIN FL as a reporter substrate. Penicillin G and amoxicillin at 64 μM and cephalothin at 1 mM was incubated with OXA-58 K86A at 1 μM and at different time intervals an aliquot of the reaction mixture was taken and incubated with BOCILLIN FL for 30 s and then the reaction was quenched by addition of SDS loading dye. The aliquots were loaded on a 12.5 % SDS-gel and the gel was visualized at 488 nm excitation and 520 nm emission.

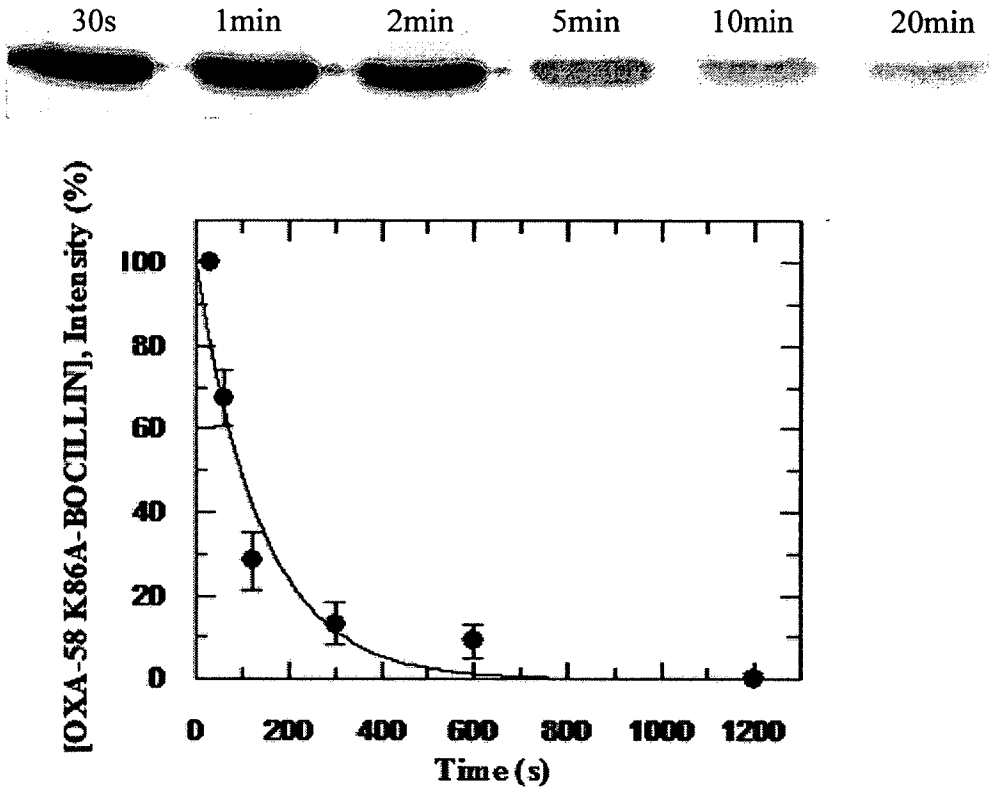

Figure 6 Deacylation of the acyl-enzyme intermediate formed between OXA-58 K86A and BOCILLIN FL. In this experiments OXA-58 K86A at 3 μM was incubated with50 μM BOCILLIN FL for 30 s and was desalted using Zeba mini centrifugal columns (Pierce, Rockford, IL, USA) equilibrated with 50 mM sodium phosphate buffer pH 7.0, to remove the excess of BOCILLIN FL and at different time intervals (30s to 20 min) aliquots were taken and the reaction was quenched by addition of SDS loading dye. All samples were loaded on a 12.5 % SDS-PAGE. The gel was imaged using a Typhoon Trio^{+} Variable Mode Imager (GE Healthcare) at 488 nm excitation and 520 nm emission.

A

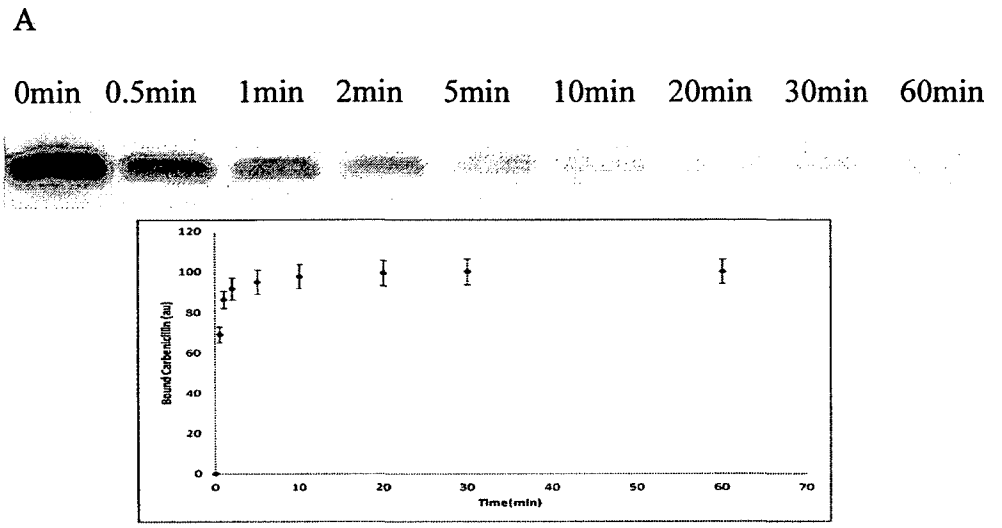

B

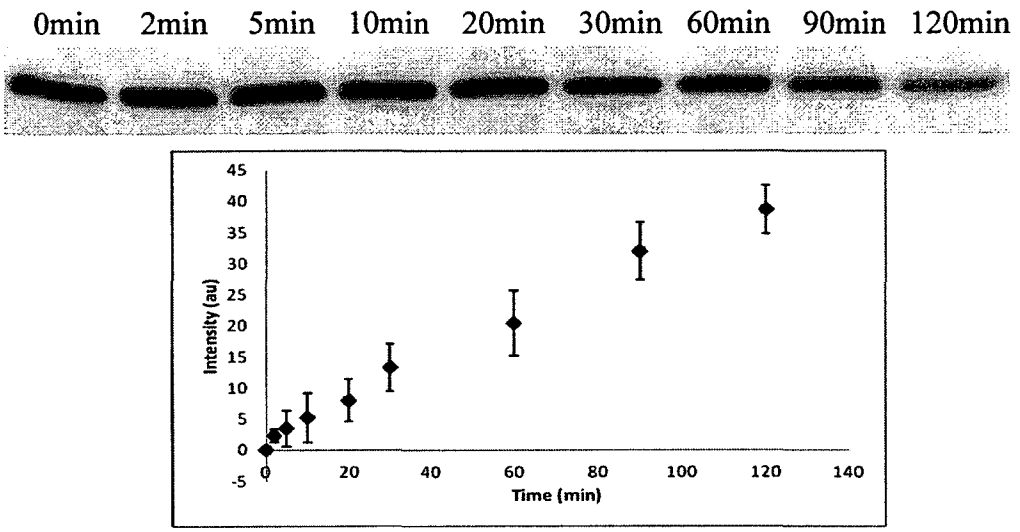

Figure 7. (A) Carbenicillin acylation profile of OXA-58 K86A mutant assessed by SDS-PAGE. Carbenicillin at 64 μM was incubated with OXA-58 K86A at 1 μM and at different time intervals an aliquot was taken and incubated with 10 μM BOCILLIN FL for 30s and then the reaction was quenched by addition of SDS loading dye and the samples were loaded on a 12.5% SDS-PAGE. (B) Imipenem acylation profile of OXA-58 K86A mutant assessed by SDS-PAGE. The experiment was performed similar to carbenicillin.

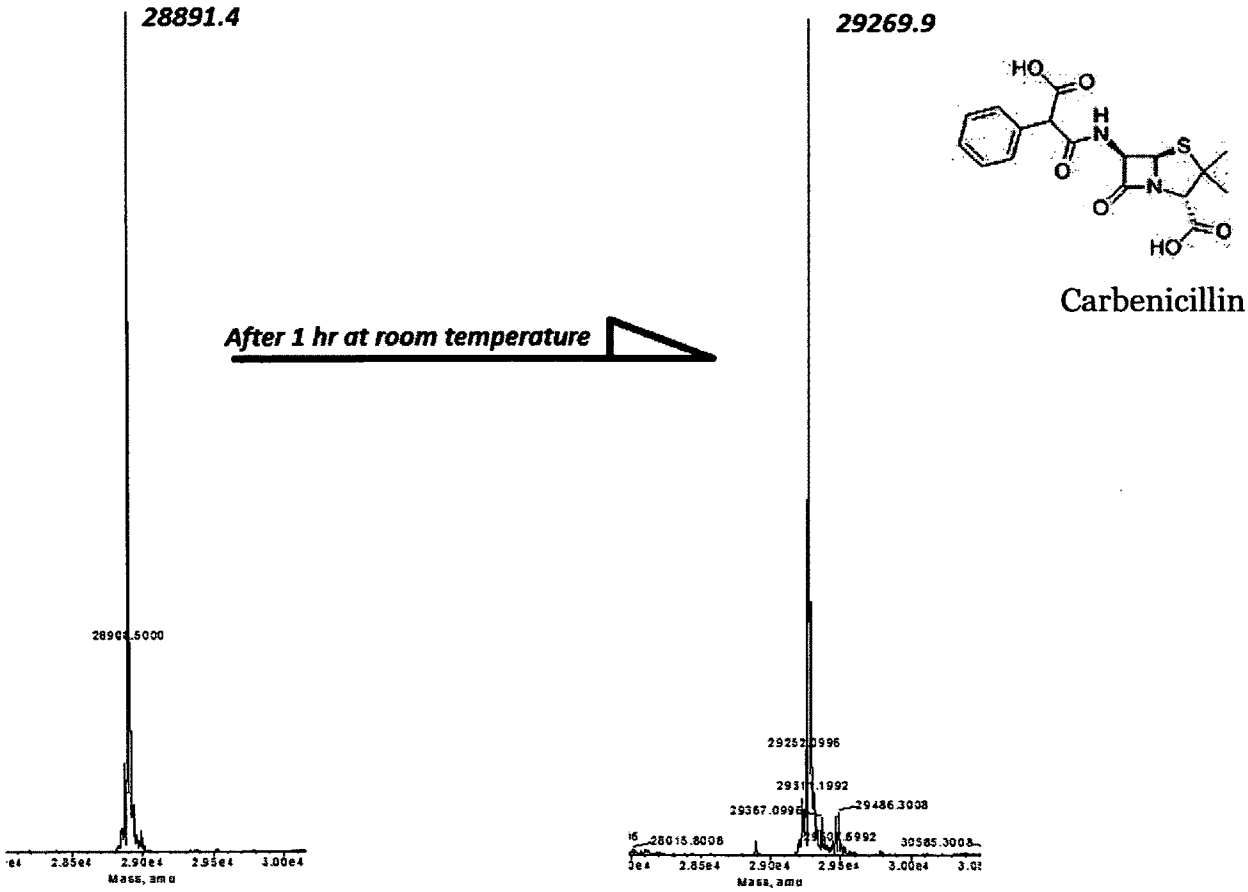

Figure 8. Examination of the formation of an acyl-enzyme species between OXA-58 K86A and carbenicillin. In this experiment carbenicillin at 800 μM was incubated with OXA-58 K86A at 10 μM for 1 hr at room temperature (total reaction mixture was 100 μL). Then the reaction was stopped by addition of trichloroacetic acid (final concentration = 10 %) and the protein precipitate was separated by centrifuge and was dissolved in 10 μL water (total concentration of protein = 10 μM). The control solution was made in a similar way to the above mentioned sample with the only difference being that carbenicillin was not added.

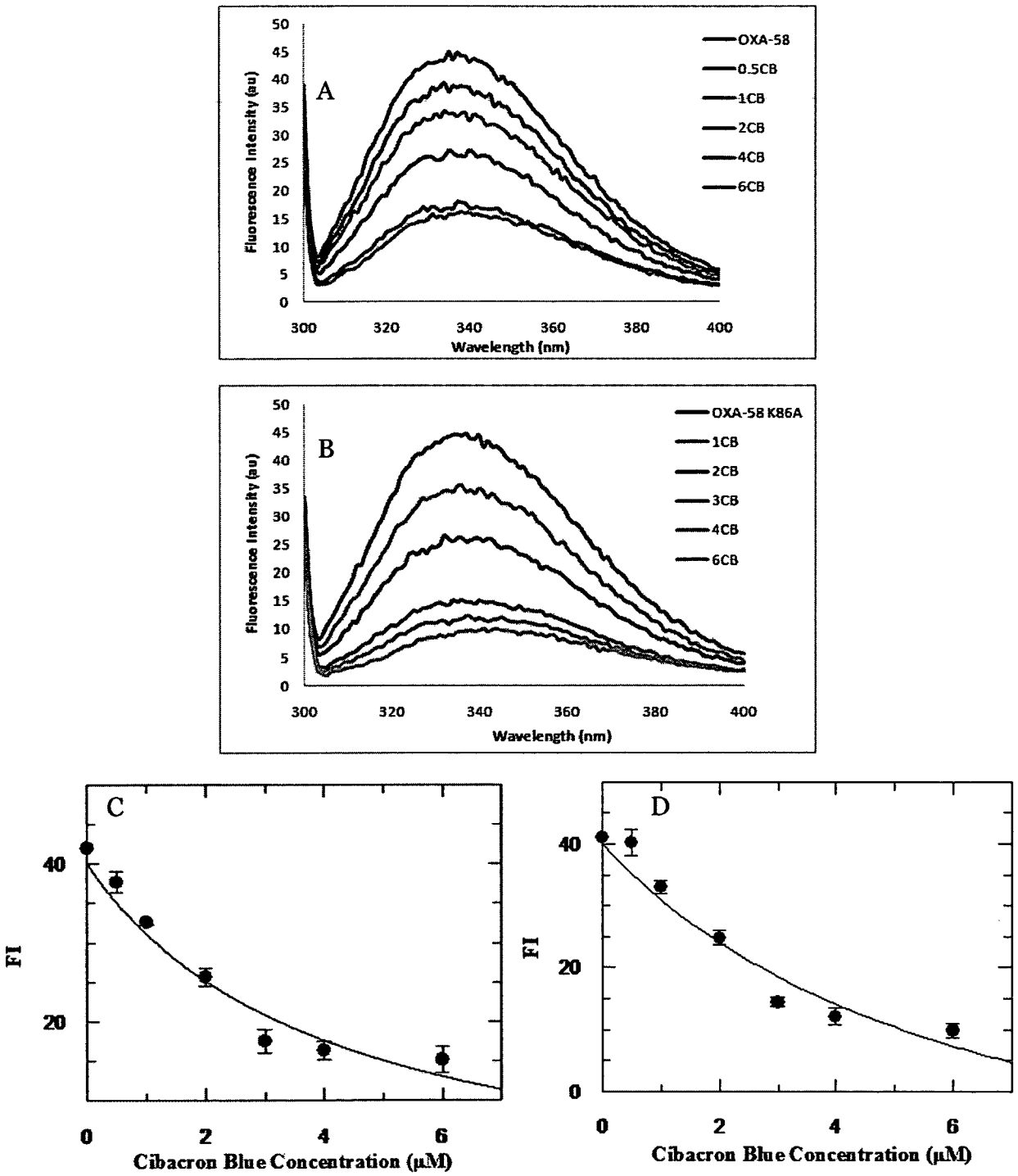

Figure 9. (A) Quenching of the fluorescence emission of OXA-58 Wild type and (B) OXA-58 K86A mutant in the presence of different concentrations of Cibacron blue 3GA (CB stands for Cibacron blue 3GA and the concentrations mentioned in the graphs are in μM). Non-linear fitting of the fluorescence quench of OXA-58 by Cibacron blue 3GA on (C) wild type OXA-58 and (D) OXA-58 K86A mutant recorded at 345 nm.

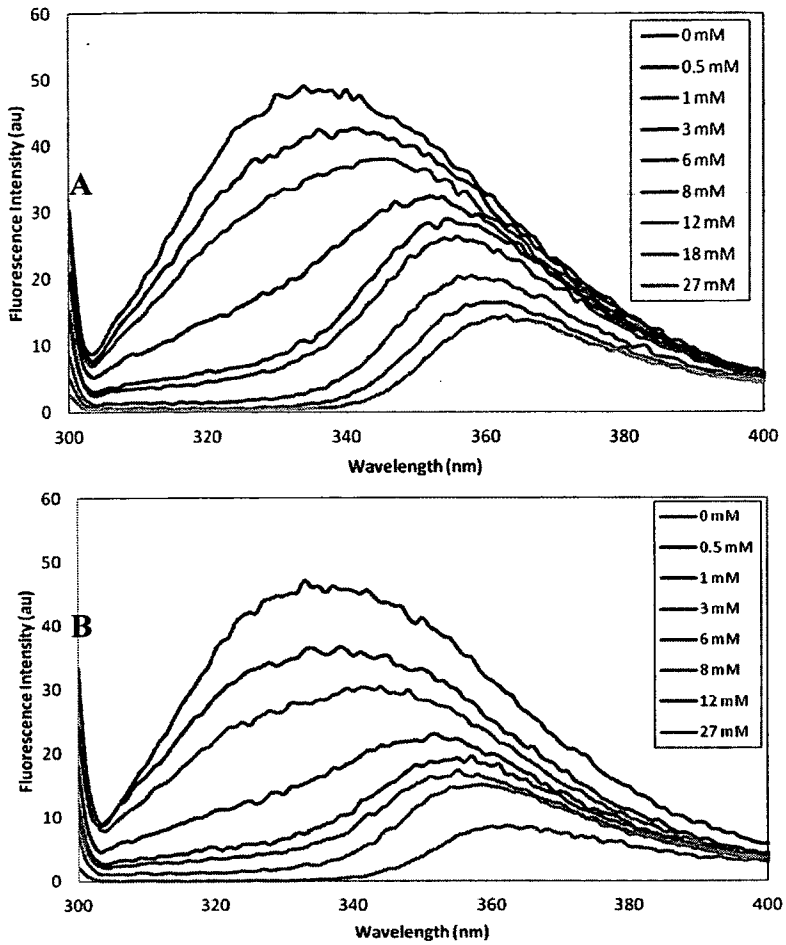

Figure 10. Quenching effect of different Carbenicillin on OXA-58 and OXA-58 K86A fluorescence emission. (A) Quenching the fluorescence of OXA-58 by carbenicillin. (B) Quenching the fluorescence of OXA-58 K86A by carbenicillin.

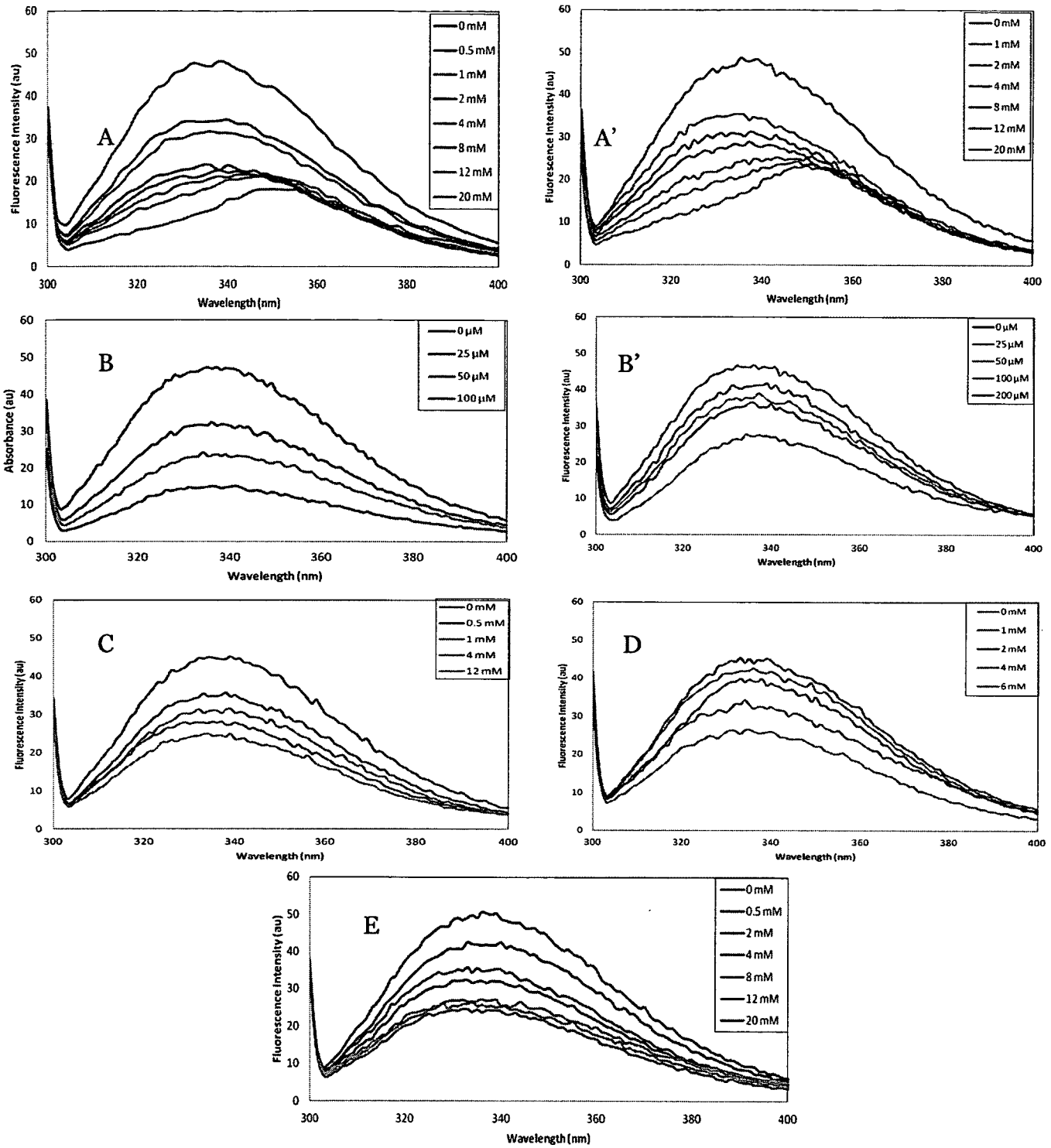

Figure 11. Quenching the fluorescence of OXA-58 by (A) Penicillin G (B) Imipenem (C) Ampicillin (D) Amoxicillin and (E) Oxacillin and Quenching the fluorescence of OXA-58 K86A by (A') Penicillin G (B') Imipenem.

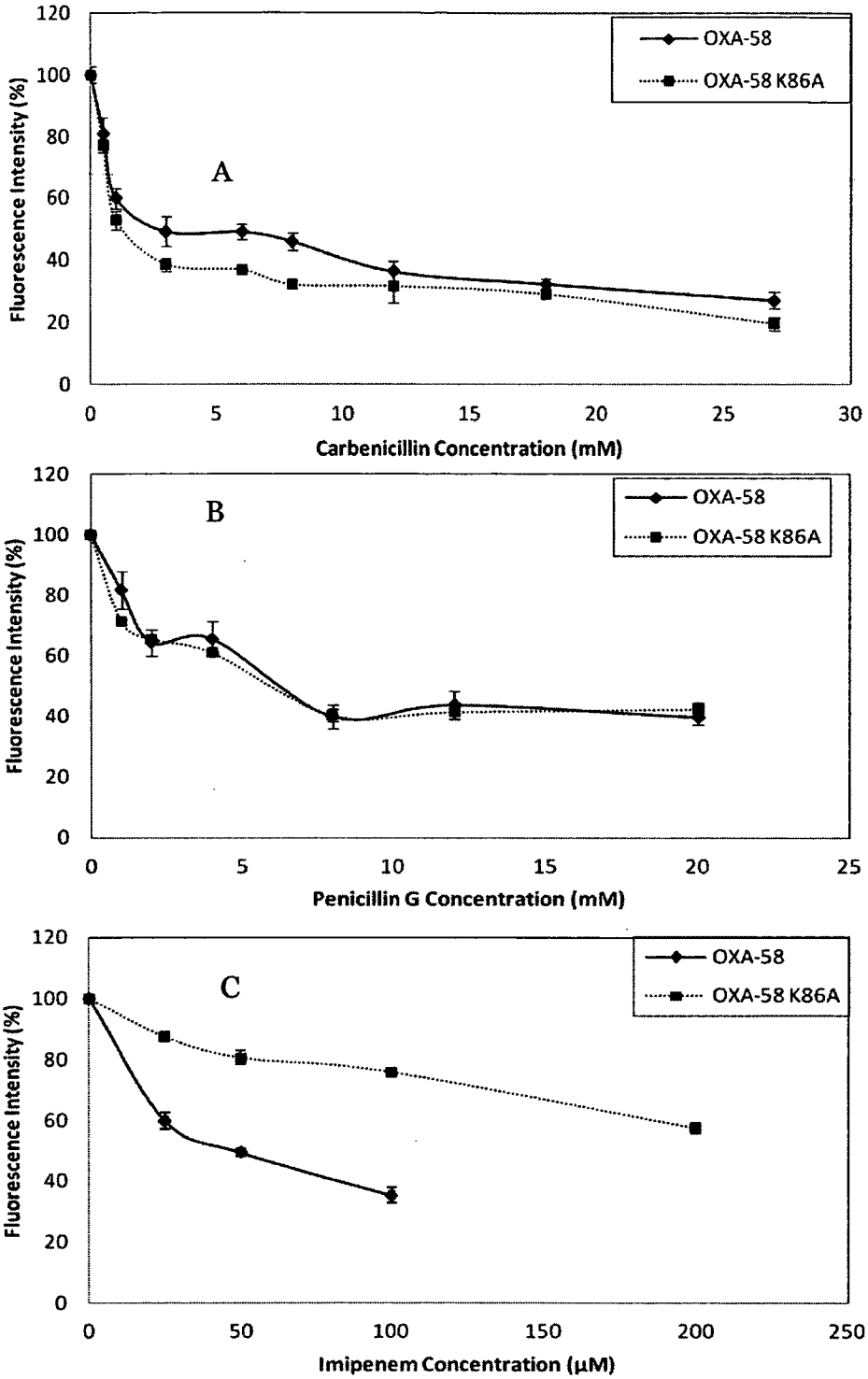

Figure 12. Comparison of the quenching effect of (A) carbenicillin, (B) penicillin G and (C) imipenem on the fluorescence emission (at 360-370 nm for carbenicillin and 345 nm for penicillin G and imipenem) of wild type OXA-58 and OXA-58 K86A mutant.

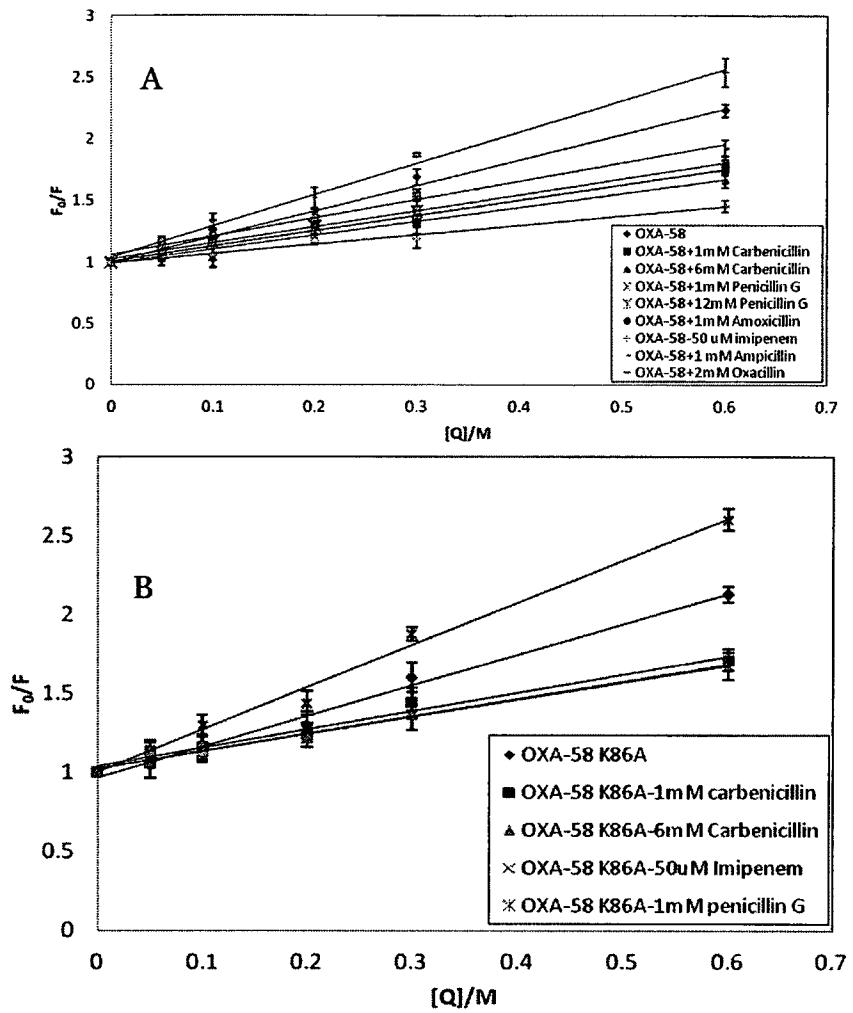

Figure 13. Stern-Volmer plots for (A) wild type OXA-58 and (B) OXA-58 K86A mutant in the absence and presence of different β-lactams. The data have been recorded at 345 nm.

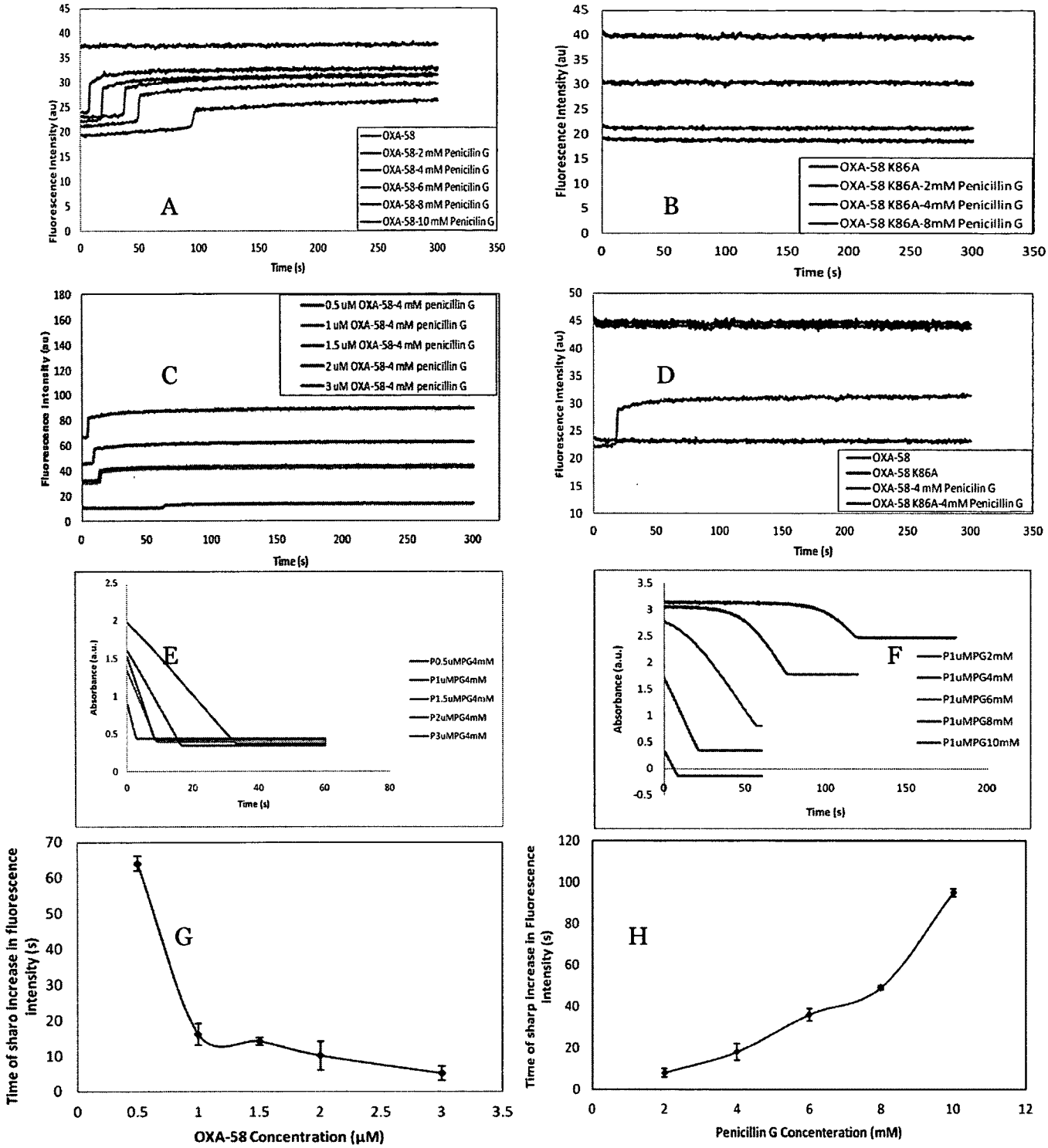

Figure 14 Monitoring the fluorescence intensity of (A) 1 μM of OXA-58 and (B) OXA-58 K86A in the presence of different concentrations of penicillin G. (C) Monitoring the fluorescence intensity of different concentrations of OXA-58in the presence of 4 mM penicillin G. (D) Comparison of the fluctuation of the fluorescence intensity of OXA-58 and OXA-58 K86A in the presence of 4 mM penicillin G. Monitoring the hydrolysis of (E) 4 mM of penicillin G by different concentrations of OXA-58 and (F) different concentrations of penicillin G by 1 μM OXA-58 using UV-Vis spectrophotometery. Dependence of the sudden increase in the fluorescence intensity on (F) OXA-58 and (H) penicillin G concentration.

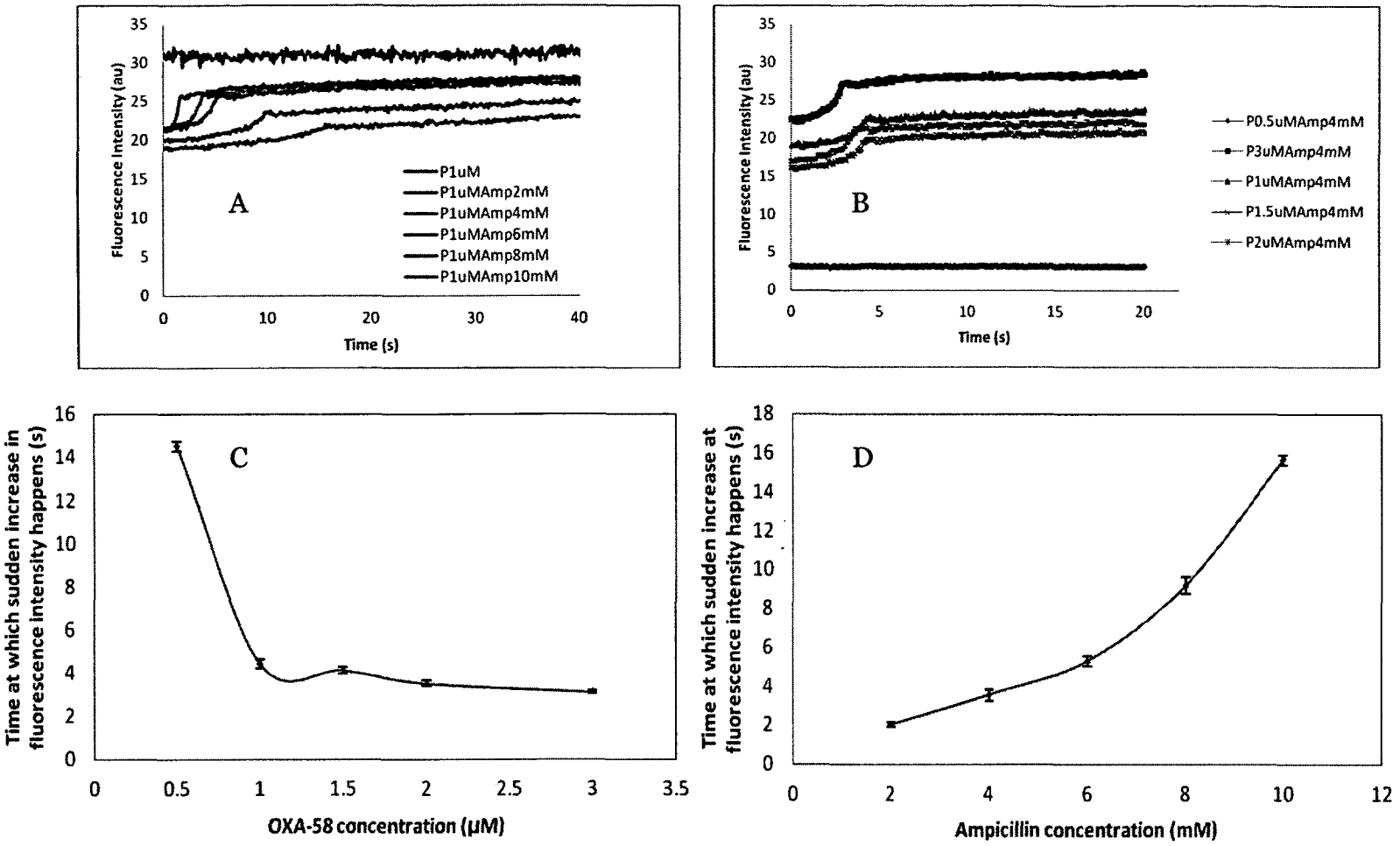

Figure 15. Monitoring the fluorescence intensity of OXA-58 in the presence of different concentrations of ampicilin (A). Monitoring the fluorescence intensity of different concentrations of OXA-58 in the presence of 4 mM ampicilin (B). Dependence of the sudden increase in the fluorescence intensity on (C) ampicillin and (D) OXA-58 concentration.

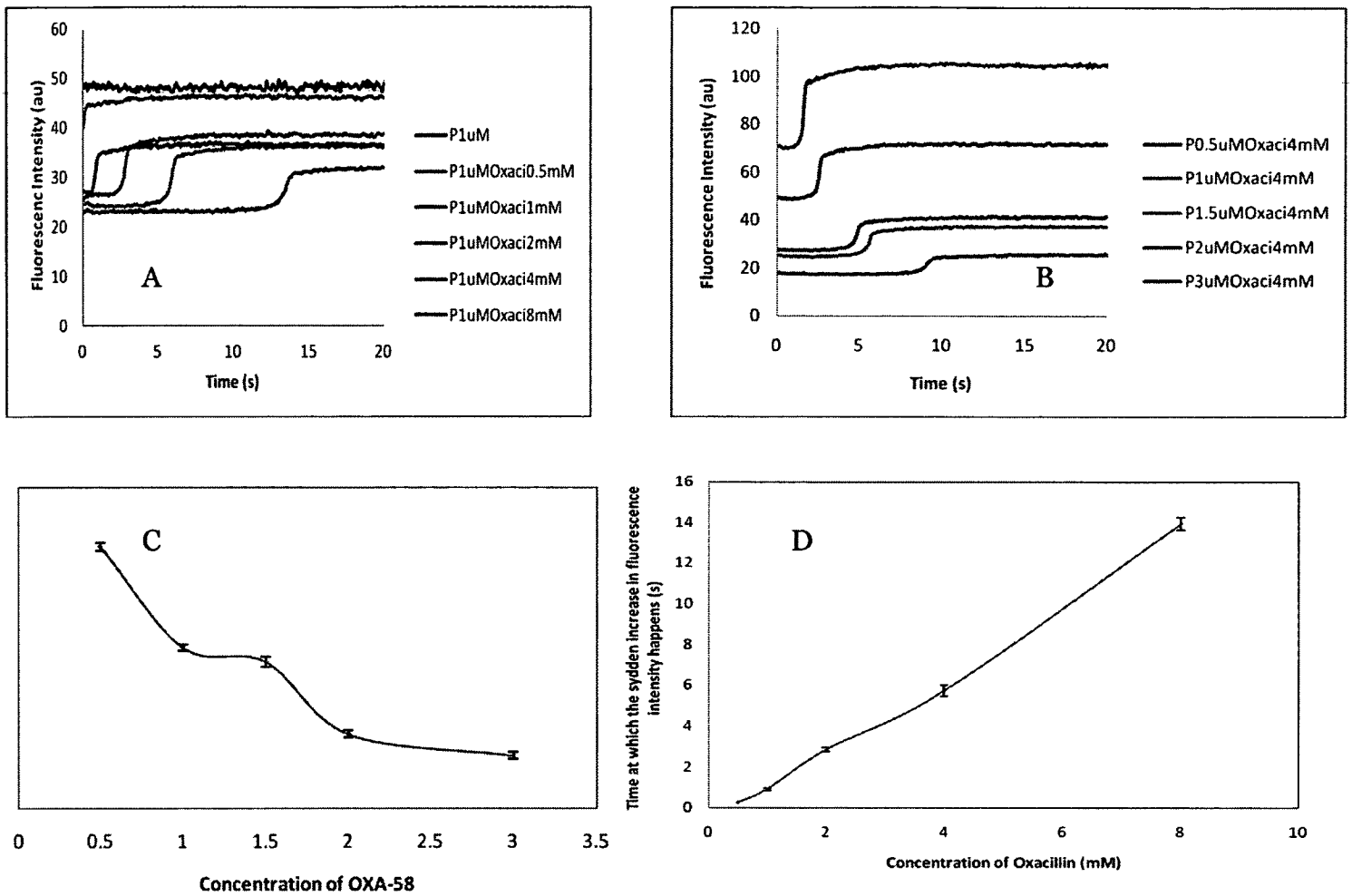

Figure 16. Monitoring the fluorescence intensity of OXA-58 in the presence of different concentrations of Oxacillin (A). Monitoring the fluorescence intensity of different concentrations of OXA-58 in the presence of 4 mM Oxacillin (B). Dependence of the sudden increase in the fluorescence intensity on (C) OXA-58 and (D) Oxacillin concentration.

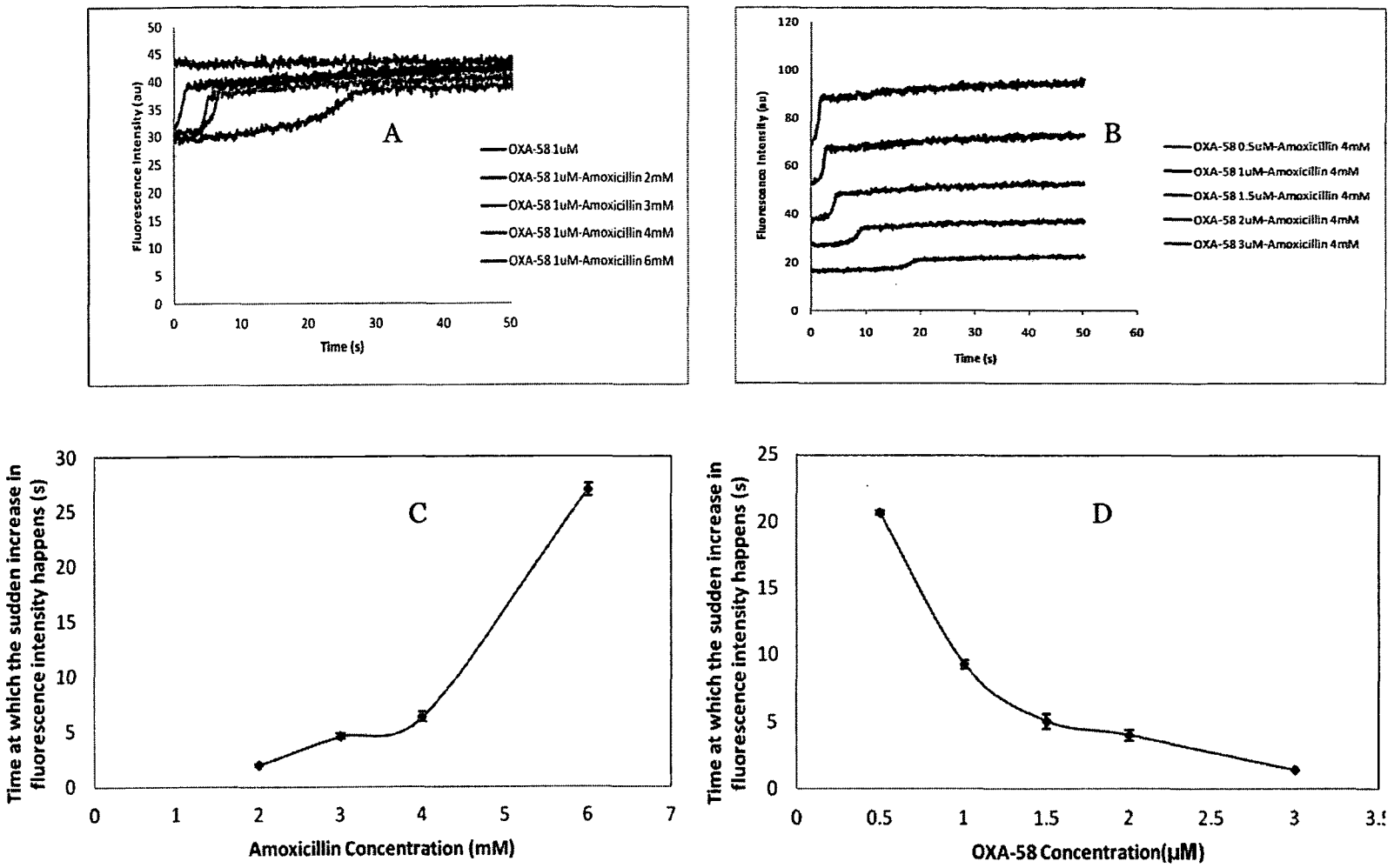

Figure 17. Monitoring the fluorescence intensity of OXA-58 in the presence of different concentrations of Amoxicillin (A). Monitoring the fluorescence intensity of different concentrations of OXA-58 in the presence of 4 mM Amoxicillin (B). Dependence of the sudden increase in the fluorescence intensity on (C) Amoxicillin and (D) OXA-58 concentration.

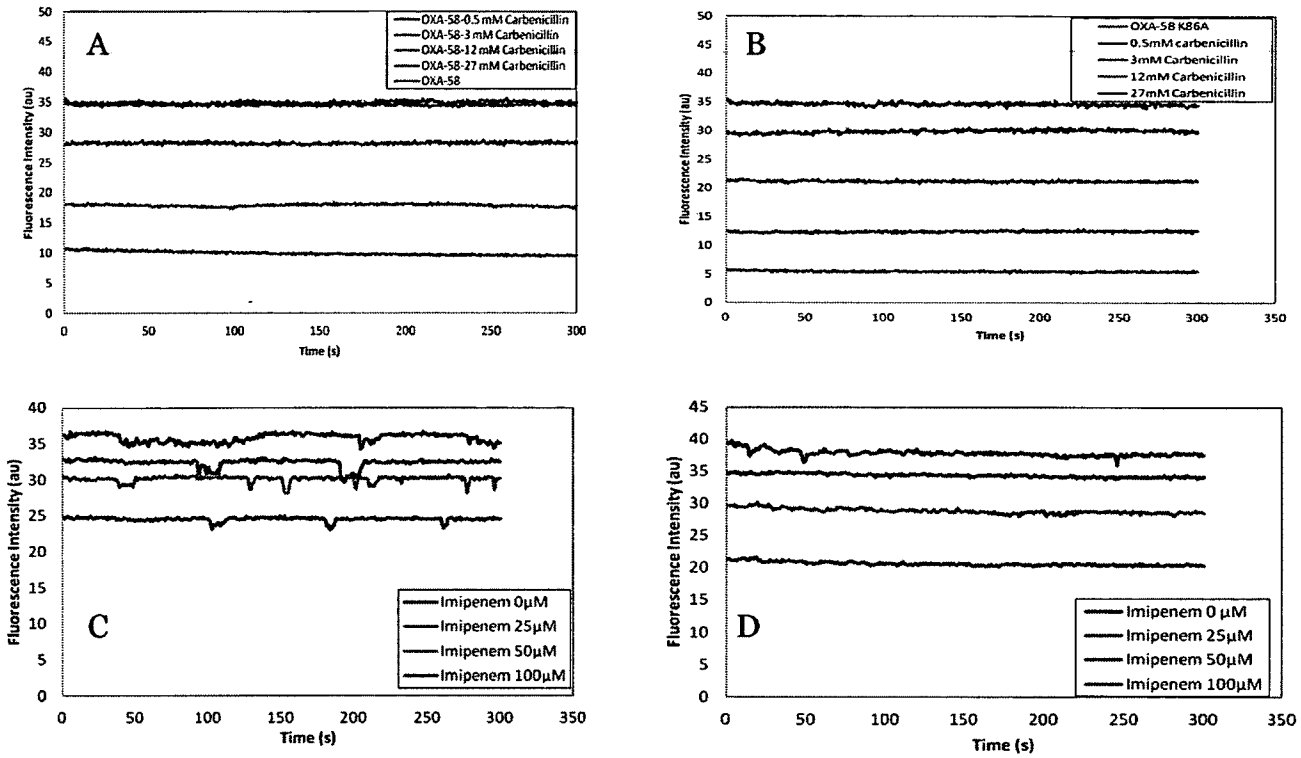

Figure 18. Monitoring the fluorescence intensity of 1 μM of (A) OXA-58 and (B) OXA-58 K86A in the presence of different concentrations of Carbenicillin and monitoring the fluorescence intensity of 1 μM of (C) OXA-58 and (D) OXA-58 K86A in the presence of different concentrations of Imipenem. In all cases the fluorescence data were collected right after mixing.

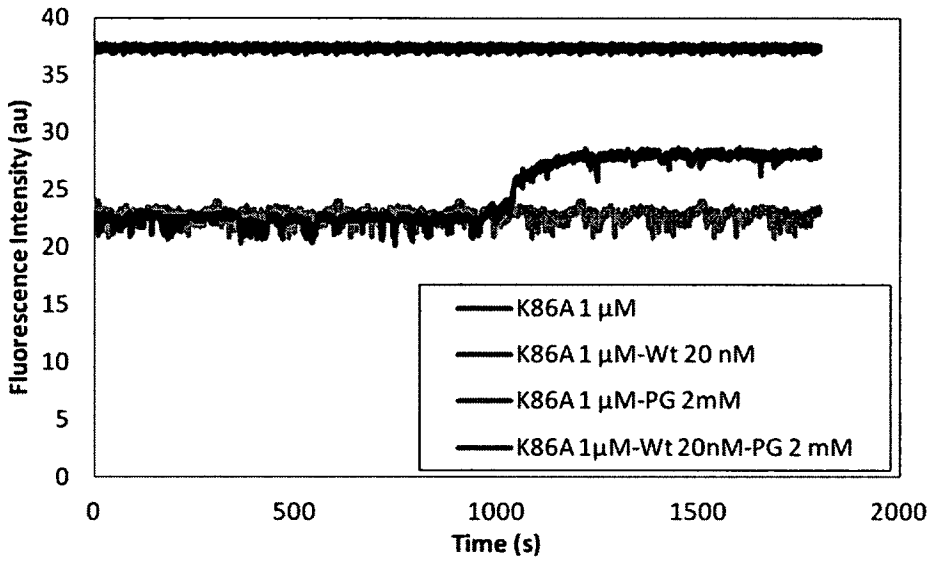

Figure 19. Monitoring the fluorescence intensity of 1 μM of OXA-58 K86A while interacting with 2 mM penicillin G. After addition of 20 nM of wild type OXA-58 to the incubation solution of OXA-58 K86A and penicillin G the sudden increase in the fluorescence intensity of K86A mutant is also observed which indicates that after the hydrolysis of excess of penicillin G, the acyl-enzyme species between K86A and penicillin G is deacylated and the sudden increase happens at the end of hydrolysis.

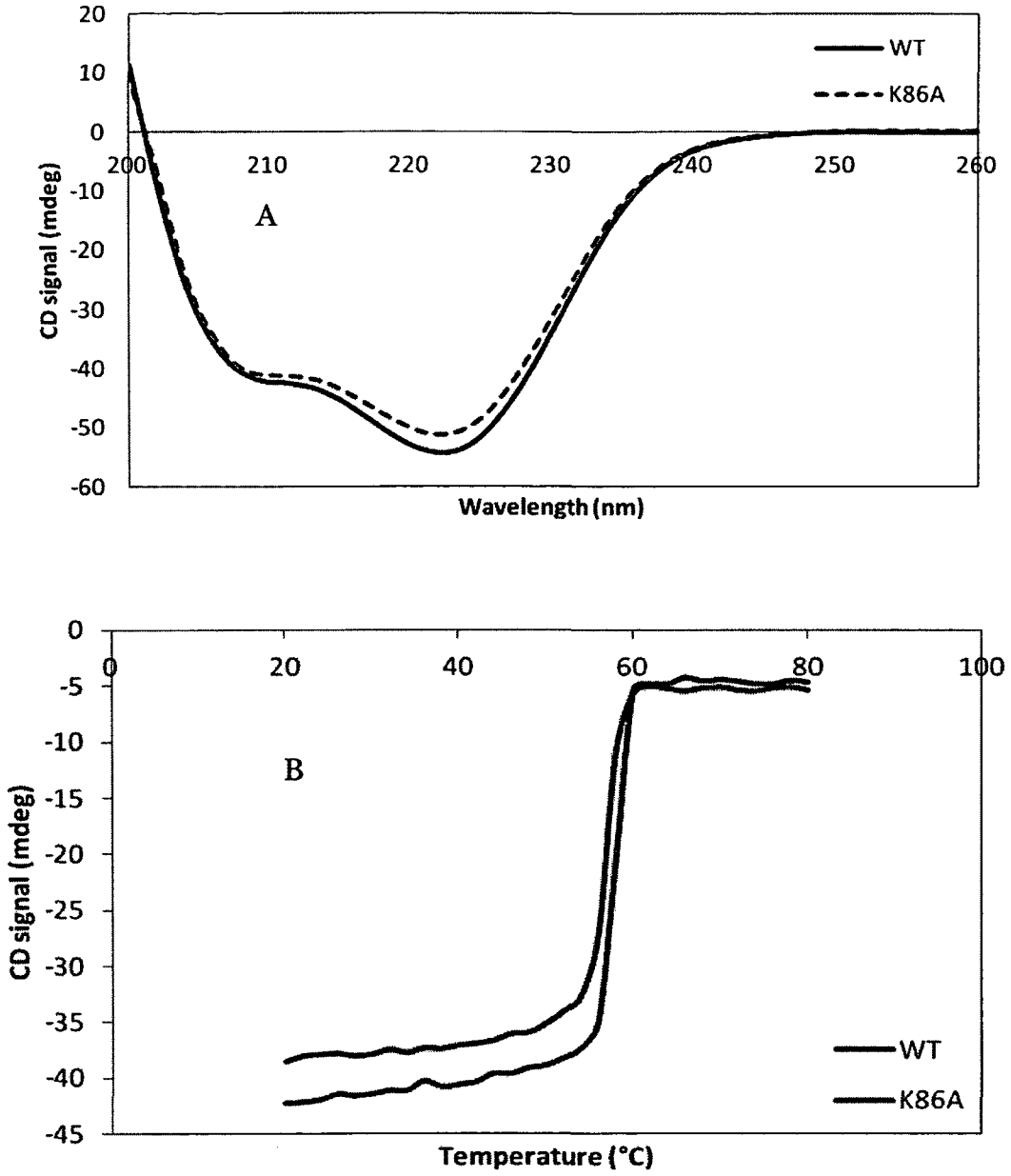

Figure 20. Comparison of the (A) CD spectrum and (B) thermal melting of the wild type OXA-58 with that of the OXA-58 K86A mutant.

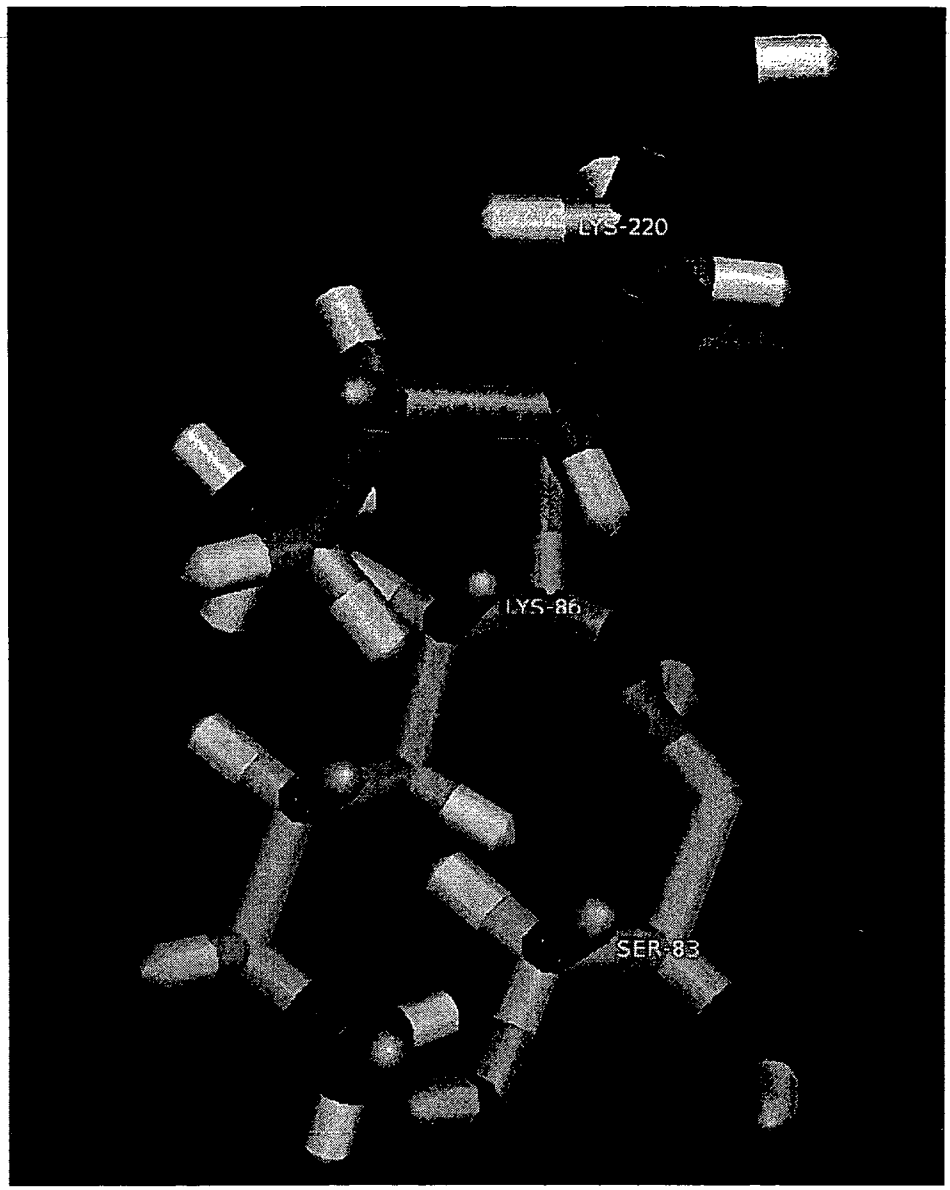

Figure 21. Positions of Ser83, Lys86 and Lys220 with respect to each other in the structure of the protein.

Tables

Table 1 Half minimal inhibitory concentrations (IC_{50}) for different β-lactams on the activity of OXA-58 K86A

β-Lactam	*IC_{50} ± SD (μM)*
BOCILLIN FL	1.05 ± 0.03*
Penicillin G	15 ± 2
Ampicillin	10.4 ± 0.8
Amoxicillin	21200 ± 2500
Oxacillin	3100 ± 200
Cephalothin	3800 ± 200
Carenicillin	18 ± 3
Imipenem	4700 ± 300

* This value is the dissociation constant (K_d).

Table 2 Stern-Volmer constants (Ksv) for quenching of wild type OXA-58 and OXA-58 K86A mutant by acrylamide in the presence and absence of different β-lactams.

β-lactam (Concentration)	*K_{sv} (M^{-1}) WT*	*K_{sv} (M^{-1}) K86A*
In the Absence of any β-lactam	2.1 ± 0.1	2.0 ± 0.2
Carbenicillin (1 mM-6 mM)	1.1 ± 0.1-1.1 ± 0.1	1.2 ± 0.1-1.1 ± 0.1
Penicillin G (1 mM)	1.7 ± 0.2	1.0 ± 0.1
Ampicillin (1 mM)	1.5 ± 0.1	N.D.*
Oxacillin (2 mM)	0.7 ± 0.1	N.D.
Amoxicillin (1 mM)	1.1 ± 0.1	N.D.
Imipenem (50 μM)	2.5 ± 0.2	3.0 ± 0.2

* Not Determined.

Chapter Four: Investigation of the role of Phen113, Phen114 and Met225 residues in the active-site of OXA-58 on its catalytic activity

4.1 Introduction

4.1.1 The importance of different residues in the active site of OXA-58

The structural homology model of OXA-58 has already been shown to be similar to that of OXA-24 and OXA-48 carbapenemases (Figure 1)[1]. The Arg-244 in OXA-10 that enters into an interaction with the carboxylic group of β-lactams is also conserved in OXA-58 (Arg-263). Similar to OXA-10, OXA-24, and OXA-48, the hydrophobic pocket formed by the side chains of hydrophobic residues in which the carbamylated lysine residue in the active site lies, is also present in OXA-58 (Phe-85, Val-132, Phe-135, Trp-169, and Leu-170)[1].

The most significant conformational differences between the OXA-58 homology model and the OXA-10 crystal structure are observed in the loop between the β4 and β5 strands and in the overall topology of the active site[1] (Figure 1). The loop which connects the β4 and β5 strands has been shown to be shorter in OXA-58 than in OXA-10[1]. In addition, similar to the conformation of the loop in OXA-24 and OXA-48 [2,3], the OXA-58 loop has a closed conformation (Figure 1 and Figure 2). OXA-58 active site, according to its predicted topology, has been shown to be narrower in comparison to the active site of OXA-10 and OXA-24. [1]This is because of the location of the side chains of

hydrophobic residues such as Phe-113, Phe-114, Ala-226, Gln-167, Met-225, and Ile-250 which are toward the active site (Figure 2).

The side chain of Met-225 located in the β4-β5 loop (comparable to Met-223 in OXA-24 and Ser-244 in OXA-48) and the side chains of Phe-113 (comparable to Tyr-112 in OXA-24 and Ile-104 in OXA-48) and Phe-114 of the α3-α4 loop have been predicted to be in an interaction according to the homology model of OXA-58 model[1]. Consequently, probably due to the flexibility of both loops, a better tunnel-like topology is observed in comparison to the active sites of OXA-10 and OXA-24 (Figure 2).[1] According to the OXA-58 homology model, side chains of Leu-170 and Val-132 in this protein don't have much interaction with each other which may lead to a pocket with less hydrophobicity as in oxacillinases such as OXA-10 and OXA-13 (Leu-155 and Val-117) (Figure 2).

In this part of the project, we have tried to elucidate the role of Phen113, Phen114 and Met225 residues located right above the active site in the catalytic mechanism of OXA-58 by studying the kinetics of Phen113Ala, Phen114Ala, Phen113Tyr, Phen114Ile, Met225Ala and Met225Thr mutants. The logic behind mutating any of these residues to Alanine is to investigate the role of them in the active site. The reason for studying F113Y mutant is the result of the finding by Santillana et al.[2] In the OXA-24 crystal structure, a hydrophobic tunnel substructure is observed at the entrance of the active site which is suggested to have a critical role in substrate specificity. In OXA-24, Met223 and Tyr112 form the hydrophobic tunnel, the latter of which is the Phe113 equivalent in OXA-58. The steric obstruction dictated by the hydrophobic barrier, makes the entrance

of bulky substrates like oxacillin into the active site difficult and limits their hydrolysis. However, smaller substrates have the chance to manoeuvre around the hydrophobic tunnel and enter the active site pocket without any significant hindrance. Hence, the plausible model for β-lactam hydrolysis is investigated by mutating the Phen113 to a tyrosine residue in OXA-58.

The tunnel-like entrance of the active site seen in OXA-24 (the Tyr-112 and Met-223 hydrophobic barrier) [2], and also in OXA-58 (the Phen-113, Phen-114 and Met-225 hydrophobic barrier) is missing in OXA-48.[3] This corresponds to the different behavior of the two enzymes toward oxacillin. However, by mutating Phen114 to an Isoleucine and the Met225 to a Therionine, we have investigated the model of β-lactam hydrolysis by simulating the active site of OXA-48 in OXA-58 (Figure 2).

4.1.2 Employment of isothermal titration calorimetry for enzyme kinetic studies

The ITC protocol developed by Kotra and co-workers [4] was employed as an appropriate tool to determine the steady state kinetic parameters of OXA-58 against β-lactams with low extinction coefficients. High sensitivity, direct rate measurement, and easy data analysis are the advantages of this method.

ITC progress curves are named as thermal power and are reported in the form of microcalories per unit time (Figure 3A). The thermal power (ITC signal) is proportional with the rate of substrate consumption. As the substrate is metabolized by the enzyme, the thermal power decreases up to the base line. Using equations 1-2 we can convert thermal power into reaction rates (Figure 3B), which are then plotted against substrate concentration (Equation 3).

$$\text{power (P)} = dQ/dt = (dP_t/dt)V_0\Delta H_{app} \qquad \text{(eq. 1)}$$

$$R_t = dP_t/dt = (1/(V_0\Delta H_{app})) \times dQ/dt \qquad \text{(eq. 2)}$$

$$S_t = S_0 - \frac{\int_0^t Pdt}{V_0\Delta H_{app}} \qquad \text{(eq. 3)}$$

where, P is thermal power (μcal/s); R_t is the rate of the reaction at time t; S_t is the substrate concentration at time t; Q is the heat released during the enzymatic reaction; V_0 is the volume of the ITC cell; ΔH_{app} is the molar enthalpy (calculated by dividing the net heat by the number of moles of substrate in the assay).

4.2 Experimental section

Materials and Methods

All chemicals and antibiotics were purchased from Sigma or Fisher unless otherwise stated. Growth media were purchased from EMD Biosciences (Mississauga, Ontario, Canada). Chromatography media and columns were purchased from GE Healthcare.

The plasmids for mutants were obtained from Mutagenex (Piscataway, NJ).

4.2.1 Purification of the mutants

The mutants were constructed by the Mutagenex (Piscataway, NJ).

All the mutants were purified employing the same purification protocol for the wild type OXA-58.[1]

4.2.2 Circular dichroism spectroscopy

The far-UV CD spectra of OXA-58 and OXA-58 Phen113Ala, Phen114Ala, Phen113Tyr, Phen114Ile, Met225Ala and Met225Thr (10 μM) were recorded using a Jasco J-810 instrument. All measurements were carried in 50 mM sodium phosphate buffer, pH 7.0, in a rectangular cuvette with a path length of 0.1 cm. Spectra were recorded from 260 to 200 nm at a scan rate of 10 nm/min and a 1.0-nm bandwidth, at 20 °C. All spectra were corrected for buffer as appropriate.

4.2.3 Cibacron blue 3GA titrations

Tryptophan fluorescence quench of OXA-58 and OXA-58 K86A by Cibacron Blue 3GA was conducted in a Cary Eclipse fluorescence spectrophotometer (Varian Inc., Palo Alto, CA, USA). The fluorescence spectra of OXA-58 and OXA-58 F113A, F114A, F113Y, F114I, M225T and M225A (1 μM) were acquired in the presence of increasing concentrations of Cibacron Blue from 0.5 to 6 μM in 50 mM sodium phosphate buffer pH 7.0. The fluorescence (F_I) was fit to the equation below:

$$F_I = F_{max} - F_{change}\{[\text{Cibacron Blue}] / (K_d + [\text{Cibacron Blue}])\}$$

where F_{max} is the initial fluorescence intensity, F_{change} is the total fluorescence quench, and K_d is the dissociation constant.[6]

4.2.4 Determination of the K_d for CO_2 with the lysine 86 residue in the active site

The dissociation constants (K_d) of CO_2 to lysine 86 in wild type OXA-58 and mutants (F113A, F114A, F113Y, F114I, M225A and M225T) were determined using the activity assay method.[4] The dependence of the activity of the enzyme on carbon dioxide concentration has been explored using penicillin G as a substrate at varying concentrations of sodium bicarbonate as a source of CO_2 in solution. The K_d determination for CO_2 and lysine residue in the active site of the enzyme using activity studies were performed as described previously.[4]

All the buffers were degassed and purged with argon to remove CO_2. Enzymes were decarbamylated by incubation with 25mM sodium acetate (pH 4.5) under vacuum for 8 min. Carbon dioxide was supplemented using sodium bicarbonate at different concentrations ranging from 0-1500 μM. The concentration of CO_2 in the solution on the basis of sodium bicarbonate added was calculated using the equations below[7]:

$$H_2CO_3\ (aq) \rightleftharpoons H^+ + HCO_3^- \qquad k_{a1} = 10^{-6.3}$$

$$HCO_3^- \rightleftharpoons H^+ + CO_3^{2-} \qquad k_{a2} = 10^{-10.3}$$

$$[CO_2] = C_T([H^+]/k_{a1}k_{a2} + k_{a1}[H^+] + [H^+]^2)$$

$$C_T = [CO_3^{2-}] + [HCO_3^-] + [CO_2] + [H_2CO_3]$$

k_{a1} and k_{a2} are acid dissociation constants for two different steps of dissociation of H_2CO_3. The enzyme activity (100-200 nM) was studied by monitoring the hydrolysis of penicillin G (1 mM) in 100 mM sodium phosphate buffer pH = 7.5. The ionic strength was kept constant at 0.3 M by addition of Na_2SO_4. The dissociation constant was

determined by fitting the results using GraFit 5.0 software to a single-site binding equation.

4.2.5 Determination of the kinetic parameters by isothermal titration calorimetry

Isothermal titration calorimetry (ITC) experiments were performed using a MicroCal VP-ITC instrument (GE Healthcare) according to the protocol developed by Kotra and co-workers.[5] The measurements were performed at 25 °C. Substrate (antibiotic) stock solutions were prepared in 100 mM sodium phosphate buffer, pH 7.0.

A single injection method for all enzyme kinetic studies was used where the sample cell contained the antibiotic solution (substrate), and the syringe added the enzyme into the sample cell and the signal was recorded versus 100 mM sodium phosphate buffer, pH 7.0 in the reference cell contained. The final concentration of enzyme in the sample cell was 20-200 nM following injection of a 5 µl aliquot. The injection flow rate was 1 µl/s. After single injection of the enzyme, the change in heat was measured until a stable base line was obtained, showing the end of the enzymatic reaction. The reaction mixtures were stirred at 500 rpm. All reactions were carried out in triplicate. The buffer was supplemented with 50 mM sodium bicarbonate to ensure full carbamylation of the enzyme. The raw data were analyzed using Origin version 7.0 software and as described previously by fitting the data to Michaelis-Menten equation.[5]

4.2.6 Preparation of protein samples for mass spectrometry studies

A 10 µM solution of each mutant (100 µl) was prepared and the protein was precipitated by addition of 10% Trichloroacetic acid and separated by centrifugation at 18000 ×g for 5

min. Then the protein precipitate was resuspended in 10 µl water to yield the 100 µM protein solution.

4.3 Results and discussion

4.3.1 Comparison of the conformation of wild type OXA-58 to that of mutants

Comparison of the CD spectra of OXA-58 and mutants although shows slight differences, however no significant change is introduced to the structure of the protein due to the mutation (Figure 4). Also, the thermal melting of the wild type OXA-58 and Lys86Ala mutant did not show a significant change in the melting point (i.e. the stability) of the proteins because of mutation (Melting point for the wild type is 57, for Phen114Ala is 55, for Phen113Ala is 58, for Phen113Tyr is 58, for Phen114Ile is 58, for Met225Ala is 57 and for Met225Tyr is 57) (Figure 4).

4.3.2 Determination of the dissociation constant (K_d) of CO_2 for lysine 86

All mutants and also the wild type enzyme showed between 20 and 30% residual activity after decarbamylation and in the absence of CO_2 (figure 5). An increase in the activity of the enzyme was observed in the presence of increasing concentrations of CO_2. The K_d values (Table 1) were extracted using the GraFit by fitting the data to the equation below:

$$\text{Bound} = ([L].\text{capacity}) / (K_d + [L])$$

where Bound is the amount bound which is directly proportional with the fluorescence intensity, L is the concentration of the β-lactam and capacity is the binding capacity.

All mutants showed around two times higher K_d values in comparison to the wild type enzyme indicating that the CO_2 affinity to the lysine residue in the active site is decreased due to these mutations.

4.3.3 Kinetic studies on OXA-58 mutants using isothermal titration calorimetry

It was already determined experimentally in our research group that it was best to inject the enzyme, rather than substrate into the assay buffer.[1] The single injection method was used to determine the k_{cat} and K_m of OXA-58 for several β-lactam antibiotics. Control experiments including the injection of buffer into antibiotic solution in the sample cell, or OXA-58 into buffer were performed to ensure that the heat observed during the assays was from the enzymatic reaction.

Carbenicillin which had already reported not to get hydrolyzed [1], turned to be a substrate of this enzyme in this study (Table 2). Carbenicillin was the poorest substrate ($k_{cat}/K_m = 0.7 \pm 0.1$ $s^{-1}\mu M^{-1}$). Imipenem ($\Delta\varepsilon_{298}$ = -9000 $M^{-1}cm^{-1}$) has been shown to have a slow turnover rate [1], however, in this study although a slight slope was seen in the absorbance versus time graph (2.5×10^{-8} to 8×10^{-8} Ms^{-1}) for the interaction of imipenem with wild type OXA-58, however the slope did not change significantly at different concentrations of imipenem and enzyme and due to the low turnover rate the kinetic parameters could not be determined (Figure 6). M225A and F113Y did show hydrolysis when investigated by ITC however the curves could not be fitted to determine the kinetic parameters (figure 7).

F114A did not show a significant change in k_{cat} value however, the K_m value was increased around 3-fold for different substrates. This indicates that this mutation has

negatively affected the affinity of the substrate to the enzyme. In the case of F114I a dramatic decrease in the k_{cat} was observed, however, K_m was not changed significantly for different substrate which means the affinity of the substrate to the protein has not changed however the ability of the protein to hydrolyze the substrate has been decreased. For other mutants both the K_m and k_{cat} have been affected negatively which means the catalytic efficiency has decreased for these enzymes.

When determining the K_d between CO_2 and lysine 86 residue, OXA-58 displayed high levels of residual activity before supplementation with bicarbonate. Two hypotheses are proposed to explain why this high enzyme activity is seen in the absence of CO_2. Removal of the carbon dioxide that is covalently linked to the lysine residue is carried out by degassing the enzyme in sodium acetate buffer. It is possible that all the enzyme molecules are not decarbmylated fully and certain population of the enzyme solution still remain bound to carbon dioxide yielding the observed high levels of residual activity. A second hypothesis is that OXA-58 may possess a basal level enzymatic activity even when decarbamylated. Furthermore, only after the carbamylation event is the enzyme able to reach optimal residual enzyme activity. The determined dissociation constants for all mutants were higher compared with Wild type. This result suggests that the carbon dioxide affinity for these mutants of OXA-58 was reduced which may be because of the change in the hydrophobicity of the cleft over the active site of the enzyme that affects the pK_a of the lysine 86 residue.

4.3.4 Evaluation of the effect of mutation on the active site shape

To ensure that the changes in hydrolytic activity were not caused by the misfolding of the mutants (F113A, F114A, F113Y, F114I, M225T, M225A) or a change in the active site shape, fluorescence spectroscopy was used to observe the binding of the known class D active site probe, Cibacron Blue 3GA to the wild type and mutant proteins. This anthraquinone dye has already been proven to be a strong ligand to probe the proper active site formation in class D β-lactamase mutants.[6] The quenching effect of this dye on the fluorescence intensity of wild type OXA-58 and mutants was observed. This hydrophobic dye was previously shown to bind specifically to the active site of other class D β-lactamases (OXA-1 and OXA-2) with low micromolar affinities and also quench the wild-type OXA-1 tryptophan emission.[6] We found that Cibacron Blue 3GA also quenched the fluorescence intensity of wild-type OXA-58 and mutants with a large magnitude. No significant shift in the wavelength of maximal emission was seen. The K_d values obtained by fitting the fluorescence intensity as a function of cibacron blue concentration to an inverted hyperbola single-site model shown below (Figure 8, Table 3).

$$F_I = F_{max} - F_{change}\{[\text{Cibacron Blue}] / (K_d + [\text{Cibacron Blue}])\}$$

where F_{max} is the initial fluorescence intensity, F_{change} is the total fluorescence quench, and K_d is the dissociation constant[6]. In the case of the mutants for which the K_d value was obtained no dramatic change in the K_d value was observed which in turn means that the shape of active sites has not changed significantly due to this mutations.

4.3.5 Comparison of the expected mass for the wild type OXA-58 and mutants studied (K86A, F113A, F114A, F113Y, F114I, M225T, and M225A) with the obtained mass using ESI-Mass spectrometry

The expected mass and the mass obtained by mass spectrometry of the wild type and mutants have been shown in Table 4. 100 μM samples of wild type and each mutant were prepared.

All samples were submitted to the Advanced Protein Technology Centre at hospital for sick kids (Toronto, Canada) for analysis. The mass spectra for different mutants have been illustrated in Figure 6. The masses obtained by mass spectrometry are compatible with the expected ones however an extra peak with a +80 Da shift is observed for all the wild type and mutant proteins which to the most of our knowledge could be because of sulfonation or phosphorylation of the proteins.

References

(1) Verma V., Testero, S. A., Amini, K, Wei, W, Liu J., Balachandran, N., Monoharan, T., Stynes, S., Kotra, L. P., Golemi-Kotra, D. *J. Biol. Chem.* **2011**, 286:37292–37303.

(2) Santillana, E., Beceiro, A., Bou, G., and Romero, A. *Proc. Natl. Acad. Sci. U.S.A.* **2007**, 104:5354–5359

(3) Docquier, J. D., Calderone, V., De Luca, F., Benvenuti, M., Giuliani, F., Bellucci, L., Tafi, A., Nordmann, P., Botta, M., Rossolini, G. M., and Mangani, S. *Chem. Biol.* **2009**, 16:540–547

(4) Golemi, D., Maveyraud, L., Vakulenko, S., Samama J. P., and Mobasherry, S. *Proc. Natl. Acad. Sci. U.S.A* **2001**, 98:4280-5.

(5) Poduch, E., Bello, A. M., Tang, S., Fujihashi, M., Pai, E. F., and Kotra, L. P. *J. Med. Chem.* 2006, 49:4937–4945.

(6) Schneider K. D., Bethel C. R., Distler A. M., Hujer A. M., Bonomo R. A, and Leonard D. A. *Biochemistry* **2009**, 48:6136–6145.

(7) Butler James N., Carbon Dioxide Equilibria and Their Applications, 1982, Lewis Publishers.

Figures

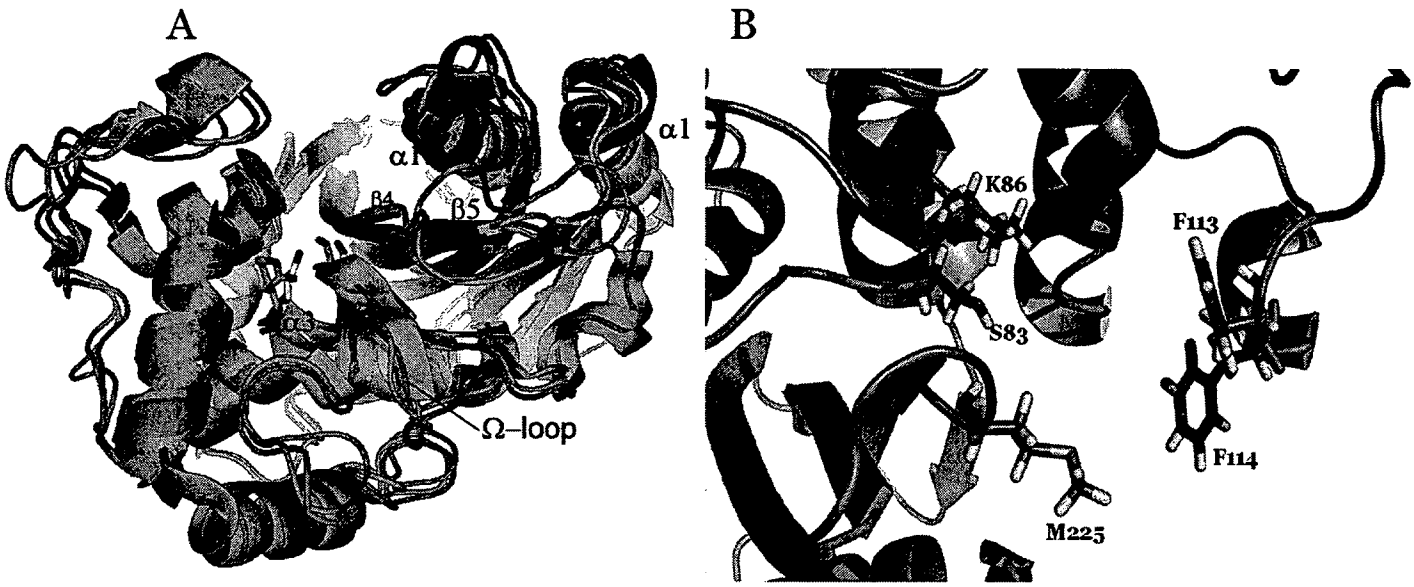

Figure 1. Comparison of the structures of Carbapenem-hydrolyzing class D β-lactamases. The OXA-58 structural homology (orange) model is superimposed on the crystal structures of OXA-10 (PDB ID 1K54, green) and OXA-24 (PDB ID 2JC7, cyan). Structures are shown in ribbons and highlighted in sticks are the sidechains of carboxylated Lys-73 and Ser-70 in OXA-10, and Lys-86 and Ser-83 in OXA-58 (figures prepared with PyMol). (Prepared by Dr. Golemi-Kotra)
(B) The positions of F113, F114 and M225 residues in the structure of OXA-58 (prepared by PyMol).

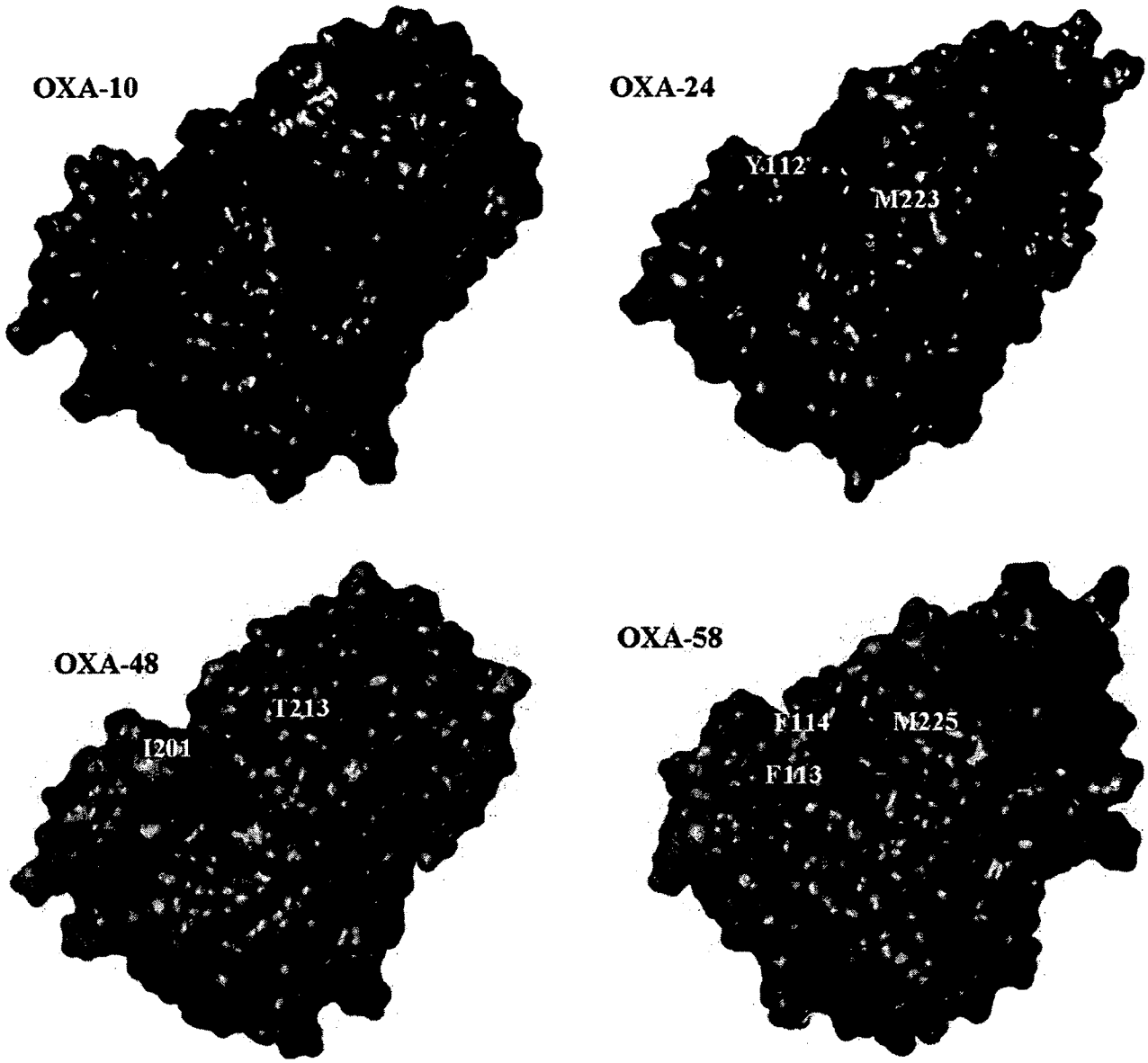

Figure 2. Molecular surfaces of OXA-10, OXA-24, OXA-48, and the OXA-58 homology model. The brown color and blue color on the surfaces show hydrophobicity and hydrophilicity. (Taken from Verma et al.[1])

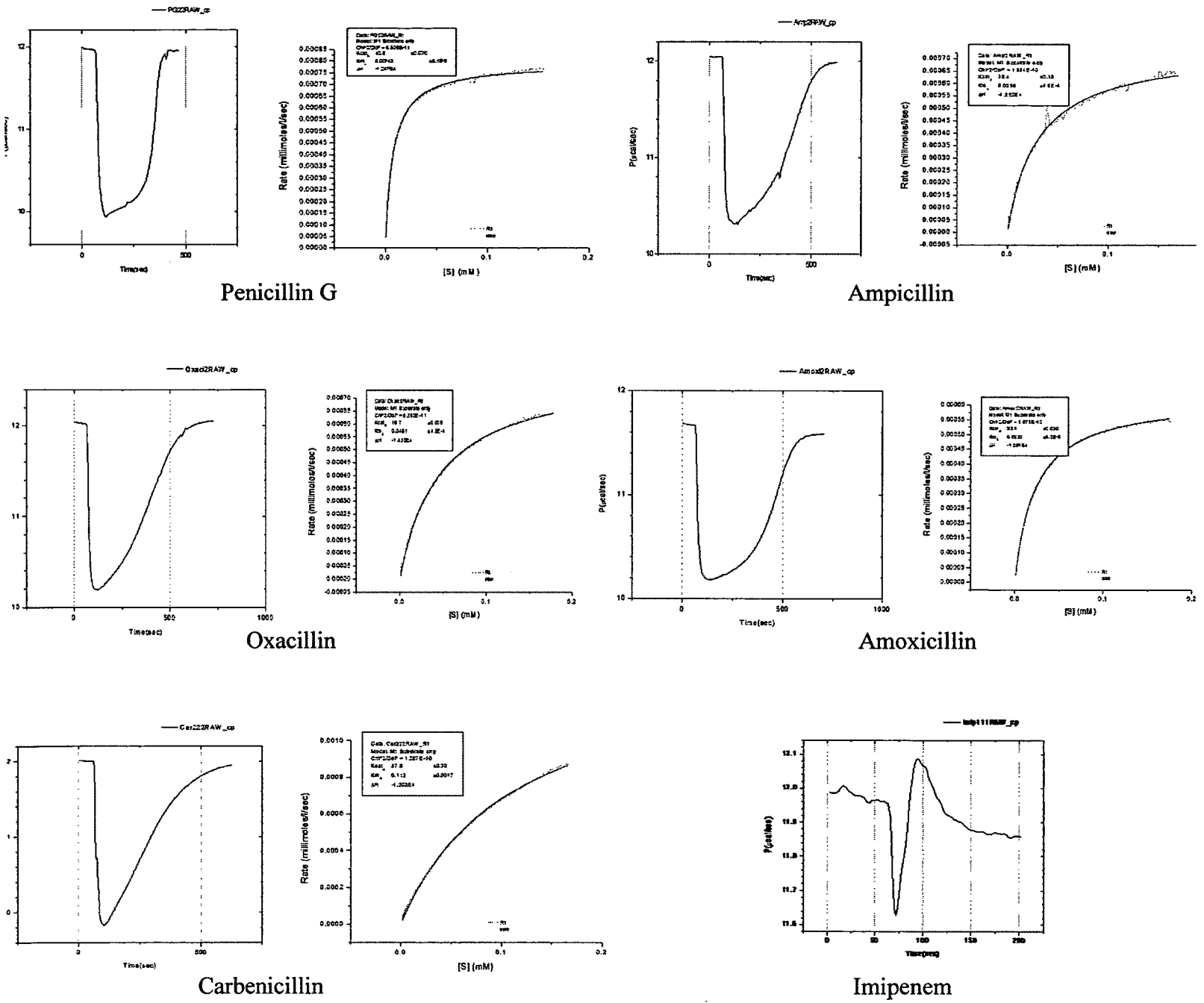

Figure 3. ITC thermograms and analysis of the data for different substrates with OXA-58 WT.

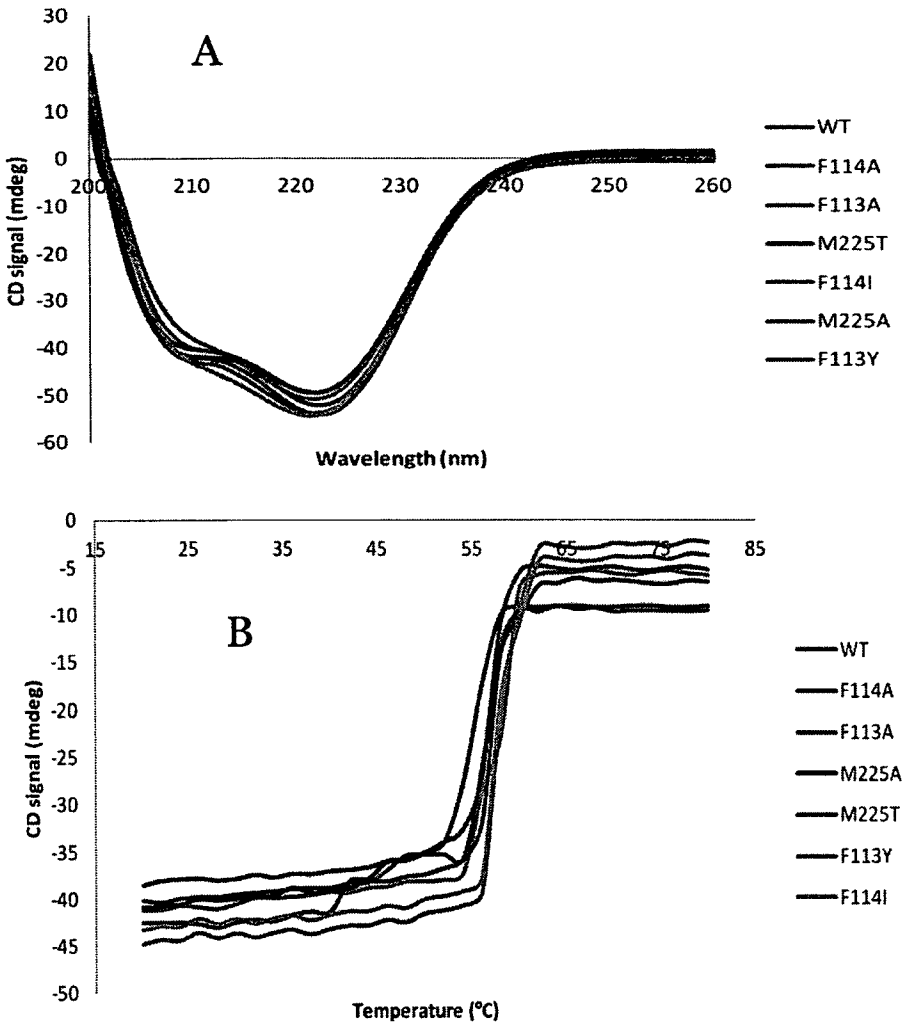

Figure 4 Investigation of effect of mutations on the structures of OXA-58. The CD spectra of 10 μM of each protein have been obtained in 50 mM sodium phosphate buffer, pH 7.0, at 20 °C.

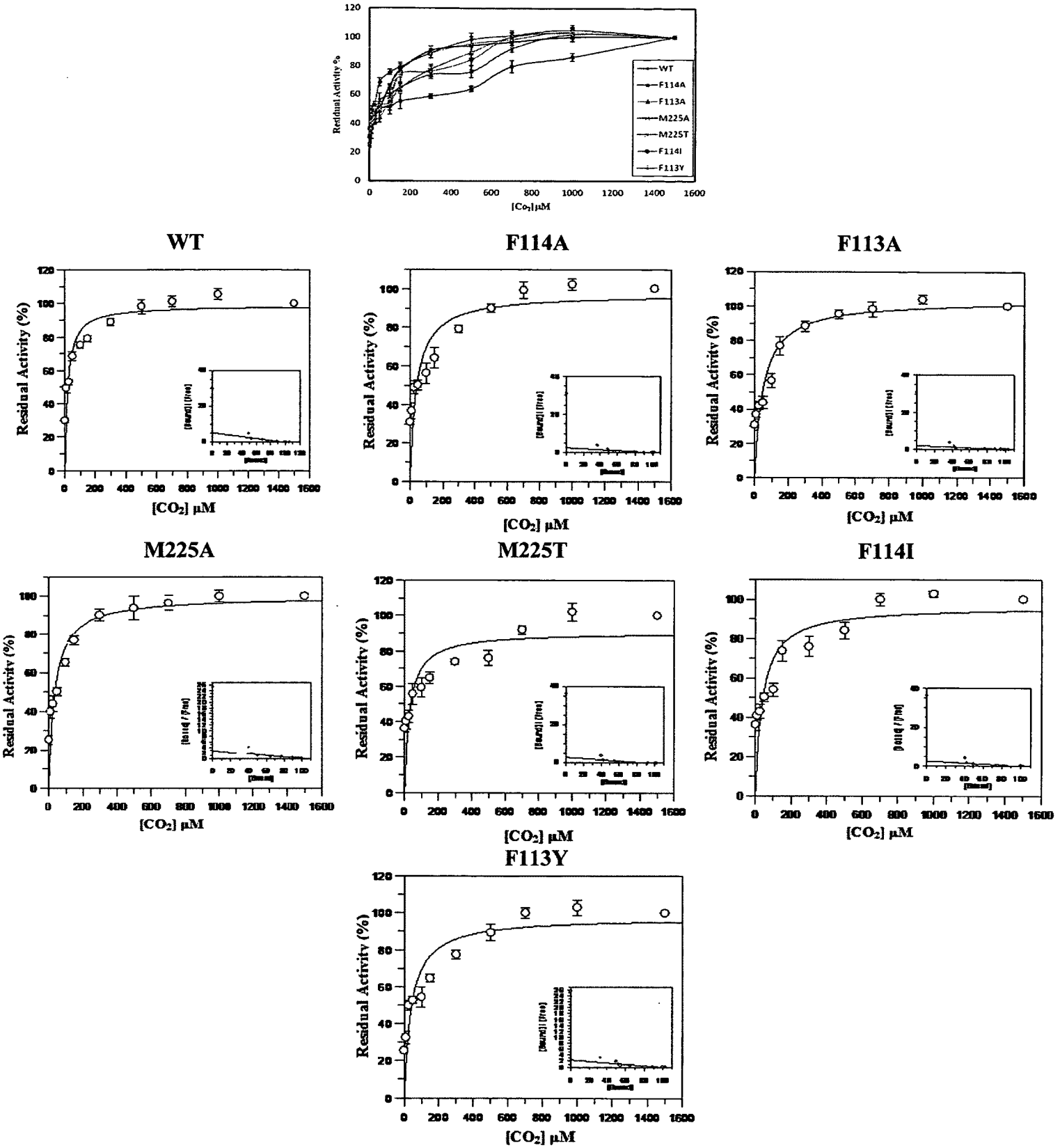

Figure 5 Determination of the dissociation constant between carbon dioxide and wild type OXA-58 and mutan

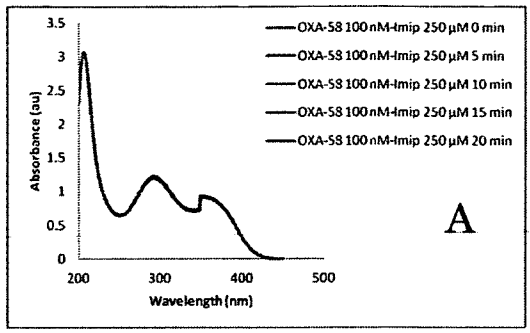

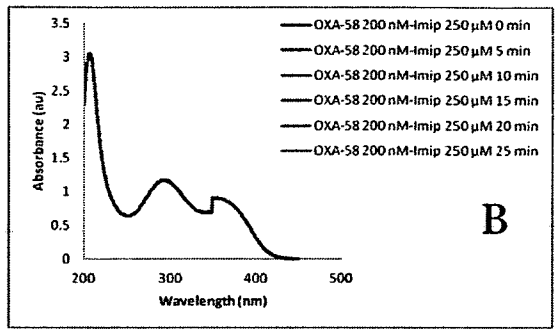

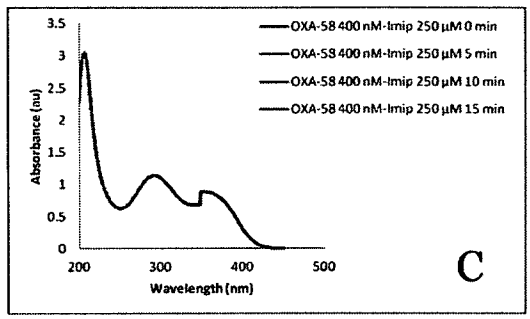

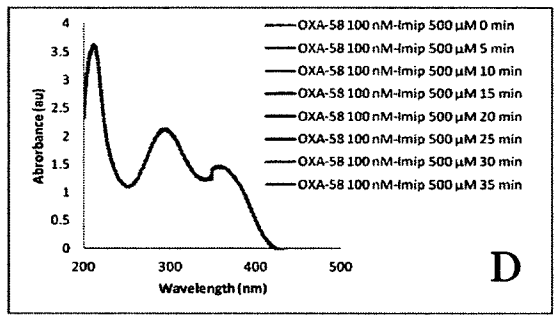

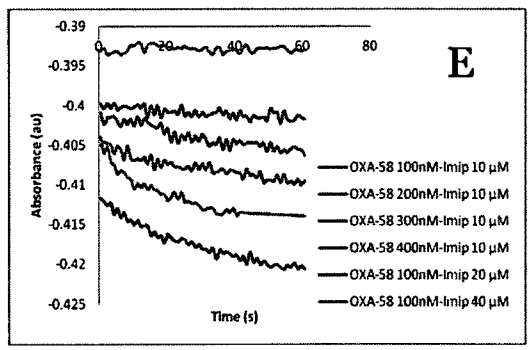

Reaction conditions	*Rate (Ms-1)*
OXA-58 100nM-Imipenem 10 µM	2.6×10^{-8}
OXA-58 200nM-Imipenem 10 µM	1.6×10^{-8}
OXA-58 300nM-Imipenem 10 µM	1.0×10^{-7}
OXA-58 400nM-Imipenem 10 µM	2.8×10^{-8}
OXA-58 100nM-Imipenem 20 µM	2.4×10^{-9}
OXA-58 100nM-Imipenem 40 µM	2.1×10^{-10}

Figure 6. (A-D) Monitoring the spectrum of imipenem at different concentrations of OXA-58 and imipenem by time. (E) The rates (Absorbance versus time) for different concentrations of OXA-58 and imipenem.

The table shows the rates (Ms^{-1}) for the reaction mixtures of different concentrations of imipenem and OXA-58

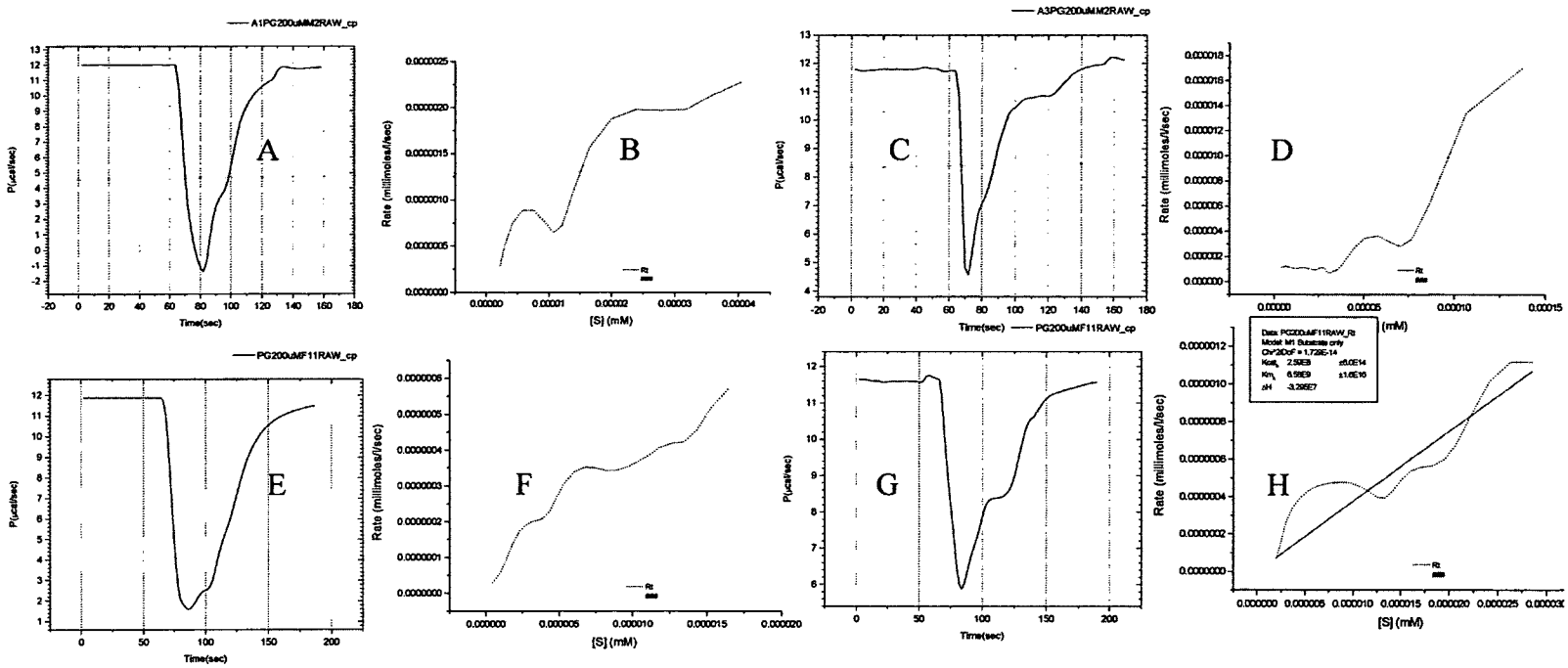

Figure 8. Thermograms for the interaction of (A) 50 nM OXA-58 M225A with 200 µM penicillin G, (C) 200 nM OXA-58 M225A with 200 µM, (E) 20 nM OXA-58 F113Y and 200 µM penicillin G, (G) 40 nM OXA-58 F113Y and 200 µM penicillin G.(B-H) Conversion of the thermal power into the reaction rates. As it can be observed data could not be fitted properly.

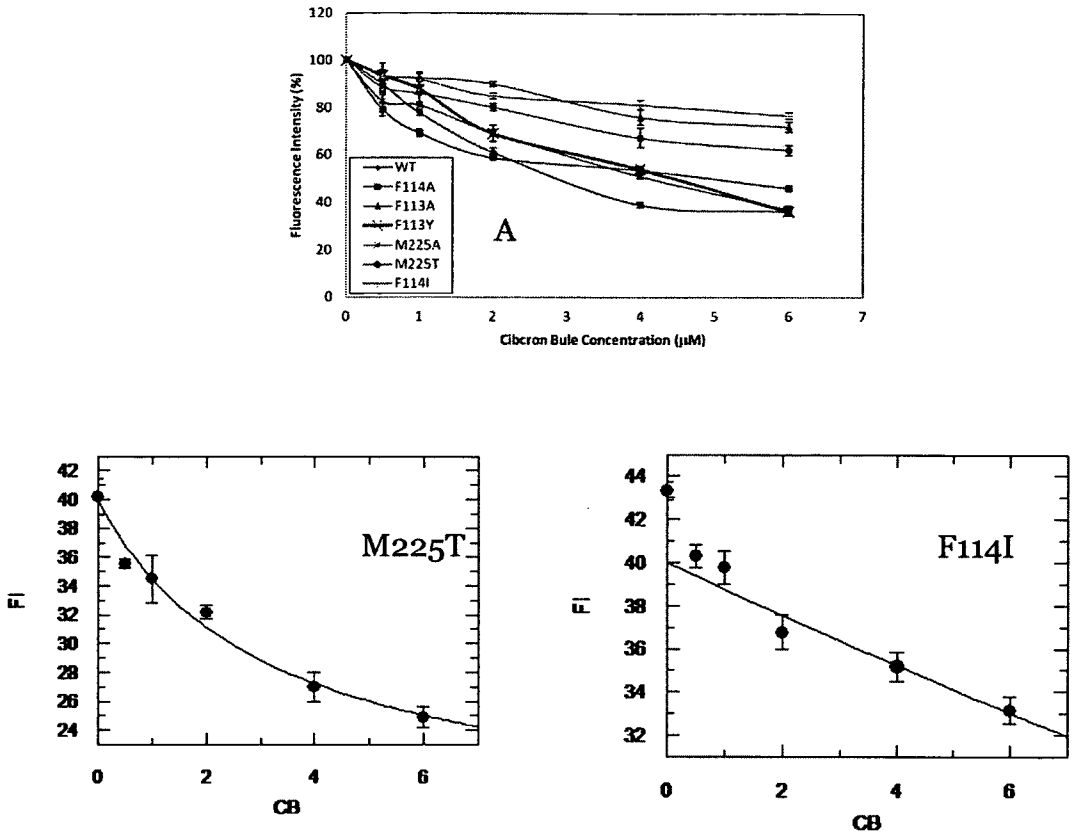

Figure 8. (A) Comparison of the quenching effect of Cibacron Blue on different mutants of OXA-58 and Non-linear fitting of the fluorescence intensity of different mutants versus cibacron blue concentration.

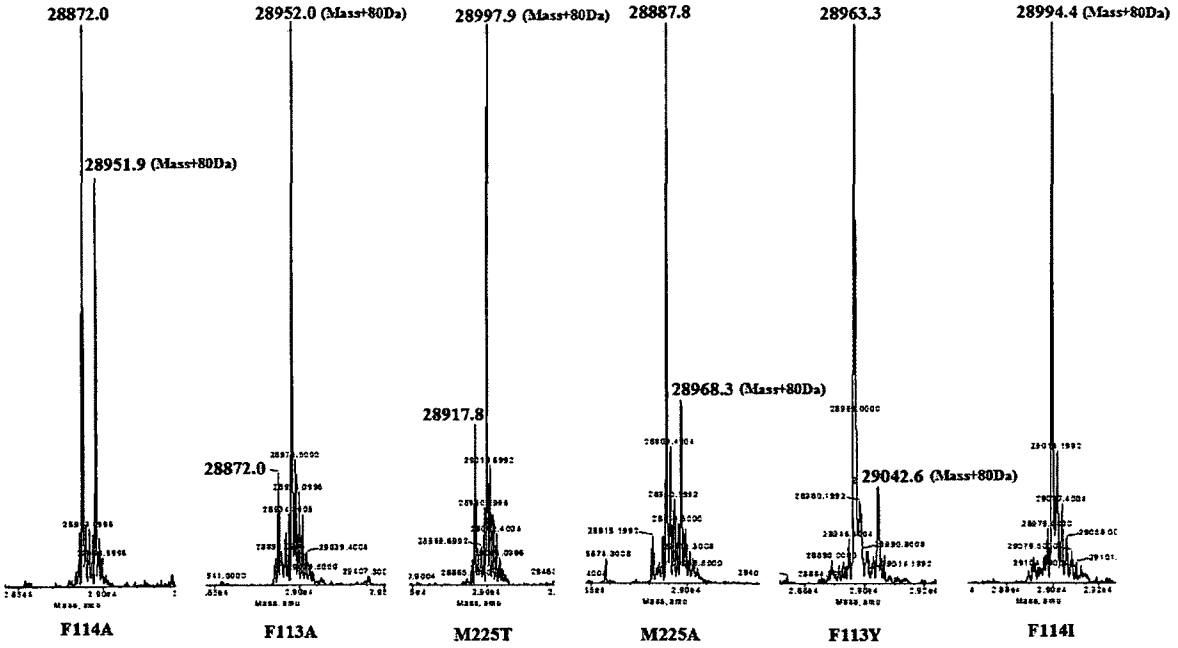

Figure 9. The Mass spectra for the OXA-58 mutants.

Tables

Table 1 Dissociation constants between wild type OXA-58 and mutants and CO_2.

Protein	K_d *(μM)*
Wild Type	18 ± 2
F114A	43± 6
F113A	50 ± 5
M225A	36 ± 4
M225T	31 ± 5
F114I	39 ± 4
F113Y	44 ± 4

Table 2 Kinetic parameters for the hydrolysis of different antibiotics with wild type OXA-58 and mutants.

Nitrocefin	*Carbenicillin*	*Oxacillin*	*Amoxicillin*	*Ampicillin*	*Penicillin G*		*Wild Type*
24 ± 3	150 ± 36	46. ± 1	25 ± 2	31 ± 2	8 ± 1	K_m (μM)	
152 ± 10	110 ± 19	85 ± 9	171± 27	185± 5	192 ± 14	K_{cat} (s^{-1})	
6.2 ± 0.3	0.7 ± 0.1	2.0 ± 0.2	7.0 ± 0.5	6.0 ± 0.5	24 ± 4	K_{cat}/K_m ($s^{-1}\mu M^{-1}$)	
487 ± 12	193 ± 19	291 ± 78	143 ± 11	104 ± 10	28 ± 2	K_m (μM)	*F114A*
120 ± 1	145 ± 16	34 ± 4	133 ± 13	233 ± 40	204 ± 28	K_{cat} (s^{-1})	
0.200 ± 0.007	0.7 ± 0.1	0.10 ±0.03	0.90 ± 0.01	2.2 0 ± 0.03	7 ± 1	K_{cat}/K_m ($s^{-1}\mu M^{-1}$)	
34 ± 1	221 ± 3	122 ± 5	67 ± 10	49 ± 3	24 ± 2	K_m (μM)	*F113A*
29 ± 2	80 ± 2	35 ± 1	80 ± 8	98 ± 11	66 ± 3	K_{cat} (s^{-1})	
0.86 ± 0.05	0.300 ± 0.004	0. 30 ± 0.01	1.2 ± 0.1	2 ± 0.1	2.6 ± 0.3	K_{cat}/K_m ($s^{-1}\mu M^{-1}$)	
14 ± 2	221 ± 3	203 ± 32	37 ± 5	41± 5	19 ± 5	K_m (μM)	*M225T*
55 ± 4	79 ± 2	13 ± 1	59 ± 2	74 ± 2	64 ± 10	K_{cat} (s^{-1})	
4.0 ± 0.3	0.300 ±0.004	0.07 ± 0.01	1.6 ± 0.2	1.7 ± 0.2	3 ± 1	K_{cat}/K_m ($s^{-1}\mu M^{-1}$)	
40 ± 2	107 ± 21	193 ± 8	84 ± 13	73 ± 5	14 ± 3	K_m (μM)	*F114I*
2.2 ± 0.1	6.5 ± 0.7	2.0 ± 0.1	11 ± 1	10 ± 2	7.0 ± 0.1	K_{cat} (s^{-1})	
0.0570 ± 0.0007	0.060 ± 0.008	0.0100 ± 0.0006	0.14 ± 0.02	0.14 ± 0.02	0.5 ± 0.1	K_{cat}/K_m ($s^{-1}\mu M^{-1}$)	
125 ± 26	N.D.	N.D.	N.D.	N.D.	N.D.	K_m (μM)	*M225A*
620 ± 77	N.D.	N.D.	N.D.	N.D.	N.D.	K_{cat} (s^{-1})	
5.0 ± 0.4	N.D.	N.D.	N.D.	N.D.	N.D.	K_{cat}/K_m ($s^{-1}\mu M^{-1}$)	
52 ± 5	N.D.	N.D.	N.D.	N.D.	N.D.	K_m (μM)	*F113Y*
329 ± 22	N.D.	N.D.	N.D.	N.D.	N.D.	K_{cat} (s^{-1})	
6.3 ± 0.2	N.D.	N.D.	N.D.	N.D.	N.D.	K_{cat}/K_m ($s^{-1}\mu M^{-1}$)	

Table 3. K_d values obtained for the interaction of cibacron blue and different OXA-58 mutants

Protein	***K_d (μM) ± SD***
OXA-58 WT	3.4 ± 0.2
K86A	4.0 ± 0.4
F114A	N.D.*
F113A	N.D.
M225A	N.D.
M225T	2.5 ± 0.3
F113Y	N.D.
F114I	3 ± 1

*Not Determined (Not enough data points to determine the K_d)

Table 4.

Protein	*Expected Mass (Da)*	*Mass obtained by Mass Spectrometry (Da)*	*Mass + 80 Da*
Wild Type	28948.1	28949.8	29029.7
K86A	28891.0	28891.5	28971.0
F114A	28872.0	28872.0	28951.9
F113A	28872.0	28872.0	28952.0
M225A	28888.0	28887.8	28968.3
M225T	28918.0	28917.8	28997.9
F113Y	28964.1	28963.3	29042.6
F114I	28914.1	28914.0	28994.4

Chapter Five: Summary and future perspectives

OXA-58 is a carbapenem-hydrolyzing class D β-lactamase from *Acinetobacter baumannii.* This enzyme uses a carbamylated lysine to activate the serine residue in its active site for a nucleophillic attack on the substrate. [1] Our findings indicate that OXA-58 uses the same catalytic machinery observed in class D β-lactamases such as OXA-10.

In this study, the hydrolytic mechanism of OXA-58 was investigated and the findings show that the hydrolyzing water molecule in the deacylation step of hydrolysis reaction approaches the acyl-enzyme intermediate from α-face. Among penicillinate derivatives studies, 6 α-hydroxyoctyl penicillinate inactivated the enzyme. All other penicillinate derivatives only were competitive inhibitors of OXA-58.

Elimination of K86 residue which in carbamylated form works as a general base to activate the active site serine residue, does not remove the activity of enzyme completely (the enzyme is still capable of hydrolyzing β-lactams although the acylation and more deacylation step have been affected) which means another lysine residue in close proximity of K86 (K220) may work as the general base in the absence of K86.

The roles of F113, F114 and Met225 in catalysis were studied by mutating these residues to Alanine and Tyrosine, Methionine, Isoleucine and Therionine which are present in the active sites of OXA-24 and OXA-48 (other carbapenem-hydrolyzing class D β-lactamases). Studies show that mutation of these residues has a negative effect on the affinity of CO_2 to the K86 in the active site of OXA-58. In the case of F114A k_{cat} value did not change significantly however, the K_m value showed around a 3-fold increase for

different substrates. This means that this mutation negatively affects the affinity of the substrate to the enzyme. In the case of F114I a remarkable decrease in the k_{cat} was observed, however, K_m was not changed significantly for different substrates which means the affinity of the substrate to the protein has not been affected however the capability of the protein to hydrolyze the substrate has been decreased. For other mutants both the K_m and k_{cat} have been affected negatively which means the catalytic efficiency has decreased for these enzymes.

In conclusion, the research work presented here provides insights into the β-lactam hydrolysis mechanism of OXA-58. In addition, the interactions of different β-lactams with this enzyme and the effect that this interaction may have on the secondary structure of this protein have been studied. Also, by mutating K86, F113, F114 and M225 residues the role of these residues in the enzymatic mechanism of OXA-58 has been investigated. X-ray crystallography of OXA-24 and OXA-48 (carbapenem-hydrolyzing class D β-lactamases) has provided invaluable information about the way they interact with their substrates.[2,3] Crystallization of OXA-58 in pure form and in complex with different β-lactams will provide a better understanding of the hydrolytic mechanism of this enzyme. Also, investigation of the acylation and deacylation rates of K86A mutant of OXA-58 with different β-lactams using a stopped flow instrument will be interesting. Tryptophan fluorescence quenching experiments can be performed on F113A, F114A, M225A, M225T, F114I and F113Y mutants to study the interaction of different β-lactams with these mutants.

References

(1) Verma V., Testero, S. A., Amini, K, Wei, W, Liu J., Balachandran, N., Monoharan, T., Stynes, S., Kotra, L. P., Golemi-Kotra, D., *J. Biol. Chem.* **2011**, 286: 37292–37303.

(2) Santillana, E., Beceiro, A., Bou, G., and Romero, A. *Proc. Natl. Acad. Sci. U.S.A.* **2007**, 104:5354–5359

(3) Docquier, J. D., Calderone, V., De Luca, F., Benvenuti, M., Giuliani, F., Bellucci, L., Tafi, A., Nordmann, P., Botta, M., Rossolini, G. M., and Mangani, S. *Chem. Biol.* **2009**, 16:540–547